Ghent University

Department of Physics and Astronomy
Theoretical High Energy Physics

Bulk Observers in Jackiw-Teitelboim Gravity

Thibaut Verhelst

Supervisor Prof. Dr. Thomas Mertens

June 4, 2024

Thibaut Verhelst

Bulk Observers in Jackiw-Teitelboim Gravity

Documentation, June 4, 2024

Reviewers: Thomas Mertens, Thomas Tappeiner and Tim Schuhmann

Supervisor: Prof. Dr. Thomas Mertens

Ghent University

Theoretical High Energy Physics

Department of Physics and Astronomy

Krijgslaan 281

9000 Ghent

Abstract

Jackiw-Teitelboim gravity is a 1+1 dimensional model of gravity which is exactly solvable not only classically but also as a model of quantum gravity. Aside from being interesting as a toy model of quantum gravity, it finds relevance in the fact that this model is emergent as the physics near the horizon of a near-extremal higher-dimensional black hole. Since this model is exactly solvable in the full quantum-gravity regime, it is possible to explicitly work out the quantum gravity corrections to many interesting known results from the semi-classical case of quantum matter on a classical gravity background. More specifically, this thesis sets out to explore the exact quantum gravity calculations of two effects related to the experience of observers living in the bulk geometry of JT gravity.

The first goal is to calculate two-point correlation functions where one of the points is located beyond the horizon of a black hole. Calculations such as these set out to better understand the experience of infalling observers. There exist already ways for defining bulk points which lie outside of a black hole in a diff-invariant way within JT gravity, but this is not the case for points on the interior. For this purpose, a method is first derived for defining such points, anchoring them to the second boundary of a TFD state. The known result for a bulk-to-bulk correlation function is then adapted using this definition of an interior point. The result was found to behave similarly to the exterior two-point function, with the addition of a finite imaginary part.

A second goal is related to the Unruh effect, which states that the concept of a vacuum is observer dependent. In the context of black holes this is related to Hawking radiation, where black holes radiate an observer-dependent Unruh heat bath. Within JT gravity, the occupation number for an uncharged Unruh heat bath of an uncharged black hole is known, but this is not so for a charged black hole emitting charged radiation. This generalisation to the charged setup is thus the second goal of this thesis. It was found that whether the exact charged occupation is higher or lower than the semi-classical approximation is dependent on the charge of the modes and the chemical potential of the black hole. This is however in disagreement with the expectations when looking at the relevant energy-stress tensor components.

Samenvatting

Jackiw-Teitelboim zwaartekracht is een $1+1$ dimensionaal zwaartekrachtmodel dat exact oplosbaar is, zowel klassiek als wanneer het een model van kwantumzwaartekracht is. Naast het feit dat een oplosbaar model van kwantumzwaartekracht op zich interessant is, heeft dit model relevantie in het feit dat het emergent is in de fysica dicht bij de horizon van een bijna-extremaal hoger dimensionaal zwart gat. Aangezien het model volledig oplosbaar is in het complete kwantumzwaartekracht regime, is het mogelijk om expliciet kwantumzwaartekracht correcties uit te voeren op vele interessante gekende resultaten uit het semi-klassieke geval van kwantum materie op een achtergrond van klassieke zwaartekracht. Meer specifiek is het doel van deze thesis om de exacte kwantumzwaartekracht berekeningen te verkennen betreffende twee effecten gerelateerd aan de ervaring van waarnemers in de bulk geometrie van JT zwaartekracht.

Het eerste doel is het berekenen van tweepuntscorrelatiefuncties waarbij één van de punten achter de horizon van een zwart gat ligt. Berekeningen zoals deze hebben als einddoel een beter begrip te ontwikkelen van de ervaring van invallende waarnemers. Er bestaan reeds manieren om bulk punten aan de buitenkant van een zwart gat te definiëren op een diff-invariante manier binnen JT zwaartekracht, maar dit geldt nog niet voor punten die binnen het zwart gat vallen. Om dit te verwezenlijken wordt er eerst een manier afgeleid om zulke punten te definiëren door ze te ankeren op de tweede rand van een TFD toestand. Het gekende resultaat voor een bulk-naar-bulk tweepuntsfunctie wordt dan aangepast gebruik makend van deze definitie van een inwendig punt. Het gevonden resultaat vertoont een gelijkaardig gedrag aan de uitwendige tweepuntsfunctie, met toevoeging van een eindig imaginair deel.

Het tweede doel is gerelateerd aan het Unruh effect, dat zegt dat het concept van een vacuüm afhankelijk is van de waarnemer. In de context van zwarte gaten is dit gerelateerd aan Hawkingstraling, waar een zwart gat een waarnemer-afhankelijk Unruh hittebad uitstraalt. De occupatie van het ongeladen Unruh hittebad van een ongeladen zwart gat is reeds gekend binnen JT zwaartekracht, maar dit is niet het geval voor het geladen hittebad van een geladen zwart gat. Deze veralgemening naar het geladen geval is concreet het tweede doel van deze thesis. Het werd gevonden dat het feit of de exacte occupatie hoger of lager ligt dan de semi-klassieke benadering, afhankelijk is van de lading van de modes en de chemische potentiaal van het zwart gat. Dit is echter in tegenspraak met de verwachtingen uit de relevante componenten van de energie-impuls tensor.

Acknowledgements

First and foremost I owe an immense gratitude to my supervisor, Prof. Dr. Thomas G. Mertens, for his continued support. It almost goes without saying that this thesis would not have been possible without his guidance. Our many personal communications proved immeasurable to my understanding of the, often times rather confusing, subject matter. Since a large part of my work was familiarising myself with the extensive literature, his directions on where to look for, and equally important how to look at, the relevant information was invaluable. When it came to performing original calculations, his continued and insightful feedback on my intermediate results were unmistakably important in getting them to a presentable state.
More generally I would like to thank him for showing an infectious amount of enthusiasm, not only about the broader subject matter but also about the specific work laid out in this thesis. His genuine excitement about the results I presented in our meetings was a great motivator when the work proved particularly daunting. On a more personal note, I would also like to thank him for his consideration and advice when it comes to my future plans in life.
Somewhere between professionally and personally, I would like to thank my colleagues. It is no secret that pursuing a higher education can be stressful, but being surrounded by like-minded peers is as good a motivator as any. I have many fond memories of discussing physics problems with them, sometimes because it is necessary and sometimes just because we like doing so.
Equally importantly, I would like to thank my family. I owe many thanks to my mom. If there is ever someone who always believes in me, it is her. While sometimes she worries perhaps a bit too much, it is nice to know that there is always someone looking out for me. I would also thank my dad, who gives me space to grow but is also there when it matters most.
Lastly I would like to thank my friends, both old and new. Life should never be all work and no play, and in this regard I could not miss them. Even just getting a moment to chat with them provided some much needed breaks during my writing process. Special thanks specifically go to my dearest friends Lies and Robin, whose unwavering support has been a beacon through many difficult times. I can honestly say I would not be where I am today were it not for them.

Thibaut Verhelst

Contents

1 Introduction

One of the biggest open questions in physics is the reconciliation of quantum mechanics and general relativity. While the unification of special relativity and quantum mechanics has seen great success in the form of quantum field theory, the same cannot be said for general relativity. When attempting to quantize general relativity in the familiar way, one finds a theory which is completely non-renormalizable in four spacetime dimensions. As such, there have been many attempts to introduce more novel theories which can explain quantum gravity as a fully UV-complete theory.

An interesting approach to tackle this search is through the so-called holographic principle, which relates theories of gravity to lower-dimensional field theories on the boundary of spacetime. A famous and useful example of such a theory is the AdS/CFT correspondence, which posits a duality between on the one hand a theory of quantum gravity in Anti de Sitter Space (AdS) and on the other hand a conformal quantum field theory (CFT) on the boundary of this AdS space.

Another possible approach is to reduce the number of spacetime dimensions altogether. This gets around the renormalizability issue, but the question remains whether such lower-dimensional models offer any insight into real physics. One such possible model is the Jackiw-Teitelboim (JT) gravity model [17], defined by the action

$$S_{JT}[g,\Phi] = \int_{\mathcal{M}} \sqrt{-g}\Phi(R-\Lambda)dx^2. \tag{1.1}$$

This model is particularly enticing, since it is exactly solvable both classically and within a full quantum-gravity framework. JT gravity is also secretly a holographic model, making use of a (nearly)AdS_2/CFT_1 correspondence to describe the physics entirely using a one-dimensional field located on the holographic boundary. Furthermore, there is a clear link between JT gravity and higher dimensional physics, as this model describes the physics near the horizon of higher dimensional, near extremal black holes. Because of this, further exploiting the exact results of JT gravity could provide pertinent insight into the nature of a more complete theory of quantum-gravity in higher dimensions.

The current work has two distinct goals in this light. Firstly, there is the question of the experience of observers falling into a black hole. Certainly, this is a question

which speaks colourfully to the imagination. While a full answer to such a question is perhaps too ambitious, JT gravity does possess the possibility of a setup which could allow us to model a "crossing" of the black hole horizon. More specifically, correlation functions between two bulk locations are already well-known, but only on the exterior of a black hole. As such, it is the goal of this thesis to extend the definition of bulk points and thus their correlators to allow for one, or both, of the points to be situated beyond the black hole horizon.

The second goal, also related to the experience of observers, is a generalisation to the description of the Unruh effect within JT gravity. The Unruh effect, in brief, describes how the concept of a vacuum is observer dependent; what appears as a vacuum to one observer can look like a heat bath to another. This effect is describable within JT gravity and one can even calculate the exact Planckian black body spectrum of the Unruh radiation, including the quantum gravity corrections. However, this result has not been fully worked out for the case of a charged black hole emitting charged Unruh radiation. Another goal of this thesis is thus to calculate the Planckian black body spectrum for charged Unruh radiation within JT gravity.

2 Introduction to JT gravity

This chapter aims to give all the background information on JT gravity necessary to follow the original work. Readers familiar with the model can opt to skip this chapter. Section 2.1 is a brief overview of some concepts from general relativity, more specifically in the case of a 1+1 dimensional spacetime, which are relevant to the rest of the thesis. Section 2.2 gives an overview of JT gravity as a classical model of gravity, largely following [26]. The next two sections discuss two different avenues of JT gravity as a quantum gravity model, i.e. including matter backreaction. Section 2.3 gives an overview of matter-coupled JT gravity, more specifically in the context of n-point correlation functions. This is the setup for the original work discussed in Chapter 3 and is based largely on [2, 26]. Section 2.4 discusses the Unruh effect, first in general terms and then within the JT gravity framework, the latter largely following [24, 30, 34]. This section forms the basis of the original work of Chapter 4.

2.1 General relativity in two dimensions

With the goal of solving the Jackiw-Teitelboim (JT) gravity model in (1+1) dimensions in mind, it is important to first take note of the relevant differences when describing general relativity in two spacetime dimensions as compared to four dimensions. Familiarly, general relativity starts from the Einstein-Hilbert action

$$S_{EH}[g] = \frac{1}{16\pi G_N}\int \sqrt{-g}R. \tag{2.1}$$

Here R is the Ricci scalar, g is the metric determinant and $d^Dx\sqrt{-g}$ is the invariant volume element (d^Dx is not explicitly written). In the case of a spacetime with a boundary there needs to be an additional term called the Gibbons-Hawking-York boundary term:

$$S_{GHY}[g] = \frac{1}{8\pi G_N}\oint \sqrt{-h}K \tag{2.2}$$

where K is the trace of the extrinsic curvature and $h_{\mu\nu}$ is the induced metric on the boundary. Note how, in natural units, the action is dimensionless. Since $[R] = L^{-2}$ and $[d^Dx] = L^D$, the dimension of the gravitational constant has to be $[G_N] = L^{D-2}$, where D is the number of spacetime dimensions. As such, G_N is dimensionless in

2d. Coupling to a matter action $S_{mat}[g]$ and using the Euler-Lagrange principle to vary this action with respect to the metric results in the Einstein field equations[1]:

$$G_{\mu\nu} \equiv R_{\mu\nu} - \frac{1}{2} g_{\mu\nu} R = 8\pi G_N T_{\mu\nu}. \tag{2.3}$$

However, in two spacetime dimensions the Einstein field tensor $G_{\mu\nu}$ becomes identically zero. This can be seen as follows [32]. The Riemann curvature tensor is antisymmetric under exchange of the first and second indices and under exchange of the third and fourth indices:

$$R_{\alpha\beta\gamma\delta} = -R_{\beta\alpha\gamma\delta} = -R_{\alpha\beta\delta\gamma} \tag{2.4}$$

Additionally, in 2d the Ricci tensor only has one degree of freedom. These properties allow us to connect the Riemann tensor with the Levi-Civita tensor $\varepsilon_{\alpha\beta}$, which is related to the Levi-Civita symbol $\varepsilon(\alpha\beta)$ by

$$\varepsilon_{\alpha\beta} = \sqrt{-g}\varepsilon(\alpha\beta). \tag{2.5}$$

The Riemann tensor in two spacetime dimensions can then be written as

$$R_{\alpha\beta\gamma\delta} = \frac{R}{2}\varepsilon_{\alpha\beta}\varepsilon_{\gamma\delta}. \tag{2.6}$$

In other words, the Riemann curvature tensor is completely defined by the value of the Ricci scalar. This means that, when given a local value of the Ricci scalar, the metric will be completely defined up to coordinate transformations [26]. This result will become important later when solving the JT gravity model. Using the property $\varepsilon_{\alpha\beta}\varepsilon_{\alpha\beta} = g_{\alpha\delta}g_{\beta\gamma} - g_{\alpha\gamma}g_{\beta\delta}$, it follows that:

$$\begin{aligned} R_{\alpha\beta} \equiv R^{\gamma}_{\alpha\gamma\beta} &= g^{\gamma\delta} R_{\gamma\alpha\delta\beta} \\ &= -\frac{R}{2} g^{\gamma\delta}(g_{\gamma\beta}g_{\alpha\delta} - g_{\gamma\delta}g_{\alpha\beta}) \\ &= -\frac{R}{2}(\delta^{\delta}_{\beta} g_{\alpha\delta} - \mathrm{Tr}(g_{\mu\nu})g_{\alpha\beta}) \\ &= -\frac{R}{2}(g_{\alpha\beta} - 2g_{\alpha\beta}) = \frac{R}{2} g_{\alpha\beta}. \end{aligned} \tag{2.7}$$

From this it indeed follows that $G_{\mu\nu} = 0$, which renders Eq. (2.3) trivial.

[1] For a derivation see e.g. [6]

2.1.1 Dilaton gravity

Instead, non-trivial results can be obtained using so-called dilaton models of gravity, where the action is coupled to a scalar field Φ called the dilaton with a corresponding potential $U(\Phi)$ called the dilaton potential:

$$S[g,\Phi] = \frac{1}{16\pi G_N}\int \sqrt{-g}(\Phi R + U(\Phi)). \tag{2.8}$$

From dimensional analysis analogous to the discussion under Eq. (2.1), it can be seen that the dilaton is dimensionless in 2d. Since the action now has an additional degree of freedom in the form of the dilaton, we can vary it with respect to both the metric and the dilaton, resulting in a system of two coupled equations of motion.

2.1.2 Euclidean gravity

It will prove useful for later discussion to give a short overview of Euclidean gravity. In contrast to Lorentzian spacetime, Euclidean spacetime holds time and space on equal footings, i.e. with a signature $(+,+)$ resulting in $ds^2 = d\tau^2 + dx^2$ for a two-dimensional flat metric. This can be obtained from the Lorentzian spacetime (with real-time t) by a Wick rotation to imaginary or Euclidean time $\tau = it$. An interesting property of such a transformation is that quantum mechanical operators at finite temperature are periodic in Euclidean time with period $\beta = 1/T$, the inverse temperature. This can be briefly illustrated as follows. The thermal average of an operator $\hat{A}$ is given by

$$\left\langle \hat{A}(\tau)\right\rangle = \frac{1}{Z}\operatorname{Tr}\left(e^{-\beta H}\hat{A}(\tau)\right). \tag{2.9}$$

where $Z = \operatorname{Tr}\left(e^{-\beta H}\right)$ is the quantum mechanical partition function. The time evolution of an operator in imaginary time is

$$\hat{A}(\tau) = e^{\tau H}A(0)e^{-\tau H}. \tag{2.10}$$

Combining these leads to the following periodicity:

$$\begin{aligned}\left\langle \hat{A}(\tau+\beta)\right\rangle &= \frac{1}{Z}\operatorname{Tr}\left(e^{-\beta H}\hat{A}(\tau+\beta)\right)\\ &= \frac{1}{Z}\operatorname{Tr}\left(e^{-\beta H}e^{\beta H}\hat{A}(\tau)e^{-\beta H}\right)\\ &= \frac{1}{Z}\operatorname{Tr}\left(\hat{A}(\tau)e^{-\beta H}\right)\\ &= \left\langle \hat{A}(\tau)\right\rangle\end{aligned} \tag{2.11}$$

Similarly, from the thermal Green's function it follows that a quantum field theory at finite temperature is periodic in Euclidean time [16]. This periodicity of

Euclidean time will be important for later discussion. These relations show a clear connection between statistical mechanics and imaginary time evolution in quantum mechanics.

A D-dimensional flat manifold in Lorentzian signature becomes a hypercylinder in Euclidean signature [35]: $\mathcal{M}_\beta = S_\beta \bigotimes \mathbb{R}^{(D-1)}$, where S_β is a circle in the Euclidean time-dimension with circumference β, imposing the cyclical nature of τ. $\mathcal{M}_\beta$ is called a Euclidean or thermal manifold. In two-dimensions this is simply a cylinder with circumference β, where τ wraps around the cylinder.

In this work Lorentzian actions will be noted with S, their Euclidean counterparts with I. For Lorentzian results, a (-, +, ..., +) metric signature convention is used.

2.2 Classical JT gravity

JT gravity is a specific model of dilaton gravity defined by the action [26]

$$S_{JT}[g,\Phi] = \frac{1}{16\pi G_N}\left(\int_{\mathcal{M}} \sqrt{-g}\Phi(R-\Lambda) + 2\oint_{\partial\mathcal{M}} \sqrt{-h}\Phi(K-1)\right), \tag{2.12}$$

i.e. setting $U(\Phi) = \Lambda\Phi$ with Λ the cosmological constant of the model. We set $\Lambda = -2/L^2$, with L the AdS length which can be set to 1. Taking the dilaton to have small fluctuations Φ about a background Φ_0, the total action of JT gravity becomes:

$$S = \frac{\Phi_0}{16\pi G_N}\left[\int \sqrt{-g}R + 2\oint \sqrt{-h}K\right] + S_{JT}[g,\Phi] + S_m[\phi,g] \tag{2.13}$$

where S_m is the matter action with a matter field ϕ and we impose explicitly that it does not couple to the dilaton. In Euclidean signature the action becomes

$$I_{JT}[g,\Phi] = -\frac{1}{16\pi G_N}\left(\int_{\mathcal{M}} \sqrt{g}\Phi(R-\Lambda) + 2\oint_{\partial\mathcal{M}} \sqrt{h}\Phi(K-1)\right). \tag{2.14}$$

This model can then be solved by applying the Euler-Lagrange principle, varying with respect to the dilaton and the metric respectively.

Note that the topological term of the total action, i.e. the constant dilaton term, is not of significant importance for the purposes of this thesis. When explicitly considered, it just leads to a constant shift in the action. It will make an appearance in Section 2.3 through the parameter $S_0 = \Phi_0/4G_N$ in the partition function, but will again not make a significant difference for the results.

2.2.1 Variation with respect to the dilaton: Anti-de Sitter space

It can be readily seen that varying (2.13) with respect to the dilaton results in

$$R = \Lambda = -2. \tag{2.15}$$

The spacetime of this model is thus a hyperbolic surface with curvature -2. A two-dimensional manifold with a constant negative curvature is called two-dimensional Anti-de Sitter (AdS_2) space.

Since the value of the Ricci scalar is defined across the entire manifold, the metric will be defined everywhere up to a local coordinate transformation [26]. More specifically, this means the metric solution will be a coordinate patch on the AdS_2 manifold. To see this, we write the metric in conformal gauge:

$$ds^2 = -e^{2\omega(u,v)} du dv \tag{2.16}$$

with u and v lightcone coordinates, related to space- and time-coordinates by $u = t + z$ and $v = t - z$. We can always do this, since any 2d pseudo-Riemannian manifold can be mapped to flat space using a conformal transformation[2]:

$$g_{\mu\nu} = e^{2\omega} \eta_{\mu\nu}, \tag{2.17}$$

where $e^{2\omega}$ is called the conformal scaling factor. Conformal transformations preserve local angles but distort distances. From the above it indeed follows that

$$\begin{aligned} ds^2 = g_{\mu\nu} dx^\mu dx^\nu &= e^{2\omega} \eta_{\mu\nu} dx^\mu dx^\nu \\ &= -e^{2\omega}(dt^2 - dz^2) \\ &= -e^{2\omega} du dv. \end{aligned} \tag{2.18}$$

The Ricci scalar becomes $R = 8e^{-2\omega} \partial_u \partial_v \omega$. Substituting this into Eq. (2.15) gives

$$4 \partial_u \partial_v \omega = -e^{2\omega} \tag{2.19}$$

which is exactly the form of Liouville's equation, which relates the conformal factor of a metric to the (constant) Gaussian curvature of its manifold. The general solution for Liouville's equation takes the form [26]

$$e^{2\omega} = \frac{4 \partial_u U(u) \partial_v V(v)}{(U(u) - V(v))^2}. \tag{2.20}$$

[2] In other words they are conformally flat.

The chiral functions $U(u)$ and $V(v)$ are determined up to homographies [18]. More specifically all representations of $e^{2\omega}$ are related by Möbius transformations of these functions:

$$U(u) \to \frac{aU+b}{cU+d}, \qquad V(v) \to \frac{-aV+b}{cV-d} \tag{2.21}$$

where $ab - cd \neq 0$. We can now write the metric as

$$ds^2 = -\frac{4\partial_u U(u)\partial_v V(v) du dv}{(U(u)-V(v))^2} = -\frac{4dUdV}{(U-V)^2}. \tag{2.22}$$

2.2.1.1 Anti-de Sitter coordinate patches

Since any metric solution of this model will be a coordinate patch on the AdS_2manifold, it is constructive to give an overview of some relevant patches, as laid out in [26]. These coordinate patches cover different portions of the total manifold and will prove necessary to describing the physics in JT gravity. The different patches can be seen in Fig. (2.1).

The Poincaré patch is defined by the coordinates

$$ds^2 = \frac{1}{Z^2}(dZ^2 - dT^2) = \frac{-4dUdV}{(U-V)^2} \tag{2.23}$$

with space and time coordinates Z and T and lightcone coordinates $U = T + Z$ and $V = T - Z$. With this, it is clear that the functions $(U(u), V(v))$ in Eq. (2.22) relate the lightcone coordinates of the Poincaré patch to the lightcone coordinates (u, v) of some different patch. The Poincaré patch has a boundary at $Z = 0$, where the metric blows up. The two horizons for this patch are at $U - V \to \infty$ where the metric tends to zero. These horizons are at infinite proper distance, which can be seen by setting $dT = 0 \Rightarrow ds = dZ/Z$ and noticing that $\int^{\infty} dZ/Z \to \infty$. This patch thus has, as will become more apparent later, horizons at the end of an infinite throat.

The black hole patch with lightcone coordinates (u, v) can be found from the Poincaré patch using the chiral coordinate transformations

$$U(u) = \frac{\beta}{\pi}\tanh\left(\frac{\pi}{\beta}u\right), \qquad V(v) = \frac{\beta}{\pi}\tanh\left(\frac{\pi}{\beta}v\right) \tag{2.24}$$

where β will get the interpretation of the inverse temperature of a black hole. The metric becomes

$$ds^2 = -\frac{\pi^2}{\beta^2}\frac{4dudv}{\sinh^2(\frac{\pi}{\beta}(u-v))} = \frac{4\pi^2}{\beta^2}\frac{dz^2 - dt^2}{\sinh^2(\frac{2\pi}{\beta}z)}. \tag{2.25}$$

There is a boundary at $z = 0$ and horizons at $u - v \to \infty$. These horizons are, however, at finite proper distance since $\int^{\infty} dz/\sinh(\frac{2\pi}{\beta}z) < \infty$. The black hole patch is completely contained within the Poincaré patch, since from (2.24) it follows that the black hole coordinates only cover the region of $-\frac{\beta}{\pi} < U, V < \frac{\beta}{\pi}$. As $\beta \to \infty$, the black hole patch will grow until it meets the horizons of the Poincaré patch. In other words, the Poincaré patch is the zero temperature limit of the black hole patch.
Additionally, the future horizon of the black hole patch is a black hole horizon, as described in [30]. There is a subtlety here, as this definition of a black hole in AdS_2 pure gravity differs from the four dimensional case. In four dimensions the geometry near the horizon differs from the far-away geometry, but this is not the case in AdS_2. One way to describe this is that an AdS_2 black hole is AdS_2 together with a choice of time coordinate t at infinity for which the full region $-\infty < t < \infty$ does not cover all of the time-like boundary of AdS_2, such that the black hole horizon is then the surface from behind which nothing can escape to the region $-\infty < t < \infty$ [30]. We see that this is indeed the case for the time coordinate of the black hole patch: as t runs from negative infinity to positive infinity, only a finite region of the AdS_2 boundary is covered. Anything across the future horizon of the black hole patch has no way of accessing this region and this wedge thus represents the exterior of the AdS_2 black hole and its future horizon is itself indeed a black hole horizon. Note that the same can be said for the Poincaré patch, being the zero temperature limit of the black hole patch[3].

Finally it is worth briefly mentioning the global patch, defined by the transformations

$$U(\mathbf{u}) = \tan(\mathbf{u}), \qquad V(\mathbf{v}) = \tan(\mathbf{v}). \tag{2.26}$$

This leads to the metric

$$ds^2 = -\frac{4d\mathbf{u}d\mathbf{v}}{\sin^2(\mathbf{u}-\mathbf{v})} = \frac{4}{\sin^2(2\mathbf{z})}(d\mathbf{z}^2 - d\mathbf{t}^2) \tag{2.27}$$

where $\mathbf{z} = (\mathbf{u}-\mathbf{v})/2$ and $\mathbf{t} = (\mathbf{u}+\mathbf{v})/2$. This patch gets its name from the fact that it fully covers the universal cover of AdS_2 [30], for $\mathbf{z} \in [0, \pi/2]$ and $\mathbf{t} \in]-\infty, \infty[$. Alternatively the global patch can be written in terms of the coordinates

$$ds^2 \propto \frac{-d\tau^2 + d\sigma^2}{\cos^2\sigma} \tag{2.28}$$

where then $\sigma \in [-\frac{\pi}{2}, \frac{\pi}{2}]$ and $\tau \in]-\infty, \infty[$ [30]. As per the earlier discussion, the global patch does not exhibit an AdS_2 black hole.

[3]The Poincaré patch is in fact the limit of extremality of the higher dimensional black hole which embeds the black hole patch. This statement will become more apparent later, see p.12.

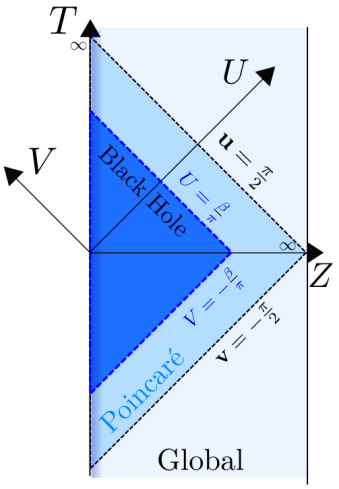

Fig. 2.1: Penrose diagram of different coordinate patches of AdS_2, all of which are solutions of JT gravity. Note that the global patch reaches infinitely up- and downwards. Figure taken from [26].

2.2.1.2 Physics of the coordinate patches

The physics in these patches is different: the Poincaré patch describes the region near the horizon of a higher dimensional extremal black hole, while the black hole patch describes the region near the horizon of a higher dimensional near-extremal black hole. To illustrate this fact, it is indicative to look at the higher-dimensional perspective in a top-down way. This derivation largely follows [26].

In 4d, the spacetime around a black hole with mass M, charge Q and no angular momentum is described by the Reissner-Nordström metric:

$$ds^2 = -f(r)dt^2 + \frac{dr^2}{f(r)} + r^2 d\Omega_2^2, \qquad f(r) = 1 - \frac{2M}{r} + \frac{Q^2}{r^2} \tag{2.29}$$

where Ω_2 is the two-dimensional angular metric element. For simplicity we take $Q > 0$. Far away (at large r), this metric becomes flat space and it has two horizons which are found by computing $f(r) = 0$, which leads to

$$r_\pm = M \pm \sqrt{M^2 - Q^2}. \tag{2.30}$$

This puts a restriction on the allowed mass of the black hole for a given charge. If $M < Q$, the roots become complex and the solution does not correspond to a physical state. In the case of $M = Q$, which is the minimal allowed value of the mass, the two horizons are degenerate and this case corresponds to a so-called extremal black hole.

A near-extremal black hole is then the regime where $M \sim Q$ or where $\Delta M \equiv M - Q$ is small. Furthermore we can consider the near-horizon regime of such a black hole by parameterizing the radial coordinate as $r = Q + Q^2\tilde{r}$, where now $\tilde{r} \sim \sqrt{\Delta M/Q^3}$. This way, for a near extremal black hole the radial coordinate is indeed close to the outer horizon r_+ since $M \sim Q$ and thus

$$\begin{aligned} r &\sim Q + Q^2\sqrt{\frac{\Delta M}{Q^3}} \sim M + \sqrt{Q(M-Q)} \\ &\sim r_+. \end{aligned} \tag{2.31}$$

In terms of the new radial coordinate $\tilde{r}$ the metric (2.29) becomes

$$ds^2 \approx -Q^2 F(\tilde{r})dt^2 + \frac{Q^2 d\tilde{r}^2}{F(\tilde{r})} + Q^2 d\Omega_2^2, \qquad F(\tilde{r}) = \tilde{r}^2 - \frac{2\Delta M}{Q^3} \tag{2.32}$$

which be written in the form

$$Q^{-2}ds^2 \approx -(\tilde{r}^2 - r_h^2)dt^2 + \frac{d\tilde{r}^2}{\tilde{r}^2 - r_h^2} + d\Omega_2^2, \qquad r_h = \sqrt{\frac{2\Delta M}{Q^3}} \tag{2.33}$$

by rescaling the length by Q^{-1}. This metric represents an $AdS_2 \times S^2$ geometry, with a black hole horizon at a distance r_h. The total geometry of the Reissner-Nordström black hole is then asymptotically flat with an $AdS_2 \times S^2$ throat leading to a horizon. This presence of a throat is unique to charged black holes [4] and its length is dependent on the extremality of the black hole.

In the extremal case $r_h = 0$, the AdS part of the metric takes the form of the Poincaré patch of AdS_2. This can be seen by defining $R = 1/Z$ in Eq. (2.23), which leads to

$$ds^2 = -R^2 dT^2 + \frac{1}{R^2} dR^2. \tag{2.34}$$

This confirms the earlier statement that the Poincaré patch describes the physics of the near-horizon regime of a near extremal higher dimensional black hole. As calculated earlier, the horizons in the Poincaré patch are at infinite proper distance. This can also be seen form the perspective of the higher dimensional black hole by calculating the distance from the horizon to an arbitrary point $r_0 > r_+$ [15]:

$$D = \int_{r_+}^{r_0} dr \sqrt{f(r)} \sim -M \log(r_+ - r_-) \tag{2.35}$$

which diverges in the extremal case since then $r_+ = r_-$. In other words, the length of the $AdS_2 \times S^2$ throat diverges as the black hole approaches extremality. The Penrose diagram for an extremal Reissner-Nordström black hole can be seen in Fig. (2.2). Since the Poincaré patch covers only a part of the AdS_2 manifold, it also covers only the near-horizon region of one patch of the Reissner-Nordström spacetime [15].

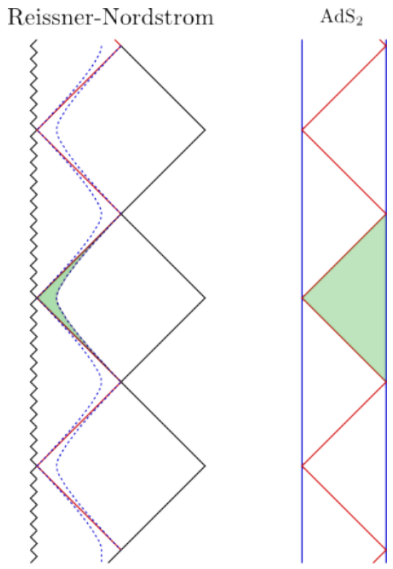

Fig. 2.2: Penrose diagrams for the extremal Reissner-Nordström black hole and corresponding AdS$_2$ region. The AdS$_2$ region is found in the near-horizon region of the higher dimensional black hole, indicated with the blue dashed line. The Poincaré patch of AdS$_2$ is colored green. Figure taken from [15]

In the near extremal case the horizon is at a finite distance r_h. The AdS part of the metric (2.33) has the form of the black hole patch of AdS$_2$, given by Eq. (2.25). This can be seen by defining the coordinate $r = r_h \coth(\frac{2\pi z}{\beta})$ where $r_h = 2\pi/\beta$, which leads to

$$ds^2 = -(r^2 - r_h^2)dt^2 + \frac{dr^2}{r^2 - r_h^2} \tag{2.36}$$

which does indeed correspond to Eq. (2.33). The black hole patch is thus found in the near-horizon regime of a near extremal, higher dimensional black hole and the parameter β is the inverse temperature of this black hole.
As was apparent in Sec. (2.2.1.1), the Poincaré patch is the zero temperature limit $(\beta \to \infty)$ of the black hole patch. This can be directly related to the extremality limit of the higher dimensional black hole. The Hawking temperature of a Reissner-Nordström black hole in terms of the horizons is given by [30]

$$T_H = \frac{r_+ - r_-}{2\pi r_+^2}, \tag{2.37}$$

and since in the extremal limit $r_+ = r_-$, the Hawking temperature becomes zero for an extremal black hole.

The fact that the different patches are found in different physical systems introduces an ambiguity to this description, since the patches are related by simple coordinate transformations which on their own are not physical. As such, the theory will need some way of clarifying this ambiguity and specifying which patch is relevant for a

given system by way of offering physical meaning to the coordinates. This will be achieved by taking a closer look at the dynamics near the boundary and introducing a preferred time coordinate as well as boundary-intrinsic bulk coordinates, resulting in a fixed physical metric.

2.2.2 Variation with respect to the metric

The next step is to vary the action (2.13) with respect to the metric. The constant dilaton part of the action is exactly the Einstein-Hilbert action, which when varied results in the Einstein field tensor which is zero in two dimensions. The first steps of the derivation of the remaining terms also follow in large part the variation of the Einstein-Hilbert action, which can be found in [6].

The variation to be calculated is

$$\delta S = \frac{1}{16\pi G_N}\left(\int_{\mathcal{M}} \Phi\delta(\sqrt{-g}(R-\Lambda)) + 2\oint_{\partial\mathcal{M}} \Phi\delta(\sqrt{-h}(K-1))\right). \tag{2.38}$$

The variation in the bulk integral can be written as

$$\begin{aligned}\delta(\sqrt{-g}(R+2)) &= (R+2)\delta\sqrt{-g} + \sqrt{-g}\delta R \\ &= (R+2)\delta\sqrt{-g} + \sqrt{-g}\left(g^{\mu\nu}\delta R_{\mu\nu} + R_{\mu\nu}\delta g^{\mu\nu}\right).\end{aligned} \tag{2.39}$$

The final term is already in the correct form, $(\dots)\delta g^{\mu\nu}$, but the other terms need further work. The variation of the Ricci tensor can be calculated using the Palatini identity:

$$\begin{aligned}\delta R^{\lambda}{}_{\mu\sigma\nu} &= \nabla_\sigma\left(\delta\Gamma^\lambda_{\mu\nu}\right) - \nabla_\nu\left(\delta\Gamma^\lambda_{\mu\sigma}\right) \\ \Rightarrow \delta R_{\mu\nu} = \delta R^{\lambda}{}_{\mu\lambda\nu} &= \nabla_\lambda\left(\delta\Gamma^\lambda_{\mu\nu}\right) - \nabla_\nu\left(\delta\Gamma^\lambda_{\mu\lambda}\right)\end{aligned} \tag{2.40}$$

where ∇ is the covariant derivative. From this it follows that the second term can be written as

$$\begin{aligned}g^{\mu\nu}\delta R_{\mu\nu} &= g^{\mu\nu}(\nabla_\lambda(\delta\Gamma^\lambda_{\mu\nu}) - \nabla_\nu(\delta\Gamma^\lambda_{\mu\lambda})) \\ &= g^{\mu\nu}\nabla_\lambda\delta\Gamma^\lambda_{\mu\nu} - g^{\mu\lambda}\nabla_\lambda\delta\Gamma^\alpha_{\mu\alpha} \\ &= \nabla_\lambda(g^{\mu\nu}\delta\Gamma^\lambda_{\mu\nu} - g^{\mu\lambda}\delta\Gamma^\alpha_{\mu\alpha} - \delta\Gamma^\lambda_{\mu\nu}\nabla_\lambda g^{\mu\nu} + \delta\Gamma^\alpha_{\mu\alpha}\nabla_\lambda g^{\mu\lambda}).\end{aligned} \tag{2.41}$$

The Levi-Civita connection is the unique connection which is both torsion free and metric compatible [6], meaning that $\nabla_\lambda g_{\mu\nu} = 0$. From this it follows also that $\nabla_\lambda g^{\mu\nu} = 0$ and $\nabla_\lambda g^{\mu\lambda} = 0$. Eq. (2.41) becomes

$$g^{\mu\nu}\delta R_{\mu\nu} = \nabla_\lambda(g^{\mu\nu}\delta\Gamma^\lambda_{\mu\nu} - g^{\mu\lambda}\delta\Gamma^\alpha_{\mu\alpha}). \tag{2.42}$$

The variation of the Christoffel symbols is a known identity:

$$\delta\Gamma^{\lambda}_{\mu\nu} = \frac{1}{2}g^{\lambda\rho}(\nabla_\mu\delta g_{\nu\rho} + \nabla_\nu\delta g_{\mu\rho} - \nabla_\rho\delta g_{\mu\nu}) \tag{2.43}$$

such that

$$\begin{aligned} g^{\mu\nu}\delta R_{\mu\nu} = \frac{1}{2}\nabla_\lambda \Big[& g^{\mu\nu}g^{\lambda\rho}(\nabla_\mu\delta g_{\nu\rho} + \nabla_\nu\delta g_{\mu\rho} - \nabla_\rho\delta g_{\mu\nu}) \\ & - g^{\mu\lambda}g^{\alpha\rho}(\nabla_\mu\delta g_{\alpha\rho} + \nabla_\alpha\delta g_{\mu\rho} - \nabla_\rho\delta g_{\mu\alpha})\Big] . \end{aligned} \tag{2.44}$$

By renaming the dummy indices we notice that the first term is equal to the sixth term, the second term is cancelled by the fifth term and the third term is equal to the fourth term, resulting in

$$g^{\mu\nu}\delta R_{\mu\nu} = \nabla_\lambda \left[g^{\mu\nu}g^{\lambda\rho}(\nabla_\mu\delta g_{\nu\rho} - \nabla_\rho\delta g_{\mu\nu})\right] . \tag{2.45}$$

Next, the $\delta\sqrt{-g}$ term in Eq. (2.39) needs to be worked out. To do this, we use Jacobi's formula, which states that for an invertible matrix A:

$$\begin{aligned} \delta \det A &= \det A \,\mathrm{Tr}(A^{-1}\delta A) \\ \Rightarrow \delta g &= g g^{\mu\nu}\delta g_{\mu\nu} \end{aligned} \tag{2.46}$$

Additionally, from $g_{\mu\nu}g^{\nu\lambda} = \delta^\lambda_\mu$ it follows that $g_{\mu\nu}\delta g^{\nu\lambda} = -g^{\nu\lambda}\delta g_{\mu\nu}$ such that $\delta g = -g g_{\mu\nu}\delta g^{\mu\nu}$ and

$$\begin{aligned} \delta\sqrt{-g} &= \frac{-1}{2\sqrt{-g}}\delta g \\ &= \frac{1}{2}\frac{g}{\sqrt{-g}}g_{\mu\nu}\delta g^{\mu\nu} \\ &= \frac{-1}{2}\sqrt{-g}g_{\mu\nu}\delta g^{\mu\nu} \end{aligned} \tag{2.47}$$

The variation in the bulk integral becomes:

$$\begin{aligned} \delta(\sqrt{-g}(R+2)) = & -\frac{1}{2}\sqrt{-g}g^{\mu\nu}\delta g_{\mu\nu}(R+2) \\ & + \sqrt{-g}\left(\nabla_\lambda\left[g^{\mu\nu}g^{\lambda\rho}(\nabla_\mu\delta g_{\nu\rho} - \nabla_\rho\delta g_{\mu\nu})\right] + R_{\mu\nu}\delta g^{\mu\nu}\right) . \end{aligned} \tag{2.48}$$

The full bulk part of Eq. (2.38) then becomes:

$$\begin{aligned} & \frac{1}{16\pi G_N}\int_{\mathcal{M}}\sqrt{-g}\Phi\left(-\frac{1}{2}g^{\mu\nu}\delta g_{\mu\nu}(R+2)\right. \\ & \qquad \left. + \nabla_\lambda\left[g^{\mu\nu}g^{\lambda\rho}(\nabla_\mu\delta g_{\nu\rho} - \nabla_\rho\delta g_{\mu\nu})\right] + R_{\mu\nu}\delta g^{\mu\nu}\right) \\ & = \frac{1}{16\pi G_N}\int_{\mathcal{M}}\sqrt{-g}\Phi\left(\left(R_{\mu\nu} - \frac{1}{2}g_{\mu\nu}\right)\delta g^{\mu\nu} - g_{\mu\nu}\delta g^{\mu\nu}\right. \\ & \qquad \left. + \nabla_\lambda\left[g^{\mu\nu}g^{\lambda\rho}(\nabla_\mu\delta g_{\nu\rho} - \nabla_\rho\delta g_{\mu\nu})\right]\right) . \end{aligned} \tag{2.49}$$

The first term is the Einstein field tensor and is thus zero in two dimensions. The third term is where this derivation differs from the Einstein-Hilbert action due to the presence of the dilaton field. Here, this term needs to be worked out by splitting the derivative twice. Introducing the notation

$$V^\lambda = g^{\mu\nu} g^{\lambda\rho} (\nabla_\mu \delta g_{\nu\rho} - \nabla_\rho \delta g_{\mu\nu}), \tag{2.50}$$

the term becomes

$$\int \sqrt{-g} \Phi \nabla_\lambda V^\lambda = \int \sqrt{-g} \nabla_\lambda (\Phi V^\lambda) - \int \sqrt{-g} \nabla_\lambda \Phi V^\lambda. \tag{2.51}$$

The first term has solely a boundary contribution using the generalised Stokes' theorem:

$$\int_{\mathcal{M}} \sqrt{-g} \nabla_\mu V^\mu = \int_{\partial \mathcal{M}} \sqrt{-h} n_\mu V^\mu, \tag{2.52}$$

which will be left implicit for now. We get

$$\int \sqrt{-g} \Phi \nabla_\lambda V^\lambda = \text{BDY} - \int \sqrt{-g} \nabla_\lambda \Phi V^\lambda. \tag{2.53}$$

Splitting again the derivative the integral can be further worked out to be

$$\begin{aligned} \int \sqrt{-g} \nabla_\lambda \Phi V^\lambda &= \int \sqrt{-g} g^{\mu\nu} g^{\lambda\rho} \left(\nabla_\lambda \Phi \nabla_\mu \delta g_{\nu\rho} - \nabla_\lambda \Phi \nabla_\rho \delta g_{\mu\nu} \right) \\ &= \int \sqrt{-g} g^{\mu\nu} g^{\lambda\rho} \left(\nabla_\mu (\nabla_\lambda \Phi \delta g_{\nu\rho}) - \delta g_{\nu\rho} \nabla_\mu \nabla_\lambda \Phi \right. \\ &\qquad \left. - \nabla_\rho (\nabla_\lambda \Phi \delta g_{\mu\nu}) + \delta g_{\mu\nu} \nabla_\rho \nabla_\lambda \Phi \right). \end{aligned} \tag{2.54}$$

Again using the metric compatibility requirement $\nabla_\alpha g^{\mu\nu} = 0$, the metric can be brought into the covariant derivatives, meaning the first and third term are full derivatives which can be reduced to boundary terms using again Stokes' theorem. Also using $g^{\mu\nu} \delta g_{\nu\rho} = -g_{\nu\rho} \delta g^{\mu\nu}$ we get

$$\begin{aligned} \int \sqrt{-g} \nabla_\lambda \Phi V^\lambda &= \text{BDY} - \int \sqrt{-g} g^{\mu\nu} g^{\lambda\rho} \left(\delta g_{\nu\rho} \nabla_\mu \nabla_\lambda \Phi - \delta g_{\mu\nu} \nabla_\rho \nabla_\lambda \Phi \right) \\ &= \text{BDY} - \int \sqrt{-g} \left(g^{\mu\nu} \delta g_{\nu\rho} \nabla_\mu \nabla^\rho \Phi - g^{\mu\nu} \delta g_{\mu\nu} \nabla^2 \Phi \right) \\ &= \text{BDY} + \int \sqrt{-g} \left(g_{\nu\rho} \delta g^{\mu\nu} \nabla_\mu \nabla^\rho \Phi - g_{\mu\nu} \delta g^{\mu\nu} \nabla^2 \Phi \right) \\ &= \text{BDY} + \int \sqrt{-g} \left(\nabla_\mu \nabla_\nu \Phi - g_{\mu\nu} \nabla^2 \Phi \right) \delta g^{\mu\nu}. \end{aligned} \tag{2.55}$$

Plugging this into Eq. (2.49) gives

$$\frac{1}{16\pi G_N} \left(\text{BDY} - \int \sqrt{-g} \left(\nabla_\mu \nabla_\nu \Phi - g_{\mu\nu} \nabla^2 \Phi + g_{\mu\nu} \Phi \right) \delta g^{\mu\nu} \right). \tag{2.56}$$

Analogously to the treatment of the Einstein-Hilbert action, it turns out that the boundary terms are perfectly cancelled by the variation of the boundary term in Eq. (2.38)[4]. From this expression we can read out the vacuum equations for the dilaton. With the introduction of the matter sector $S_m[\phi, g]$, we get a term containing the energy-momentum tensor, the derivation of which is completely analogous to the usual matter coupled Einstein-Hilbert action. The total field equation for the dilaton becomes:

$$\nabla_\mu \nabla_\nu \Phi - g_{\mu\nu} \nabla^2 \Phi + g_{\mu\nu} \Phi = -8\pi G_N T_{\mu\nu} \tag{2.57}$$

Since any 2d metric is conformally flat we can write this in conformal gauge $ds^2 = -e^{2\omega} du dv$:

$$\begin{cases} -e^{2\omega} \partial_u (e^{-2\omega} \partial_u \Phi) & = 8\pi G_N T_{uu} \\ -e^{2\omega} \partial_v (e^{-2\omega} \partial_v \Phi) & = 8\pi G_N T_{vv} \\ 2\partial_u \partial_v \Phi + e^{2\omega} \Phi & = 16\pi G_N T_{uv} \end{cases} \tag{2.58}$$

These equations together with Eq. (2.15) have an interesting consequence: it is only the dilaton, not the metric, which is sensitive to backreaction in this model. In other words, the matter content only has an effect on the dilaton and not on the geometry.

2.2.2.1 The dilaton solution

It is now possible to construct a general solution for the dilaton starting from Eq. (2.58). We first take the case of the vacuum solutions, largely following [1, 26]. In Poincaré coordinates we have

$$e^{2\omega} = \frac{4}{(U - V)^2} \tag{2.59}$$

such that the general vacuum solution becomes (remember that the Poincaré coordinates are related to other lightcone coordinates through the chiral functions $U(u)$ and $V(v)$)

$$\Phi(u, v) = \frac{a + b(U + V) - \mu UV}{U - V} \tag{2.60}$$

where a, b, μ are integration constants. It is useful to perform dimensional analysis on this result. Since the dilaton is dimensionless and lightcone coordinates have dimensions $[U] = L$, the parameter a will also have the dimension of length. Similarly, b will be dimensionless and μ will have dimension $[\mu] = 1/L = E$. The parameter b actually has no physical meaning and can be set to zero without loss of generality due to the symmetry of AdS_2: AdS_2 has the PSL(2, $\mathbb{R}$) isometry group,

[4] For an explicit calculation see e.g. [13].

or the projective special linear group. This group acts on the Poincaré lightcone coordinates as the Möbius transformations [26]:

$$U \to \frac{\alpha U + \beta}{\gamma U + \delta}, V \to \frac{\alpha V + \beta}{\gamma V + \delta} \tag{2.61}$$

where $\alpha, \beta, \gamma, \delta$ are real parameters which satisfy $\alpha\delta - \beta\gamma = 1$. Recall that a similar result was earlier already obtained as a property of the general solution of Liouville's equation. By choosing $\gamma = 0$ and $\alpha = 1 \Rightarrow \delta = 1$ the dilaton transforms as:

$$\begin{aligned} \Phi &\to \frac{a + b(U + V + 2\beta) - \mu(U + \beta)(V + \beta)}{U + \beta - V - \beta} \\ &= \frac{a + 2b\beta - \mu\beta^2 + b(U + V) - \mu\beta(U + V) - \mu UV}{U - V} \end{aligned} \tag{2.62}$$

We can now choose β such that $b = \mu\beta$ (as a check note that $[\beta] = [U] = L$ and $[\mu] = 1/L$ such that b is indeed dimensionless) and rescale $a \to a + b\beta$ resulting in

$$\Phi \to \frac{a - \mu UV}{U - V}. \tag{2.63}$$

In other words we can always perform a Möbius transformation such that the term in b disappears.

The solution with conformal matter is given by [26]

$$\Phi(u, v) = \frac{a - \mu UV}{U - V} - \frac{8\pi G_N}{U - V}(I_+ + I_-) \tag{2.64}$$

where

$$\begin{aligned} I_+(u, v) &= \int_U^{+\infty} ds(s - U)(s - V)T_{UU}(s) \\ I_-(u, v) &= \int_{-\infty}^{V} ds(s - U)(s - V)T_{VV}(s) \end{aligned} \tag{2.65}$$

2.2.3 The preferred time frame: boundary dynamics

Since every metric solution in JT gravity is a coordinate patch of the AdS_2 manifold, the boundary at $Z = 0$ or $U = V$ is of special interest and will play the role of a holographic boundary [26]. In other words, we will be able to describe the two-dimensional physics of the model using one-dimensional boundary dynamics. This is particularly useful since boundary coordinates in this setup are physical. Formally, this is because the boundary explicitly breaks diffeomorphism gauge invariance [2]. Practically, this will later allow us to use the boundary to define local bulk observables in an invariant way.

Since the boundary is completely in the time direction, such a physical boundary coordinate (which we will call the preferred time coordinate) describes time evolution along the holographic boundary. A possible choice is the proper time t of an observer situated on the holographic boundary, which naturally fits such a description. The next step is now to implement suitable boundary conditions, keeping in mind that this derivation does not rely on the specific choice of preferred time coordinate.

2.2.3.1 Boundary conditions

The first step is to fix the asymptotics of the metric of a bulk solution. This section largely follows [10, 26]. The dynamics of the boundary time coordinate will depend on the energy-momentum flow of the matter sector. It is possible to describe these dynamics relative to some reference frame, for example the Poincaré frame $ds^2 = -4dUdV/(U-V)^2$. In other words, the dynamics are parameterized as a deformation relative to the vacuum solution [10]:

$$ds^2 = -\frac{4dudv}{(u-v)^2} + (\text{subleading as } z \to 0 \text{ or } u \to v) \tag{2.66}$$

expressed in terms of some lightcone coordinates (u, v). On the boundary we have $u = v$ and we can choose the lightcone coordinates such that they are equal to our preferred boundary time coordinate t, and the boundary is then defined as $u = v \equiv t$. We can relate these lightcone coordinates to the Poincaré ones through the chiral functions $U(u)$ and $V(v)$. The $u = v$ boundary should then coincide with the unperturbed boundary in the Poincaré patch $U(u) = V(v)$, such that we can define the dynamical boundary time

$$F(t) \equiv U(t) = V(t) \tag{2.67}$$

in terms of some field F which encodes the relation between the Poincaré time coordinate and the preferred time coordinate. It is possible to derive an equation of motion for this field, meaning that the time coordinate at the boundary will become a dynamical variable, hence the name dynamical boundary time. Note that the physics is independent on the specific choice of preferred time coordinate, since the physical meaning is contained in the relation $F(t)$.

The metric diverges at the boundary, so we introduce a near-boundary cutoff ϵ which moves the boundary inward to

$$u = t + \epsilon, \quad v = t - \epsilon \quad \text{or} \quad z = \epsilon. \tag{2.68}$$

The Poincaré space and time coordinates are defined in terms of the lightcone coordinates as $U = T + Z = F + Z$ and $V = F - Z$. We can write these as

$$F(t) = \frac{1}{2}\left(U(t+\epsilon) + V(t-\epsilon)\right) \tag{2.69}$$

and

$$Z(t) = \frac{1}{2}\left(U(t+\epsilon) - V(t-\epsilon)\right). \tag{2.70}$$

As $z \to 0$, $V(t-\epsilon) = U(t-\epsilon)$ such that

$$\begin{aligned} Z(t) &= \frac{1}{2}\left(U(t+\epsilon) - U(t-\epsilon)\right) \\ &= \epsilon U'(t) \\ &= \epsilon(F'(t) + Z'(t)) \\ &= \epsilon(F'(t) + \epsilon(F''(t) + Z''(t)) \\ &= \epsilon F'(t) + \mathcal{O}(\epsilon^2) \end{aligned} \tag{2.71}$$

The dynamical boundary is then described by $(F(t), Z(t)) = (F(t), \epsilon F'(t))$, where $Z(t)$ is the distance between the dynamical boundary and the unperturbed AdS_2 boundary [10]. In other words, the boundary observer will follow a boundary curve determined completely by the function $F(t)$.

To proceed, we must also specify the asymptotics of the boundary. From Eq. (2.64), it is clear that the dilaton diverges at the boundary of the Poincaré patch. We will impose that the dilaton has the same asymptotics near the dynamical boundary by setting it to some constant, divergent value:

$$\Phi = \frac{a}{2z} \tag{2.72}$$

with additional terms subleading as $z \to 0$. In other words, the dynamical boundary curve follows a fixed value of the dilaton. By substituting Eq. (2.64), we can derive a differential equation for the field F:

$$\begin{aligned} \frac{a}{U-V}\left(1 - \frac{8\pi G_N}{a}\left(I_+ + I_-\right)\right) &= \frac{a}{2z} \\ \Leftrightarrow \frac{1}{Z}\left(1 - \frac{8\pi G_N}{a}\left(I_+ + I_-\right)\right) &= \frac{1}{z} \\ \Leftrightarrow \frac{1}{\epsilon F'(t)}\left(1 - \frac{8\pi G_N}{a}\left(I_+ + I_-\right)\right) &= \frac{1}{\epsilon} \end{aligned} \tag{2.73}$$

For this purpose, we have set $\mu = 0$ in (2.64), since it can be created by the matter in the bulk (this will become apparent in a later example). The equation becomes

$$F'(t) = 1 - \frac{8\pi G_N}{a}\left(\int_{F(t)}^{+\infty} ds (s - F(t))^2 T_{UU}(s) + \int_{-\infty}^{F(t)} ds (s - F(t))^2 T_{VV}(s)\right). \tag{2.74}$$

This result has some interesting consequences. Firstly, it confirms that the field F has physical meaning, as it is dependent on the energy content within the spacetime. This also means that the boundary curve $(F(t), \epsilon F'(t))$ will become a so-called 'wiggly boundary curve'. As the energy contents change in time, the dynamical boundary curve will respond by moving closer and further away from the true holographic boundary. Furthermore, this field is the only degree of freedom in the system and allows us to fully describe the physics in the bulk using this wiggly boundary curve. In other words, the physics is described by the relationship between two clocks: on the one hand the proper time of a boundary observer and on the other hand the Poincaré time acting as a reference time frame. Since $F(t)$ is a time reparameterization, we will want this function to be monotonically increasing as a property of a physically meaningful clock.

2.2.3.2 Example: Energy pulse injected from the boundary

As an illustration of the above principles, consider an energy pulse with energy E shot into the Poincaré patch at time $T = 0$ from the boundary, following [26]. This can be modeled as

$$T_{VV}(V) = E\delta(V) \tag{2.75}$$

with all other components of $T_{\mu\nu} = 0$. This setup can be seen in Fig. (2.3). Looking at Eq. (2.65), this leads to $I_+ = 0$ and

$$\begin{aligned} I_- &= E\int_{-\infty}^{V} ds(s-U)(s-V)\delta(s) \\ &= \begin{cases} 0 & \text{if } V < 0, \\ EUV & \text{if } V \geq 0 \end{cases} \\ &= EUV\theta(V). \end{aligned} \tag{2.76}$$

Plugging this into Eq. (2.64) (again setting a priori $\mu = 0$), we get

$$\Phi = \frac{a - 8\pi G_N EUV\theta(V)}{U - V}. \tag{2.77}$$

Before the energy pulse has passed ($V < 0$, light blue area in Fig. (2.3)), we can identify the dilaton $\Phi = a/(U - V)$ with the vacuum solution Eq. (2.63) where $\mu = 0$. After the pulse has been injected ($V \geq 0$, dark blue area in Fig. (2.3)), the dilaton takes the form of Eq. (2.63) with $\mu = 8\pi G_N E$, such that we can interpret μ in terms of the total energy in the spacetime. In other words, the parameter μ can be created by matter.

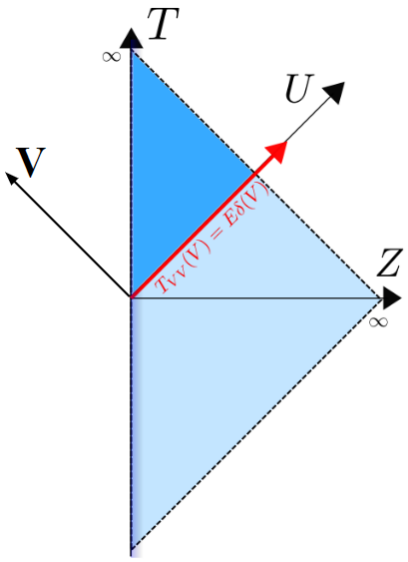

Fig. 2.3: Penrose diagram of AdS_2 in the Poincaré patch. An energy pulse is shot in from the boundary at time $T = 0$. In the dark blue region the dilaton has $\mu \neq 0$. Figure adapted from [26].

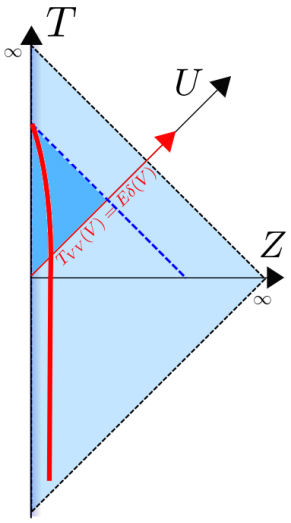

Fig. 2.4: Penrose diagram of AdS_2 in the Poincaré patch. The red line is the dynamical boundary curve, which bends towards the horizon due to the energy injection. A black hole horizon appears with the black hole patch indicated in dark blue. Figure adapted from [26].

Proceeding similarly for the field $F(t)$, we get

$$\begin{aligned} F' &= 1 - \frac{8\pi G_N E}{a} \int_{-\infty}^{F} ds (s-F)^2 \delta(s) \\ &= 1 - \frac{8\pi G_N E}{a} F^2 \theta(F) \\ &= \begin{cases} 1 & \text{if } F < 0, \\ 1 - \frac{\mu}{a} F^2 & \text{if } F > 0. \end{cases} \end{aligned} \tag{2.78}$$

Before the energy pulse has been injected, we simply have $F(t) = t$, such that the preferred time coordinate takes the form of the Poincaré time. After the injection, the differential equation solves to

$$\begin{aligned} F(t) &= \sqrt{\frac{a}{\mu}} \tanh \sqrt{\frac{\mu}{a}} t = \frac{\beta}{\pi} \tanh \frac{\pi}{\beta} t \\ Z(t) &= \epsilon F'(t) = \frac{\epsilon}{\cosh^2 \sqrt{\frac{\mu}{a}} t}. \end{aligned} \tag{2.79}$$

By taking the boundary limit ($U = V = F$, $u = v = t$) of Eq. (2.24), we can see that the above expression is exactly the boundary limit of the black hole patch of AdS_2 where $\sqrt{\mu/a} = \pi/\beta$. This relates the parameter μ to the temperature, and in turn the mass, of a black hole. The Poincaré vacuum is now described in the black hole frame

[8] and we call this field F the (classical) thermal boundary reparameterization[5]. The connection with the black hole patch can also be explained starting from the observation that $Z(t) \to 0$ as $t \to \infty$, at which point the Poincaré time is still finite: $F = \beta/\pi$, since the black hole patch is contained completely within the Poincaré patch (note also again the $\beta \to \infty$ limit connecting the two). As illustrated in Fig. (2.4), a black hole horizon has appeared where the boundary curve meets the true boundary, and we have essentially created an AdS_2 black hole. This acts as the future horizon of the black hole patch. This example also nicely shows the holographic nature of this model, as the entire physics in the bulk are described solely by the field $F(t)$ defined at the boundary.

2.2.3.3 The Schwarzian action

In Section 2.3, a path integral formalism is used to introduce quantum gravity into the JT model. To this end, we need an action to describe the boundary dynamics, as described in [26]. The differential equation (2.74) can be written in a more tractable form using the Schwarzian derivative:

$$\{F, t\} \equiv \frac{F'''}{F'} - \frac{3}{2}\left(\frac{F''}{F'}\right)^2 . \tag{2.80}$$

Additionally, the holographic stress tensor, which represents the total energy contained in the spacetime at time t, can be written as

$$E(t) = -\frac{a}{16\pi G_N}\{F, t\} . \tag{2.81}$$

The prefactor $\frac{16\pi G_N}{a}$ plays the role of the gravitational coupling constant and we define

$$C \equiv \frac{a}{16\pi G_N}. \tag{2.82}$$

The limit $C \to \infty$ corresponds to "freezing" gravity [26], as $G_N \to 0$. Later on in the quantum gravity treatment, taking the $C \to \infty$ limit will bring us back to the semi-classical regime of the gravitational saddle. Using these relations, it can be shown that Eq. (2.74) can be written as

$$\frac{dE(t)}{dt} = -C\frac{d}{dt}\{F, t\} = (T_{VV}(t) - T_{UU}(t))F'^2|_{\partial\mathcal{M}}. \tag{2.83}$$

As an interpretation of this result, the right hand side is the net influx of matter from the holographic boundary. In other words, this again confirms that the time reparameterization $F(t)$ and thus the wiggly boundary curve reacts explicitly to the energy inserted into the spacetime through the boundary. This was already seen in the example in Section 2.2.3.2. More specifically, we know that an influx

[5] Classical because we are on the gravitational saddle $f(t) = t$, as will become apparent later.

of positive energy causes the dynamical boundary curve to bend closer towards the true boundary [26].

The Schwarzian action is then defined as

$$S = -C \int dt \, \{F, t\} \, . \tag{2.84}$$

Using

$$\delta \{F, t\} = \frac{\partial \{F, t\}}{\partial F} \delta F = \frac{\partial \{F, t\}}{\partial t} \frac{\partial t}{\partial F} \delta F = \frac{\{F, t\}'}{F'} \delta F \tag{2.85}$$

it can be shown that variation of this action will lead to the equation of motion for the field F in the absence of matter injections:

$$\frac{d}{dt} \{F, t\} = 0. \tag{2.86}$$

2.2.3.4 Nearly AdS/CFT

Before moving on we take an aside to specify the holographic dictionary of JT gravity. There is a subtlety here, as AdS_2/CFT_1 is a notoriously tricky holographic dictionary to make sense of [26]. Namely, for a perfect AdS_2, the dual boundary field theory (CFT_1) has a stress tensor which is zero, such that the theory can only describe ground states [21]. This follows directly from the fact that the energy-stress tensor is traceless for a CFT due to scaling symmetry. Since in 0+1d there is only one component, we find $T_{tt} = 0$.

Thus, if we want to describe excitations, we need to step away from the pure AdS_2/CFT_1. As it turns out, this has already been accomplished in the previous sections through the choice of boundary condition (2.72) [26]. Recall that implementing this boundary condition led to a differential equation for the field F, in essence providing a fixed and preferred boundary time frame [26]. As such, the conformal symmetry of the boundary theory has already been broken, leading to a "nearly" CFT_1. More subtly, AdS_2 has also been deformed to nearly AdS_2 by the dilaton asymptotics (2.72). As such, the holographic dictionary for JT gravity is in fact nearly AdS_2/ nearly CFT_1 or NAdS$_2$/NCFT$_1$.

2.2.4 Euclidean perspective and the JT disk theory

The boundary dynamics can also be discussed from the Euclidean perspective, starting from the action (2.14). In this case, the boundary curve is parameterized

as $(F(\tau), \epsilon Z(\tau))$ where $\tau = it$ is the Wick-rotated preferred time coordinate. The Euclidean version of the Schwarzian action is then simply

$$I_{JT} = -C \int d\tau \{F(\tau), \tau\}, \tag{2.87}$$

where again the field $F(\tau)$ is the only dynamical degree of freedom, sufficient for explaining all the physics in the model.

The choice of reference frame is not binding, since it is only the relation between the reference frame and the preferred time coordinate which carries meaning. More concretely, instead of choosing the Poincaré time we can choose some other reference frame. In the case of the thermal system which has been discussed so far, i.e. a black hole with inverse temperature β, it is more natural to define the reparameterization [26]

$$F(\tau) \equiv \tan \frac{\pi}{\beta} f(\tau), \tag{2.88}$$

where the physics is now described in terms of the field $f(\tau)$. Since $f(\tau)$ is a time reparameterization we require again $f'(\tau) \geq 0$, and we now have the additional periodicity requirement

$$f(\tau + \beta) = f(\tau) + \beta \tag{2.89}$$

to ensure that $F(\tau+\beta) = F(\tau)$. This new field f is thus a time reparameterization of the boundary thermal circle: the circle with circumference β around which Euclidean time revolves. In other words, f belongs to the set of diffeomorphisms of the circle: $f \in \text{Diff}(S^1)$, i.e. the set of all maps between circles where the maps are both differentiable and have a differentiable inverse. This can simply be seen as the set of well-behaved clocks in imaginary time. Using this field to solve the equation of motion for the thermal system starting from the Euclidean action

$$I_{JT} = -C \int d\tau \{\tan \frac{\pi}{\beta} f, \tau\} \tag{2.90}$$

results in the unique classical solution [26]:

$$f(\tau) = \tau \quad \Rightarrow \quad F(\tau) = \tan \frac{\pi}{\beta} \tau, \tag{2.91}$$

which we will refer to as the gravitational saddle[6]. We can check this result by verifying that it is indeed the Wick-rotated black hole solution from before:

$$F(t) = \tanh \frac{\pi}{\beta} t, \tag{2.92}$$

[6] In contrast to the full quantum gravity theory, which involves a path integral over the field f. In other words the backreaction will move the location of the gravitational saddle.

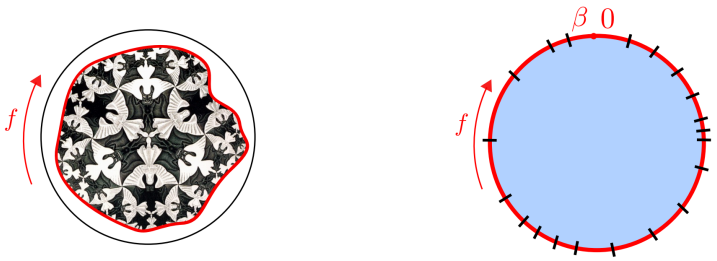

Fig. 2.5: Left: In red the wiggly boundary curve as the boundary of the Poincaré disk, represented by the tiled surface. Right: Ticking of the f clock along the thermal circle. Figure taken from [26].

where we have omitted the prefactor (which is not observable due to the gauge isometry group [26]). More generally the reparameterization (2.88) is simply the Wick rotated version of the real-time thermal reparameterization:

$$F(t) = \tanh \frac{\pi}{\beta} f(t) \xrightarrow{\text{Wick rotation}} F(\tau) = \tan \frac{\pi}{\beta} f(\tau). \tag{2.93}$$

Which is apparent from $F \to -iF$, $f \to -if$ and $\tanh -ix = -i \tan x$.

In terms of the field $f(\tau)$, the wiggly boundary curve can now be depicted on the Poincaré disk, a two-dimensional hyperbolic geometry contained within the thermal circle. The boundary curve is the effective boundary of the Poincaré disk and $Z(\tau) = \epsilon F'(\tau)$ determines the distance from the true boundary, which is the thermal circle. The reparameterization $f(\tau)$ determines the ticking of a clock along this circle, i.e. the spacing between consecutive ticks of the f time coordinate. These two perspectives are illustrated in Fig. (2.5). Keep in mind that, due to Eq. (2.89), the number of ticks along one full rotation (i.e. τ going from $\tau_0 \to \tau_0 + \beta$) is fixed, and it is only their spacing which can vary. In fact it is exactly this stretching and compressing along the circle which defines maps belonging to $\mathrm{Diff}(S^1)$.

In summary, since $f(\tau)$ is governed by a Schwarzian action, we can say that the JT disk theory is dual to a Schwarzian field theory on the boundary [2], again highlighting the holographic nature of the JT gravity model.

2.2.5 Bulk frames

The field $F(t)$, which relates the proper time t of an observer on the wiggly boundary curve to the Poincaré time T, offers a solution to the ambiguity of the physics of the different coordinate patches by fixing a certain patch in terms of the preferred boundary time coordinate t. We can extend this notion to define the bulk metric in a boundary-intrinsic way, making use of the physicality of the boundary to ensure that this definition is diffeomorphism invariant. Furthermore, this definition of a

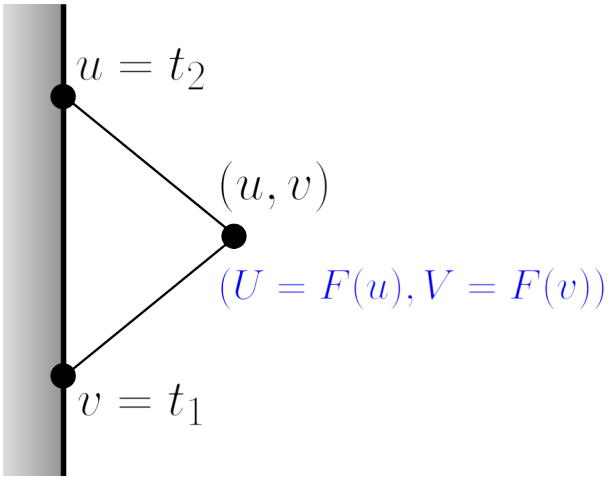

Fig. 2.6: Radar definition of a bulk point, anchored to the holographic boundary.

bulk frame will allow us to define observables located in the bulk, such as two-point functions, in an invariant way. This will become important in later sections.

There are many possible ways to construct a suitable bulk frame. One possibility is for an observer on the boundary to construct a bulk frame using outgoing and ingoing lightrays, following [2]. First, They shoot out a light ray from the boundary at their proper time t_1. The light ray is reflected by an imaginary mirror situated at some point in the bulk and arrives back at the boundary when the observer's proper time is t_2. The lightcone coordinates of that point are then defined as $(u = t_2, v = t_1)$ with $v = t - z$ and $u = t + z$. This procedure is entirely physical and should thus produce identical results when viewed from the Poincaré frame. From this perspective, a light ray is sent out from the boundary at Poincaré time T_1, is reflected at the mirror and reaches the boundary again at time T_2. The bulk point where the mirror is situated is assigned the Poincaré coordinates $(U = T_2, V = T_2)$ with again $V = T - Z$ and $U = T + Z$. Since the physical field F relates the boundary observer's proper time to the Poincaré time, it also relates the new bulk coordinates (u, v) to the Poincaré coordinates (U, V):

$$U = F(u), \qquad V = F(v). \tag{2.94}$$

This way of constructing bulk points is the so-called radar definition and can be seen in Fig. (2.6).

Starting from the Poincaré metric, this mapping leads to a metric of the form

$$ds^2 = -\frac{4\partial_u U(u)\partial_v V(v) du dv}{(U(u) - V(v))^2} = \frac{\dot{F}(u)\dot{F}(v)}{(F(u) - F(v))^2}(dz^2 - dt^2). \tag{2.95}$$

The conformal scaling factor is dependent on the field F, which has physical meaning. Thus, the earlier procedure of setting up suitable boundary conditions, leading to a differential equation for F, has fixed the form of the metric. Considering for example the thermal boundary reparameterization $F(t) = \tanh \frac{\pi}{\beta} t$, we find that the bulk metric takes the form of the black hole patch of AdS_2:

$$ds^2 = \frac{4\pi^2}{\beta^2} \frac{dz^2 - dt^2}{\sinh^2(\frac{2\pi}{\beta} z)} \tag{2.96}$$

showing that this specific field F describes the physics near the horizon of a higher dimensional near-extremal black hole with inverse temperature β.

It is important to note that, as it stands, this definition of bulk points can only be used to define points within a certain region of the AdS_2 spacetime. For the case where the bulk metric is that of the black hole patch, only this patch itself and thus the exterior of the black hole is accessible. Since the Poincaré coordinates reach further, it isn't implausible to try to extend or generalise this definition to be able to reach points outside of this patch. In fact, doing so would allow for a diff-invariant way of defining points which lie beyond the black hole horizon. This idea is further explored in Chapter 3.

2.3 Correlators in JT gravity

It is now possible to extend the classical JT gravity model to a quantum gravity model using the path integral formulation of quantum mechanics. As it turns out, JT gravity allows for exact calculations of quantum gravity expectation values of observables and it is thus possible to construct exact matter correlators.

2.3.1 Schwarzian path integral formalism

Reformulating the dynamics of JT gravity in terms of the boundary field F has the attractive property that it makes the quantum-gravity theory of the model more tractable. To see this, we start from the partition function of the thermal system with inverse temperature β [26]:

$$\begin{aligned} Z(\beta) &= e^{S_0} \int [\mathcal{D}g][\mathcal{D}\Phi] e^{-I_{JT}} \\ &= e^{S_0} \int [\mathcal{D}g][\mathcal{D}\Phi] \exp\left(\frac{1}{16\pi G_N} \left[\int_{\mathcal{M}} \sqrt{g}\Phi(R+2) + 2 \oint_{\partial\mathcal{M}} \sqrt{h}\Phi(K-1) \right] \right) \end{aligned} \tag{2.97}$$

This expression is a quantum gravitational path integral over the metric and the dilaton in Euclidean signature. Since this theory is dual to the Schwarzian theory on the boundary, we can reduce this double path integral to a path integral solely over the time reparameterization f:

$$Z(\beta) = e^{S_0} \int_{\mathrm{Diff}(S^1)/\mathrm{SL}(2,\mathbb{R})} [\mathcal{D}f] e^{C \int_0^\beta d\tau \{\tan \frac{\pi}{\beta} f(\tau), \tau\}}. \tag{2.98}$$

Note how the integral covers $\mathrm{Diff}(S^1)$ modulo $\mathrm{SL}(2,\mathbb{R})$. As discussed before, $\mathrm{Diff}(S^1)$ is the set of all "well-behaved" clocks or time reparameterizations. Furthermore, the solutions $f(\tau)$ have an $\mathrm{SL}(2,\mathbb{R})$ gauge freedom, which acts on F according to Eq. (2.61). As such, we can restrict the path integral to only cover fields f specified up to such transformations, thus avoiding double-counting physically identical solutions. This partition function will later also be referred to as $Z_{\mathrm{SL}(2,\mathbb{R})}$, and turns out to be one-loop exact [31]:

$$Z(\beta) = \left(\frac{2\pi C}{\beta}\right)^{3/2} e^{\frac{2\pi^2 C}{\beta}}. \tag{2.99}$$

Where here, and moving forward, we have neglected the factor e^{S_0}. Recall that S_0 is in fact related to the constant part of the dilaton Φ_0 [26]. For our purposes however, this prefactor is not of significant importance. This result can in turn be written as an energy integral

$$Z(\beta) = \int_0^\infty \sinh(2\pi\sqrt{2CE}) e^{-\beta E} dE, \tag{2.100}$$

where

$$\rho(E) = \sinh 2\pi\sqrt{2CE} \tag{2.101}$$

is then interpreted as a density of states[7] and is often called the Schwarzian density of states.

2.3.2 Matter fields and correlators

The goal is now to couple quantum JT gravity to matter fields. As before the matter sector is taken to not explicitly depend on the dilaton. In general we can couple JT gravity to scalar fields ϕ_i with mass m, whose action is given by:

$$S_{\mathrm{mat}}[\phi, g] = \frac{1}{2} \int d^2x \sqrt{-g} [g^{\mu\nu} \partial_\mu \phi \partial_\nu \phi + m^2 \phi^2] \tag{2.102}$$

As a first step it is relevant to review the holographic dictionary for these matter fields. As described in [15], according to the GKPW dictionary of $\mathrm{AdS}_{d+1}/\mathrm{CFT}_d$,

[7] There is a subtlety to this interpretation. See [31] for details.

there exists a duality between massive bulk fields ϕ_i and boundary CFT operators $\mathcal{O}_i$:

$$Z_{\text{grav}}[\phi_i(x), \partial\mathcal{M}] = \left\langle \exp\left(-\sum_i \int d^d x \phi_i(x)\mathcal{O}_i(x)\right)\right\rangle_{\text{CFT on } \partial\mathcal{M}} = Z_{\text{CFT}}[\phi], \tag{2.103}$$

such that each field in gravity corresponds to a local operator in the boundary CFT. The left hand side is the gravitational partition function and the right hand side is the generating functional for CFT correlation functions, where the bulk fields ϕ_i take the role of sources for the operators $\mathcal{O}_i$. The mass m of the bulk fields[8] is related to the scaling dimension or weight Δ of the boundary dual operators through $\Delta = d/2 + \sqrt{d/4 + m^2}$ or $m^2 = \Delta(d - \Delta)$. The scaling dimension determines how a CFT operator behaves under coordinate rescalings: $\langle \mathcal{O}_\Delta(x)\rangle_{CFT} = \lambda^\Delta \langle \mathcal{O}_\Delta(\lambda x)\rangle_{CFT}$. For the present case of AdS_2/CFT_1, we get $\Delta = 1/2 + \sqrt{1/4 + m^2}$. In the Euclidean picture, these operators are located on the thermal circle, $\mathcal{O}_\Delta(\tau)$, as can be seen in Fig. (2.7).
Given scalar fields ϕ_i, the n-point correlation function is the time-ordered vacuum expectation value of the field operators:

$$\langle \phi_1 \dots \phi_n \rangle = \langle 0|\mathcal{T}(\phi_1 \dots \phi_n)|0\rangle\,. \tag{2.104}$$

Alternatively, the CFT correlator can be obtained from the generating functional $Z_{CFT}[\phi]$ by taking consecutive functional derivatives with respect to the matter fields:

$$\langle \mathcal{O}_1(x_1) \dots \mathcal{O}_n(x_n)\rangle_{\text{CFT}} \sim \frac{\delta}{\delta\phi_1(x_1)} \dots \frac{\delta}{\delta\phi_n(x_n)} Z_{\text{CFT}}[\phi]|_{\phi_i=0}. \tag{2.105}$$

$Z_{CFT}[\phi]$ is a path integral, and the correlator itself can also be written as a path integral. In general, in the path integral formulation for a theory with action S, the (normalized) thermal n-point correlation function of the variables $x(\tau)$ is given by [19]:

$$\langle x(\tau_1)x(\tau_2)\dots x(\tau_n)\rangle = Z^{-1}\int [\mathcal{D}x] x(\tau_1)x(\tau_2)\dots x(\tau_n)e^{-I}. \tag{2.106}$$

2.3.3 Boundary two-point functions

The first step is now to calculate the quantum gravity two-point function of these boundary operators. This section follows in large parts [26] and [2]. Taking for

[8] For simplicity we take the fields to all have the same mass, in full generality the field ϕ_i has mass m_i and the corresponding operator $\mathcal{O}_i$ has weight Δ_i.

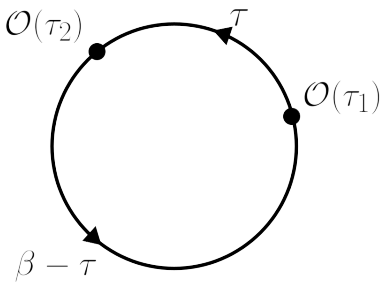

Fig. 2.7: Boundary dual CFT operators on the thermal circle. The operators are separated by Euclidean time $\tau = \tau_2 - \tau_1$ on one side and $\beta - \tau$ on the other side.

example the 2d CFT matter sector $S_{mat}[\phi, g]$ (or equivalently $S_{mat}[\phi, f]$), the matter two-point function is given by [2]:

$$\begin{aligned} \langle \phi_1 \phi_2 \rangle_{\text{mat}} &= Z_{\text{mat}}^{-1} \int [\mathcal{D}\phi] \phi_1 \phi_2 e^{-I_{\text{mat}}[\phi, g]} \\ &= \langle \mathcal{O}_\Delta(\tau_1) \mathcal{O}_\Delta(\tau_2) \rangle_{\text{CFT}} \,, \end{aligned} \tag{2.107}$$

where the last line relates the matter correlation function of the bulk fields to the CFT correlation function of the dual operators. The normalization is the matter sector partition function

$$Z_{\text{mat}}[f] = \int [\mathcal{D}\phi] e^{-I_{\text{mat}}[\phi, f]}. \tag{2.108}$$

In order to quantize this result we should now insert this into the Schwarzian path integral:

$$\langle \phi_1 \phi_2 \rangle = \int [\mathcal{D}f] \left(Z_{\text{mat}}^{-1} \int [\mathcal{D}\phi] \phi_1 \phi_2 e^{-I_{\text{mat}}[\phi, f]} \right) e^{-I[f]} \tag{2.109}$$

or, in terms of the boundary dual operators:

$$\langle \mathcal{O}_\Delta(\tau_1) \mathcal{O}_\Delta(\tau_2) \rangle = \int [\mathcal{D}f] \, \langle \mathcal{O}_\Delta(\tau_1) \mathcal{O}_\Delta(\tau_2) \rangle_{\text{CFT}} \, e^{-I[f]}. \tag{2.110}$$

The CFT two-point function for operators of weight Δ is a known result:

$$\begin{aligned} \langle \mathcal{O}_\Delta(\tau_1) \mathcal{O}_\Delta(\tau_2) \rangle_{\text{CFT}} &= \left(\frac{F'(\tau_1) F'(\tau_2)}{(F(\tau_1) - F(\tau_2))^2} \right)^\Delta \\ &= \left(\frac{f'(\tau_1) f'(\tau_2)}{\frac{\beta^2}{\pi^2} \sin^2 \frac{\pi}{\beta} (f(\tau_1) - f(\tau_2))} \right)^\Delta \\ &= G_\Delta(\tau_1, \tau_2) \end{aligned} \tag{2.111}$$

for a field of weight Δ, where again the (Euclidean time) thermal reparameterization $F(\tau) = \tan \frac{\pi}{\beta} f(\tau)$ was used. This operator $G_\Delta(\tau_1, \tau_2)$ is called the Schwarzian bilocal operator of weight Δ and is, like the field f itself, invariant under $\text{SL}(2, \mathbb{R})$ [26]. The bilocal can be interpreted as a matter source being inserted at τ_1 and reabsorbed

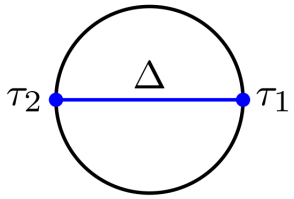

Fig. 2.8: Diagrammatic representation of the two-point function of boundary dual operators with weight Δ. Matter insertions are located at τ_1 and τ_2, the insertion of the Schwarzian bilocal is represented by the line going through the bulk. Figure from [26].

at τ_2. The symmetry in this interpretation is necessitated by the periodicity of the thermal circle, as the situation after the insertion at τ_2 needs to be identical to that before the insertion at τ_1 (see e.g. Fig. (2.8)). The two-point function of the boundary dual operators is then just the Schwarzian expectation value with the Schwarzian bilocal as an operator insertion:

$$\begin{aligned}\langle \mathcal{O}_\Delta(\tau_1)\mathcal{O}_\Delta(\tau_2)\rangle &= \langle G_\Delta(\tau_1,\tau_2)\rangle_{\text{Sch}} \\ &= \int [\mathcal{D}f] G_\Delta(\tau_1,\tau_2) e^{C\int_0^\beta \{\tan\frac{\pi}{\beta}f,\tau\}},\end{aligned} \tag{2.112}$$

which can be represented by the diagram in Fig. (2.8). It is insightful to recall that this operator insertion in the path integral is itself the result of a path integral, namely one over the matter/CFT sector. Similar to Eq. (2.105) for the CFT correlator, we can also write the full quantum gravity correlator as the functional derivative of a generating functional [26]:

$$\langle \mathcal{O}(\tau_1)\dots\mathcal{O}(\tau_n)\rangle = \frac{\delta}{\delta\phi(\tau_1)}\dots\frac{\delta}{\delta\phi(\tau_n)} Z(\beta,\phi)|_{\phi=0} \tag{2.113}$$

where now

$$Z(\beta,\phi) = e^{S_0}\int [\mathcal{D}f] e^{\frac{1}{2}\int d\tau_1 d\tau_2 \left(\frac{f'(\tau_1)f'(\tau_2)}{\frac{\beta^2}{\pi^2}\sin^2\frac{\pi}{\beta}[f(\tau_1)-f(\tau_2)]}\right)^\Delta \phi(\tau_1)\phi(\tau_2)} e^{-I_{\text{Sch}}[f]}. \tag{2.114}$$

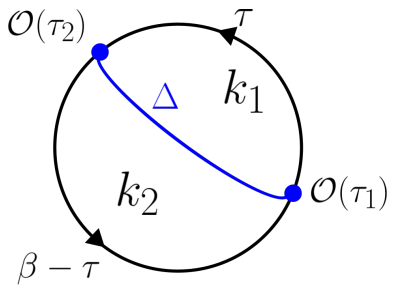

Fig. 2.9: Diagrammatic representation of the two-point function for dual operators with weight Δ with $\tau \equiv \tau_2 - \tau_1$. The energy insertions $E = k^2/2C$ are explicitly written and determine the time evolution operator for that sector.

2.3.3.1 Exact two-point function solution

The (normalized) two-point function has a closed form exact solution [24, 26] [9][10]

$$\langle \mathcal{O}_\Delta(\tau_1)\mathcal{O}_\Delta(\tau_2)\rangle = Z^{-1}(\beta)\int_0^\infty \prod_{i=1,2}(dk_i^2 \sinh 2\pi k_i) e^{-\tau\frac{k_1^2}{2C}} e^{-(\beta-\tau)\frac{k_2^2}{2C}} \frac{\Gamma(\Delta \pm ik_1 \pm ik_2)}{2\pi^2(2C)^{2\Delta}\Gamma(2\Delta)} \tag{2.115}$$

Here $\tau = |\tau_1 - \tau_2|$, and the partition function is given by Eq. (2.99). The two-point function is a double integral over k_1 and k_2 which, from a group theoretical perspective, are intermediate $\mathrm{SL}(2,\mathbb{R})$ labels [27]. We can relate them to intermediate energies $E = k^2/2C$, with the measure $d\mu(k) = 2k\sinh(2\pi k)dk$ representing the Schwarzian density of states, cf. Eq. (2.101). The exponential factors ensure that the integrals do not diverge and are most easily interpreted by looking at Fig. (2.9), associating an energy $k_1^2/2C$ with the operator insertion $\mathcal{O}(\tau_1)$ and $k_2^2/2C$ with $\mathcal{O}(\tau_2)$, and thus dividing the thermal circle into two propagators. After the first insertion, the intermediate energy eigenstate with energy $k_1^2/2C$ is propagated along an imaginary time span τ, until it reaches the second insertion. The factor $e^{-\tau\frac{k_1^2}{2C}}$ is then simply the familiar Schrödinger picture time evolution operator for this sector. After the second insertion, the propagation covers the other part of the thermal circle, i.e. $(\beta - \tau)$, which in turn explains the factor $e^{-(\beta-\tau)\frac{k_2^2}{2C}}$.
The gamma functions make use of the notation convention where $\pm$ denotes a product of all possible combinations[11]. These factors represent the "interaction" between the bilocal operator and the energy eigenstates. More formally they originate from the matrix element of each endpoint of the bilocal operator between the two energy eigenstates [20]. Diagrammatically this occurs where the line of the bilocal operator insertion meets the thermal circle.

[9] There is a slight variation in convention here: sometimes a factor $1/4\pi^2$ is included in the partition function (such as in [26]), in which case (2.115) has $8\pi^4$ in the denominator.
[10] For a collection of a few possible derivations of this result, see [26].
[11] i.e. $\Gamma(\Delta \pm ik_1 \pm ik_2) = \Gamma(\Delta + ik_1 + ik_2)\Gamma(\Delta + ik_1 - ik_2)\Gamma(\Delta - ik_1 + ik_2)\Gamma(\Delta - ik_1 - ik_2)$.

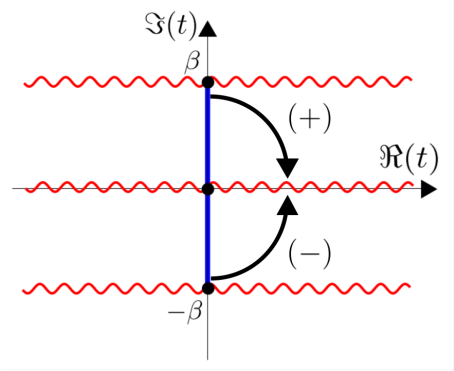

Fig. 2.10: Wick rotation of the Euclidean correlator to real-time. The complex t-plane has Euclidean time on the imaginary axis and real-time on the real axis. The red squiggly lines are the branch cuts of the correlator. The two non-equivalent rotations are labeled $(+)$ and $(-)$. Figure adapted from [26].

Taking the $C \to \infty$ limit corresponds to the semi-classical regime, i.e. quantum matter in classical gravity, which in the case of light operators ($\Delta \sim 1$) is the same as taking the gravitational saddle $f(t) = t$ [26].

Following [26], it is possible to write the result Eq. (2.115) in terms of the Lorentzian time t, but this Wick rotation requires special care. We can see that, along the imaginary time axis, the two-point function has singularities at $\tau = 0$ and $\tau = \beta$, since there the k_i integrals no longer have damping. We extend our focus to the complex t plane, where then $\text{Im}(t) = -\tau$. The singularities at $\tau \to 0, \beta$ are extended to branch cuts, parallel to the real-t axis. Furthermore, these branch cuts appear periodically at $\text{Im}(t) = n\beta$. In other words, there is a branch cut on the real axis, such that we have to specify if we approach the real axis from above $(+)$ or below $(-)$ when performing the Wick rotation, as can be seen in Fig. (2.10) This choice corresponds to taking different time orderings of the two operators: $G_+ = \langle \mathcal{O}(t_1)\mathcal{O}(t_2)\rangle$ and $G_- = \langle \mathcal{O}(t_2)\mathcal{O}(t_1)\rangle$, which are each others complex conjugate. They are given by

$$G_\pm = \int_0^\infty \prod_{i=1,2} \left(dk_i^2 \sinh 2\pi k_i \right) e^{\mp it\frac{k_1^2}{2C} - (\beta \mp it)\frac{k_2^2}{2C}} e^{-\epsilon\frac{k_1^2}{2C} - \epsilon\frac{k_2^2}{2C}} \frac{\Gamma\left(\Delta \pm ik_1 \pm ik_2\right)}{8\pi^4 (2C)^{2\Delta}\Gamma(2\Delta)}, \tag{2.116}$$

where ϵ is a Euclidean regulator. Semi-classically, the differently ordered correlators differ only with an infinitesimal imaginary part $\pm i\varepsilon$, whereas the quantum gravity correlators have a finite imaginary part and are thus inequivalent beyond infinitesimals [26]. This trend of time orderings being equivalent in the semi-classical regime but inequivalent in the full quantum gravity picture appears again in Section 2.4 and in Chapter 3.

2.3.4 Bulk two point functions

Equipped with the invariant definition of bulk frames described in Sec. (2.2.5) and the knowledge on how to calculate boundary two-point functions, it is possible to define two-point functions between matter operators $\mathcal{O}(U = F(u), V = F(v))$ located in the bulk. This approach is laid out in [2], and as such this section mostly follows this work. For the remainder of this section we will consider massless scalar fields ϕ such that $\Delta = 1$. The CFT two-point function for these bulk fields is now the relevant operator to be inserted into the Schwarzian path integral in order to obtain the full quantum gravity two-point function:

$$\langle \phi(u_1, v_1)\phi(u_2, v_2)\rangle = \int [\mathcal{D}f]\, \langle \phi(u_1, v_1)\phi(u_2, v_2)\rangle_{\text{CFT}}\, e^{C\int_0^\beta d\tau \left\{\tan\frac{\pi}{\beta}f,\tau\right\}}. \tag{2.117}$$

The CFT bulk two-point function can be determined following a brief derivation[12]. A 2d CFT massless scalar field ϕ in flat space has the action

$$S = \frac{1}{2}\int d^2x \partial_\mu\phi\partial^\mu\phi, \tag{2.118}$$

such that the CFT two-point function for ϕ is then given by [5, 12][13]:

$$\langle \phi(\mathbf{x_1})\phi(\mathbf{x_2})\rangle_{\text{CFT}} = -\frac{1}{4\pi}\ln|\mathbf{x_1} - \mathbf{x_2}|. \tag{2.119}$$

The first question is now whether this result is applicable to AdS_2 as opposed to Minkowski space. For a general metric $g_{\mu\nu}$ we have the action

$$S = \int d^2x\sqrt{-g}g^{\mu\nu}\partial_\mu\phi\partial_\nu\phi \tag{2.120}$$

Now we again make use of the fact that in 2d, it is always possible to write a metric in conformal gauge $ds^2 = e^{\omega(x,y)}(-dt^2 + dx^2)$, such that

$$g_{\mu\nu} = \begin{bmatrix} -e^\omega & 0 \\ 0 & e^\omega \end{bmatrix}. \tag{2.121}$$

From this it follows that $\sqrt{-g} = e^\omega$ and $g^{tt} = g^{xx} = e^{-\omega}$. These factors cancel each other out, such that the action (2.120) is independent of the conformal scaling factor. Thus, the result (2.119) is also valid for any patch of AdS_2 and thus any metric solution of JT gravity. The next step is to consider the boundary of our AdS_2 spacetime. For this, Dirichlet boundary conditions are implemented using a

[12] The outline of which follows a personal communication with Prof. Dr. Thomas G. Mertens.

[13] Note that there are different conventions for the normalisation of the action and subsequently the two-point function. In [12], for example, a prefactor $1/8\pi$ in the action is used, while in [5] the action has a prefactor $g/4\pi$, leading to a prefactor of $1/2g$ for the two-point function. From this it can be seen that indeed for the $1/2$ normalisation here the $1/4\pi$ prefactor follows.

method analogous to the image charge method from electrostatics, where the image "charges" are placed opposite the real "charges" on the other side of the holographic boundary. We can introduce the complex coordinates z with the imaginary axis perpendicular to the boundary, such that the z coordinate of an image charge is the complex conjugate of the corresponding real charge. More specifically, we can define the z coordinates such that the imaginary z axis aligns with the Poincaré Z axis and the real z axis with the Poincaré T axis. This setup can be seen in Fig. (2.11). We can then write the fields in terms of these coordinates $\phi(z, \overline{z})$, since z and $\overline{z}$ can be treated as independent variables. The two-point function in complex coordinates takes the form [12]

$$\langle \phi(z_1, \overline{z}_1)\phi(z_2, \overline{z}_2)\rangle_{\text{CFT}} = -\frac{1}{4\pi}\left(\ln|z_1 - z_2| + \ln|\overline{z}_1 - \overline{z}_2|\right) \tag{2.122}$$

Taking into account the image charges, the two-point function now gets additional terms of this form corresponding to the interaction between the image charges and the real charges belonging to the other field. These terms get a relative minus sign, leading to:

$$\begin{aligned}\langle \phi(z_1, \overline{z}_1)\phi(z_2, \overline{z}_2)\rangle_{\text{CFT}} &= -\frac{1}{4\pi}\left(\ln|z_1 - z_2| - \ln|z_1 - \overline{z}_2|\right. \\ &\qquad \left. + \ln|\overline{z}_1 - \overline{z}_2| - \ln|z_2 - \overline{z}_1|\right) \\ &= -\frac{1}{4\pi}\ln\left|\frac{(z_1 - z_2)(\overline{z}_1 - \overline{z}_2)}{(z_1 - \overline{z}_2)(z_2 - \overline{z}_1)}\right|\end{aligned} \tag{2.123}$$

Relating this back to the Poincaré coordinates $(U = F(u), V = F(v))$ through $z = T + iZ \to U = T + Z$ and $\overline{z} = T - iZ \to V = T - Z$, the CFT bulk two-point function is then given by

$$\langle \phi(u_1, v_1)\phi(u_2, v_2)\rangle_{\text{CFT}} = -\frac{1}{4\pi}\ln\left|\frac{(F(u_1) - F(u_2))(F(v_1) - F(v_2))}{(F(u_1) - F(v_2))(F(v_1) - F(u_2))}\right|. \tag{2.124}$$

We can quickly check that this result does indeed have Dirichlet boundary conditions, since at the boundary $z = 0$, we have $u = v$ such that

$$\begin{aligned}\langle \phi(u_1, v_1)\phi(u_2, v_2)\rangle_{\text{CFT}} &= -\frac{1}{4\pi}\ln\left|\frac{(F(u_1) - F(u_2))(F(u_1) - F(u_2))}{(F(u_1) - F(u_2))(F(u_1) - F(u_2))}\right| \\ &= 0.\end{aligned} \tag{2.125}$$

The result Eq. (2.124) can now be inserted into the Schwarzian path integral:

$$\langle \phi(u_1, v_1)\phi(u_2, v_2)\rangle = -\frac{1}{4\pi}\int [\mathcal{D}f]\ln\left|\frac{(F(u_1) - F(u_2))(F(u_1) - F(u_2))}{(F(u_1) - F(u_2))(F(u_1) - F(u_2))}\right| e^{-I_{\text{Sch}}[f]}. \tag{2.126}$$

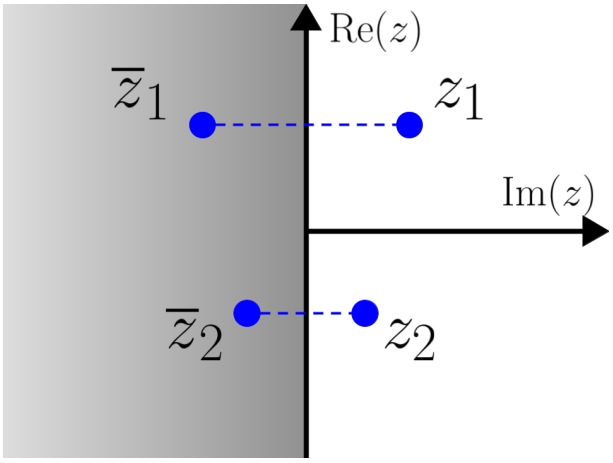

Fig. 2.11: Real charges and their images on the opposite side of the holographic boundary in the complex z coordinates. The holographic boundary is at $\mathrm{Im}(z) = 0$.

For this purpose, we can make use of the following observation:

$$\ln\left|\frac{(F(u_1)-F(u_2))(F(v_1)-F(v_2))}{(F(u_1)-F(v_2))(F(v_1)-F(u_2))}\right| = \int_{v_1}^{u_1} dt \int_{v_2}^{u_2} dt' \frac{\dot{F}(t)\dot{F}(t')}{(F(t)-F(t'))^2}. \tag{2.127}$$

This trick is particularly useful since the operator in the double integral is the familiar Schwarzian bilocal operator $G_\Delta(t_1, t_2)$, Eq. (2.111), with weight $\Delta = 1$. In this way, we can directly connect the calculation of the bulk two-point function to the known results of the two-point function of the boundary dual operators. As a consistency check, it makes sense that $\Delta = 1$ since we started from the action of a massless scalar field, such that $\Delta = 1/2 + \sqrt{1/4 + m}$ should indeed equal one. Again making use of the (real-time) thermal reparameterization $F(t) = \tanh \frac{\pi}{\beta} f(t)$, we get

$$\begin{aligned}\ln\left|\frac{\sinh\frac{\pi}{\beta}(f(u_1)-f(u_2))\sinh\frac{\pi}{\beta}(f(v_1)-f(v_2))}{\sinh\frac{\pi}{\beta}(f(u_1)-f(v_2))\sinh\frac{\pi}{\beta}(f(v_1)-f(u_2))}\right| \\ = \int_{v_1}^{u_1} dt \int_{v_2}^{u_2} dt' \frac{\dot{f}(t)\dot{f}(t')}{\frac{\beta}{\pi}\sinh\frac{\pi}{\beta}(f(t)-f(t'))^2}.\end{aligned} \tag{2.128}$$

Such that the bulk two-point correlator becomes, neglecting for now the $1/4\pi$ prefactor:

$$\begin{aligned}\langle\phi(u_1,v_1)\phi(u_2,v_2)\rangle &= \int_{v_1}^{u_1} dt \int_{v_2}^{u_2} dt' \int [\mathcal{D}f] \frac{\dot{f}(t)\dot{f}(t')}{\frac{\beta}{\pi}\sinh\frac{\pi}{\beta}(f(t)-f(t'))^2} e^{-I_{\mathrm{Sch}}[f]} \\ &= \int_{v_1}^{u_1} dt \int_{v_2}^{u_2} dt' \,\langle \mathcal{O}_\Delta(\tau_1)\mathcal{O}_\Delta(\tau_2)\rangle\end{aligned} \tag{2.129}$$

Again, the boundary two-point function $\langle \mathcal{O}_\Delta(\tau_1)\mathcal{O}_\Delta(\tau_2)\rangle$ is given by Eq. (2.115). By replacing the irrep labels k with energies $E, M = k^2$ and setting for now $C = 1/2$, we can write this result as

$$\begin{aligned}\langle \mathcal{O}_\Delta(\tau_1)\mathcal{O}_\Delta(\tau_2)\rangle = \frac{1}{8\pi^4 Z^{-1}(\beta)} \int_0^\infty dM \sinh(2\pi\sqrt{M}) e^{-\beta M} \\ \times \int_0^\infty dE \sinh(2\pi\sqrt{E}) e^{i(t-t')(E-M)} \Gamma(1 \pm i\sqrt{M} \pm i\sqrt{E}).\end{aligned} \tag{2.130}$$

The double time integral can then be performed as follows[14]. We start from

$$\int_{v_1}^{u_1} dt \int_{v_2}^{u_2} dt' e^{i(t-t')\omega} \tag{2.131}$$

where $\omega = E - M$. Switching to space and time coordinates, the first integral is of the form

$$\begin{aligned}\int_{v_1}^{u_1} e^{it\omega} dt &= \int_{t_1-z_1}^{t_1+z_1} e^{it\omega} dt \\ &= \int_{-z_1}^{z_1} e^{i(x+t_1)\omega} dx \qquad \text{with } x = t - t_1 \\ &= e^{it_1\omega} \frac{2\sin(z_1\omega)}{\omega}.\end{aligned} \tag{2.132}$$

Similarly the second integral becomes

$$\int_{v_2}^{u_2} e^{-it'\omega} dt' = e^{-it_2\omega} \frac{2\sin(z_2\omega)}{\omega}. \tag{2.133}$$

From this it follows that the bulk two-point function is only dependent on the time difference $t \equiv t_1 - t_2$, and we can write it as $\langle G_{\text{bb}}(t, z_1, z_2)\rangle$. In total we get, neglecting the prefactors:

$$\begin{aligned}\langle G_{\text{bb}}(t, z_1, z_2)\rangle = \int_0^\infty dM \sinh(2\pi\sqrt{M}) e^{-\beta M} \int_0^\infty dE \sinh(2\pi\sqrt{E}) e^{it\omega} \\ \times \frac{\sin(z_1\omega)}{\omega} \frac{\sin(z_2\omega)}{\omega} \Gamma(1 \pm i\sqrt{M} \pm i\sqrt{E}).\end{aligned} \tag{2.134}$$

This result is plotted in Fig. (2.12) for Euclidean times.

2.3.4.1 Pure energy eigenstates

To gain some further insight into this result, we can consider the pure energy eigenstate two-point function of one of the intermediate energies M. This quantity $\langle G\rangle_M \equiv \langle M|G|M\rangle$ is, in statistical mechanics language, the microcanonical two-

[14] Alternatively (but analogously) one can rewrite the integrals using Heaviside functions and then use the known expression for the Fourier transform of the Heaviside, as in [2].

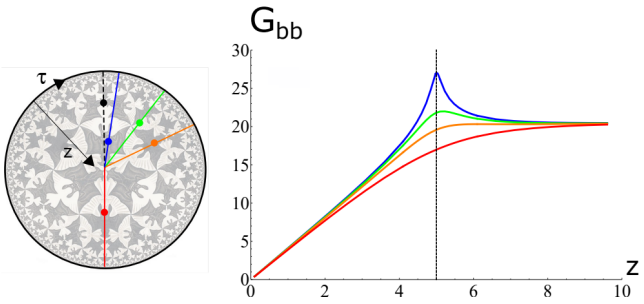

Fig. 2.12: Euclidean bulk two-point function Eq. (2.134) at finite temperature ($\beta = 2\pi, C = 1/2$), with one bulk point at $(t = 0, z' = 5)$ and the second bulk point at (it, z), as a function of z for different Euclidean times. Blue: $it = 0.1$, Green: $it = 0.5$, Orange: $it = 1$, Red: $it = \pi$. Figure taken from [2].

point function, in analogy with the microcanonical ensemble where the total energy is specified. The earlier two-point function Eq. (2.134), by contrast, is then the thermal two-point function $\langle G_{\text{bb}}(t, z_1, z_2)\rangle_\beta$. The thermal two-point function can be obtained from the pure state two-point function by taking an appropriate integral over the energy M. More specifically, the integral to take here is the Laplace transform, taking into account also the density of states. This is perhaps not surprising. If we stay in the language of statistical mechanics, the canonical partition function (NVT ensemble, thermal system) is the Laplace transform of the microcanonical partition function (NVE ensemble) [33]. In other words, the Laplace transform offers a way of constructing a function of temperature from a function of energy [29]. As such it makes sense that the relation between the microcanonical two-point function and the thermal two-point function takes this same form. As before, the Schwarzian density of states is given by Eq. (2.101), meaning that the thermal two-point function becomes[15]

$$\langle G_{\text{bb}}\rangle_\beta = \frac{1}{Z}\int_0^\infty dM \sinh(2\pi\sqrt{M})e^{-\beta M}. \tag{2.135}$$

Comparing this with Eq. (2.134), we can conclude that

$$\langle G(t, z_1, z_2)\rangle_M = \int_0^\infty dE \sinh(2\pi\sqrt{E})e^{-it\omega}\frac{\sin(z_1\omega)}{\omega}\frac{\sin(z_2\omega)}{\omega}\Gamma(1 \pm i\sqrt{M} \pm i\sqrt{E}). \tag{2.136}$$

Particularly interesting regimes to discuss for this result are the near-horizon regime and the late-time physics. It is namely in these regimes that quantum gravity effects become most pronounced. In this way, quantum effects within JT gravity are highlighted in the IR, instead of in the UV as is familiar in e.g. quantum field theory. This discussion is further expanded on in [2].

[15] Remember that we have set $C = 1/2$.

2.4 The Unruh effect in JT gravity

2.4.1 Introduction to the Unruh effect

The Unruh effect states that a uniformly accelerating observer will see a heat bath in the vacuum of an inertial observer. To see this, we can look at the different experiences of a Rindler observer and an inertial observer in 1+1d Minkowski spacetime. For this purpose, this section mostly follows [35]. Rindler coordinates are a natural coordinate frame for accelerated observers and are given by

$$X = \rho \cosh \eta, \qquad T = \rho \sinh \eta \tag{2.137}$$

where (X, T) are the Minkowski coordinates. The worldline and proper time t of an observer with a constant proper acceleration a along the X-axis are given by

$$\rho = \frac{1}{a}, \qquad \eta = at. \tag{2.138}$$

Rindler lightcone coordinates can be introduced by defining first the tortoise coordinate x:

$$\rho = \frac{1}{a} e^{ax} \tag{2.139}$$

such that the Rindler lightcone coordinates are $(u = t + x, v = t - x)$. The relation between the Minkowski lightcone coordinates $(U = T + X, V = T - X)$ and the Rindler coordinates is:

$$U = \rho e^{\eta} = \frac{1}{a} e^{au}, \qquad V = -\rho e^{-\eta} = -\frac{1}{a} e^{-av}. \tag{2.140}$$

Note that Rindler coordinates cover only one quadrant of the Minkowski spacetime. In this sense, there is an analogy between on the one hand Rindler and Minkowski coordinates and on the other hand the black hole patch and Poincaré patch respectively.

2.4.1.1 Observer dependency of the vacuum

To see the observer dependency of the concept of a vacuum, let us start with the action for a massless scalar field in Minkowski space

$$S = \frac{1}{2} \int dx^2 \partial_\mu \phi \partial^\mu \phi \tag{2.141}$$

which leads to the equation of motion

$$\Box \phi = 4 \partial_U \partial_V \phi = 0 \tag{2.142}$$

in terms of the lightcone coordinates (U, V). The general solution is then a sum of right- and left-moving waves. The left-moving waves are solely dependent on U and the right-movers on V:

$$\phi(U, V) = \phi(U) + \phi(V). \tag{2.143}$$

Moving forward we will focus solely on the right-moving waves. The most general solution takes the familiar form of a (discrete or continuous) sum over creation and annihilation operators with corresponding positive frequency plane wave modes $f_\omega(U)$:

$$\phi(V) = \int_0^{+\infty} d\omega \left(a_\omega f_\omega(V) + a_\omega^\dagger f_\omega^*(V) \right), \qquad f_\omega(V) = \frac{e^{-i\omega V}}{\sqrt{4\pi\omega}}. \tag{2.144}$$

The definition of a particle has an additional subtlety if we want to allow for a non-trivial observer dependency. For this purpose, it is sufficient to say that a particle is simply that which is detected by a particle detector. This in essence relates the concept of a particle to some specific observer (to whom the detector is attached) with proper time τ. This proper time then acts as a preferential reference time coordinate in relation to which we can define positive frequency modes. These positive frequency modes, having positive energy, thus describe particles which the observer can detect. We can again expand the field $\phi(V)$ in terms of these positive frequency modes:

$$\phi = \sum_i (a_i f_i + a_i^\dagger f_i^*), \tag{2.145}$$

where the index i can again be discrete or continuous. This in turn defines the vacuum of the "f"-observer as the state which is cancelled by these annihilation operators

$$\forall i: \quad a_i \left|0\right\rangle_f = 0. \tag{2.146}$$

In other words, the vacuum of some observer is defined as the state which is annihilated by modes which have a positive frequency with respect to this observer's proper time. However, in general a spacetime can allow for alternative mode expansions, which define positive frequency modes for some other observer:

$$\phi = \sum_i (b_i g_i + b_i^\dagger g_i^*). \tag{2.147}$$

Formally this is possible for a static spacetime if there exist multiple Killing vectors. This is for example the case for flat space, with Killing vector ∂_T for a Minkowski observer and ∂_η for a Rindler observer. Continuing for now in complete generality

without specifying the observers, both sets of modes are complete and thus can be expanded in each others bases:

$$\begin{aligned} g_i &= \sum_j (\alpha_{ij} f_i + \beta_{ij} f_i^*) \\ f_i &= \sum_j (\alpha_{ji}^* g_i - \beta_{ij} g_i^*), \end{aligned} \tag{2.148}$$

where the coefficients

$$\alpha_{ij} = (g_i, f_j), \qquad \beta_{ij} = -(g_i, f_j^*) \tag{2.149}$$

are defined according to the covariant scalar product of two modes. This inner product, sometimes called the Klein-Gordon inner product, is defined on a spacelike hypersurface Σ and is given by

$$(\phi_1, \phi_2) = i \oint_\Sigma (\phi_1^* \partial_\mu \phi_2 - \phi_2 \partial_\mu \phi_1^*)\, dS^\mu \tag{2.150}$$

where dS^μ is the surface element of the hypersurface. For modes the inner product is independent of Σ (as long as it is spacelike) and this hypersurface can thus be chosen to make the calculation easiest. The transformation Eq. (2.148) is a Bogoliubov transformation and the coefficients are Bogoliubov coefficients. They also allow to expand the creation and annihilation operators in terms of each other:

$$\begin{aligned} a_i &= \sum_j (\alpha_{ij} b_j + \beta_{ji}^* b_j^\dagger) \\ b_i &= \sum_j (\alpha_{ij}^* a_j - \beta_{ij}^* a_j^\dagger). \end{aligned} \tag{2.151}$$

This directly leads to the observer-dependency of the vacuum. Taking the f-vacuum expectation of the number operator for the modes g with energy label i, we find:

$$\begin{aligned} \langle 0|\hat{n}_{g_i}|0\rangle_f &= \langle 0|b_i^\dagger b_i|0\rangle_f \\ &= \sum_{j,k} \beta_{ij}\beta_{ik}^* \langle 0|a_j a_k^\dagger|0\rangle_f \\ &= \sum_j |\beta_{ij}|^2. \end{aligned} \tag{2.152}$$

In other words, the observer for whom the g modes have a positive frequency will see a heat bath where the f-observer only sees a vacuum.

2.4.1.2 Unruh effect

Returning now to the specific case of a Rindler observer in Minkowski space, the Rindler metric can be written in conformal gauge as

$$ds^2 = e^{2ax}(-dt^2 + dx^2). \tag{2.153}$$

The action for a massless scalar field becomes

$$S = \frac{1}{2}\int d^2x\sqrt{-g}g^{\mu\nu}\partial_\mu\phi_R\partial_\nu\phi_R. \tag{2.154}$$

As discussed before in Sec. (2.3.4), the action is independent of the conformal scaling factor such that

$$S = \frac{1}{2}\int d^2x\eta^{\mu\nu}\partial_\mu\phi_R\partial_\nu\phi_R. \tag{2.155}$$

The equation of motion thus also remains the same as before and we have again a sum of right-moving and left-moving waves as the general solution, now in terms of the Rindler lightcone coordinates (u, v):

$$\phi_R(u, v) = \phi_R(u) + \phi_R(v). \tag{2.156}$$

Focusing again on the right-mover, we can expand the field in terms of modes g_Ω which have a positive frequency with respect to the Rindler observer, i.e. with respect to their proper time:

$$\phi_R(u) = \int_0^\infty d\Omega\left(b_\Omega g_\Omega(u) + b_\Omega^\dagger g_\Omega^*(u)\right), \qquad g_\Omega(u) = \frac{1}{\sqrt{4\pi\Omega}}e^{-i\Omega u}. \tag{2.157}$$

Similarly, the field can be expanded in Minkowski modes, i.e. in the modes f_ω which have a positive frequency with respect to the proper time of an inertial (Minkowski) observer:

$$\phi_R(u) = \theta(U)\int_0^\infty d\omega\left(a_\omega f_\omega(U) + a_\Omega^\dagger f_\Omega^*(U)\right), \qquad f_\omega(U) = \frac{1}{\sqrt{4\pi\omega}}e^{-i\omega U} \tag{2.158}$$

where Heaviside function accounts for the fact that the Rindler coordinates cover only the right wedge of the Minkowski space (i.e. $U \geq 0, V \leq 0$). The Bogoliubov coefficients are again given by

$$\begin{aligned}\alpha_{\Omega\omega} &= (g_\Omega, f_\omega)\\ \beta_{\Omega\omega} &= -(g_\Omega, f_\omega^*)\end{aligned} \tag{2.159}$$

These coefficients can be calculated which results in[16]

$$\beta_{\Omega\omega} = -e^{-\frac{\pi\Omega}{a}}\alpha_{\Omega\omega} \tag{2.160}$$

such that, using the normalisation requirement for the coefficients, Eq. (2.152) becomes (now with respect to the Minkowski vacuum)

$$\langle 0|n_\Omega|0\rangle_M = \int_0^\infty d\omega|\beta_{\Omega\omega}|^2 = \frac{\delta(0)}{e^{\frac{2\pi\Omega}{a}}-1}. \tag{2.161}$$

The total number of particles with momentum k in a finite volume V in d space dimensions is given by

$$N_k = \frac{(2\pi)^d}{V}n_k = \frac{n_k}{\delta^d(0)}. \tag{2.162}$$

Using this, we find that the total number of particles observed by the Rindler observer in the Minkowski vacuum is given by

$$\langle 0|N_\Omega^R|0\rangle_M = \frac{1}{e^{\frac{2\pi\Omega}{a}}-1} \tag{2.163}$$

which is a Bose-Einstein distribution with temperature

$$T_U = \frac{a}{2\pi}, \tag{2.164}$$

the Unruh temperature. In other words, a uniformly accelerating observer in flat space sees a heat bath with temperature T_U where an inertial observers sees only a vacuum. The temperature of the heat bath increases as the observer's proper acceleration increases.

2.4.1.3 Relation to black holes

The relevance for JT gravity becomes clear when looking at the relation between Rindler coordinates and the near-horizon region of black holes. Namely, the near-horizon geometry of a non-rotating black hole is Rindler geometry[17] [15]. This is most easily seen by looking at the metric of a Schwarzschild black hole. The Rindler metric can be written as

$$-\rho^2 d\eta^2 + d\rho^2 \tag{2.165}$$

and the Schwarzschild metric is given by

$$ds^2 = -f(r)dt^2 + \frac{dr^2}{f(r)} + r^2 d\Omega^2, \qquad f(r) = 1 - \frac{2M}{r}. \tag{2.166}$$

[16] The full derivation is rather lengthy and can be found in [35].

[17] Recall that in Sec. (2.2.1.2) it was calculated that the near-horizon regime of specifically near-extremal (or indeed extremal) black holes is $AdS_2 \times S_2$. The Rindler geometry Rindler $\times S_2$ is the general case.

To take the near-horizon limit, we write $r = 2M(1+\epsilon)$ in terms of the distance ϵ to the horizon. For small ϵ it follows that $f(r) = \epsilon + \mathcal{O}(\epsilon^2)$. Thus we can rewrite the time and radial part of the metric as

$$\begin{aligned} ds^2 &= -\epsilon^2 dt^2 + \frac{dr^2}{\epsilon^2} \\ &= -\epsilon^2 dt^2 + 16M^2 d\epsilon^2 \\ &= -\rho^2 d\eta^2 + d\rho^2 \end{aligned} \tag{2.167}$$

where we have defined $\rho = 4M\epsilon$ and $\eta = t/4M$, such that we do indeed obtain the Rindler geometry. Since there is a Rindler geometry near the horizon, we expect to observe an equivalent effect to the Unruh effect near the black hole horizon. Indeed, black holes radiate like a black-body at temperature T, which is called Hawking radiation [15]. The Rindler observer in this case is an observer with a uniform acceleration close to the black hole, i.e. an observer hovering at a constant distance from the horizon. This observer will see the black hole emit Unruh radiation. The Minkowski observer in this context is simply an inertial observer and thus follows a geodesic, which means they are falling towards the black hole. This observer will not see any Unruh radiation being emitted by the black hole. Far away from the black hole, the radiation is also visible but it does not take the form of an exact black body spectrum due to the effects of the differing geometry [15].
Note how this discussion is also strongly related to the equivalence principle: uniform acceleration and being stationary in a gravitational field are indistinguishable. In this sense, Hawking radiation is just the interplay between the Unruh effect and the equivalence principle.

2.4.2 Unruh effect in JT gravity

Recall the construction of the bulk frame discussed in Section 2.2.5, where the preferred time coordinate t on the boundary is reinterpreted as lightcone coordinates $y = (u, v)$ of a bulk point using the radar definition. Our goal is now to calculate the occupation, in the Poincaré vacuum $(U = F(u), V = F(v))$, of modes which have a positive frequency with respect to the local frame y of the observer, i.e. the observer whose proper time coincides with the time coordinate of the y frame.

2.4.2.1 AdS$_2$vacuum states

We now couple JT gravity to a massless scalar field with action

$$S = \frac{1}{2}\int d^x \sqrt{-g} g^{\mu\nu} \partial_\mu \phi \partial_\nu \phi. \tag{2.168}$$

To describe the Unruh effect, we must first define the different vacuum states in AdS_2. This boils down to defining positive frequency modes with respect to the time coordinates of the coordinate patches of AdS_2. Observers at a fixed spatial coordinate x, in a coordinate system in which the metric of the patch is time-independent, then detect no particles [30]. We will find that not all of the coordinate patches described in Sec. (2.2.1.1) have equivalent vacuums. Recall that these patches are related by the reparameterization field F (or f) which defines the bulk geometry as in Sec. (2.2.5), hence we can label the vacuum states by their reparameterization [24]. Following [30], we will review the vacuums corresponding to the different patches. Starting with the global patch, recall that

$$ds^2 = \frac{-d\tau^2 + d\sigma^2}{cos^2\sigma}. \tag{2.169}$$

The global vacuum $|0\rangle_G$ is then the state which is annihilated by modes with a positive frequency with respect to τ. The question is now whether the vacua of the Poincaré patch and the black hole patch are equivalent to $|0\rangle_G$.

The Poincaré coordinates (T, Z) are related to the global coordinates (τ, σ) by

$$T \pm Z = \tan\frac{1}{2}(\tau \pm \sigma \pm \frac{\pi}{2}). \tag{2.170}$$

As discussed before, to determine whether the two vacua are equivalent we need to calculate the Bogoliubov coefficients which are determined by the inner product of the modes corresponding to each vacuum (see Eq. (2.150), where we now work in space and time coordinates instead of lightcone coordinates). Working with the Poincaré patch as a reference frame, we need to calculate the inner product between the modes which have a positive frequency in Poincaré coordinates:

$$\phi^P_{+\omega} = \frac{1}{\sqrt{\pi\omega}} e^{-i\omega T} \sin(\omega Z) \tag{2.171}$$

and the modes which have a positive $(\Omega = 1, 2, \dots)$ or negative $(\Omega = -1, -2, \dots)$ frequency in global coordinates:

$$\phi^G_\Omega = \frac{1}{\sqrt{\pi|\Omega|}} e^{-i\Omega\tau} \sin(\Omega(\sigma + \frac{\pi}{2})). \tag{2.172}$$

For the inner product we can choose the spacelike hyperplane $T = 0$ such that

$$\left(\phi^P_{+\omega}, \phi^G_\Omega\right) = i \int_0^\infty dZ \left[\phi^P_{-\omega} \partial_T \phi^G_\Omega - \phi^G_\Omega \partial_T \phi^P_{-\omega}\right]_{T=0} \tag{2.173}$$

where $\phi^P_{-\omega} = \left(\phi^P_{+\omega}\right)^*$. The choice of hyperplane $T = 0$ means $\sigma + \frac{\pi}{2} = 2\tan^{-1} Z$ and $\partial_T = \frac{2}{Z^2+1}\partial_\tau$ such that we can write the inner product as

$$\left(\phi^P_{+\omega}, \phi^G_{\Omega}\right) = \sqrt{\frac{|\Omega|}{\omega\pi^2}} \int_{-\infty}^{+\infty} dZ e^{i\omega Z}(1+iZ)^{-\Omega-1}(1-iZ)^{\Omega-1}. \tag{2.174}$$

This integral can be solved by closing the contour in the upper half plane and has a pole only when $\Omega > 0$:

$$\left(\phi^P_{+\omega}, \phi^G_{+\Omega}\right) = (-1)^{\Omega}\sqrt{\frac{\Omega}{\omega}} e^{-\omega} L^{-1}_{\Omega}(2\omega), \qquad \left(\phi^P_{+\omega}, \phi^G_{-\Omega}\right) = 0 \tag{2.175}$$

where L^{-1}_{Ω} is the associated Laguerre polynomial. As such, the Bogoliubov transformation between the Poincaré vacuum and the global vacuum is block diagonal: only the coefficients between creation operators and between annihilation operators themselves differ from zero. As such, looking at Eq. (2.152), the global vacuum will still appear as a vacuum to the Poincaré observer and vice versa; the two vacua are equivalent:

$$|0\rangle_G = |0\rangle_P . \tag{2.176}$$

The black hole patch

$$ds^2 = \frac{4\pi^2}{\beta^2}\frac{dz^2 - dt^2}{\sinh^2(\frac{2\pi}{\beta}z)} \tag{2.177}$$

with vacuum $|0\rangle_B$ is related to the global patch by

$$\tan(\frac{1}{2}(\tau \pm \sigma)) = \mp e^{\mp\frac{2\pi}{\beta}(t\pm z)}. \tag{2.178}$$

We can rewrite the black hole patch in terms of the proper distance ρ to the black hole horizon [26]. Using the coordinate transformation

$$\sinh\rho = \frac{1}{\sinh\frac{\pi}{\beta}(u-v)} \tag{2.179}$$

the metric becomes

$$ds^2 = -\frac{4\pi^2}{\beta^2}\sinh^2\rho dt^2 + d\rho^2. \tag{2.180}$$

Importantly for the discussion regarding the Unruh effect, this coordinate transformation leaves the time coordinate unchanged, such that it does not affect the definition of the black hole patch vacuum. In the near horizon limit we have $\rho \ll 1$, such that the metric becomes the Rindler metric. An observer at a constant distance from the horizon, i.e. $\rho = \rho_0$, has a proper time equal to the black hole patch time coordinate [30] and will thus not see any particles in the $|0\rangle_B$ vacuum. However, this vacuum is not equivalent to the global (and Poincaré) vacuum. To see this, we start explicitly from the action of a massless scalar field on the gravitational saddle,

i.e. in the black hole patch $F(t) = \tanh(\frac{\pi}{\beta}t)$, following [3]. The solutions are, as before, left- and right-moving plane waves which can be expanded as

$$\phi(u,v) = \int_0^\infty \frac{\omega}{\sqrt{4\pi\omega}} \left(a_\omega e^{-i\omega u} + a_\omega^\dagger e^{i\omega u} - a_\omega e^{-i\omega v} - a_\omega^\dagger e^{i\omega v}\right) \tag{2.181}$$

where (u,v) are the black hole lightcone coordinates. To show the difference between the black hole vacuum and the Poincaré vacuum, we can make use of an Unruh-DeWitt detector, which is a model of a quantum mechanical detector introduced in [9, 34]. The detector couples a quantum mechanical system with degree of freedom $\mu(t)$ to the field $\phi(u(t), v(t))$ [3]. Typically the detector system is simply a two-level system, where μ then acts as a monopole moment. The interaction Hamiltonian is given by

$$H_{\text{int}}(t) = g\mu(t)\phi(u(t), v(t)) \tag{2.182}$$

where g is the coupling and $(u(t), v(t))$ is the worldline of the detector. We now want to model the probability $P(\omega)$ that the detector, initially in its ground state $|0\rangle$, to be in the energy eigenstate $|\omega\rangle$. For this, we assume a small coupling g and use perturbation theory to work in first order in the coupling. In this case, the Hilbert space of the system is the product space $\mathcal{H} = \mathcal{H}_{\text{detector}} \bigotimes \mathcal{H}_{\text{matter}}$. The excitation of the detector $|0\rangle \to |\omega\rangle$ corresponds to the matter sector going from its initial state $|M\rangle$ (the thermal state) to some final state $|\psi\rangle$. The total transition is thus $|0, M\rangle \to |\omega, \psi\rangle$. The detector is not sensitive to the final state of the matter sector, so we need to sum over all possible ψ. The probability becomes [3, 7]

$$\begin{aligned} P(\omega) &= \sum_\psi \left| \langle \omega, \psi | - i \int_{-\infty}^{+\infty} dt H_{\text{int}}(t) |0, M\rangle \right|^2 \\ &= g^2 |\langle \omega | \mu(0) | 0 \rangle|^2 F(\omega) \end{aligned} \tag{2.183}$$

where we have used $\langle \omega|\mu(t)|0\rangle = e^{i\omega t} \langle \omega|\mu(t)|0\rangle$ and $F(\omega)$ is the response function:

$$F(\omega) = \int_{-\infty}^{+\infty} dt_1 \int_{-\infty}^{+\infty} dt_2 e^{-i\omega(t_1 - t_2)} \langle \phi(u(t_1), v(t_1)) \phi(u(t_2), v(t_2)) \rangle_{\text{CFT}} , \tag{2.184}$$

with the familiar CFT bulk two-point function Eq. (2.124), also called the Wightman two-point function. From this we can define the transition rate or response rate as the (infinite) total transition probability divided by the (infinite) total proper time:

$$\begin{aligned} R(\omega) = g^2 &|\langle \omega | \mu(0) | 0 \rangle|^2 \\ &\times \lim_{T \to +\infty} \frac{1}{T} \int_{-T}^{+T} dt_1 \int_{-T}^{+T} dt_2 e^{-i\omega(t_1 - t_2)} \langle \phi(u(t_1), v(t_1)) \phi(u(t_2), v(t_2)) \rangle_{\text{CFT}} . \end{aligned} \tag{2.185}$$

Calculating this in the black hole vacuum, i.e. from the perspective of an observer associated with the black hole time coordinate t, the probability is zero. However, in

the Poincaré vacuum this result is not zero, more specifically for a stationary detector worldline we get [3]

$$R(\omega) = g^2 |\langle \omega | \mu(0) | 0 \rangle|^2 2 \frac{\sin^2 \omega z}{\omega^2} \frac{\omega}{e^{\beta\omega} - 1} \tag{2.186}$$

which takes the form of the Planckian black body spectrum. The Unruh effect here is such that an observer associated with the black hole time coordinate sees particles in the Poincaré vacuum. In other words, an observer hovering at a constant distance from the black hole horizon will see a heat bath in the Poincaré (and thus also the global) vacuum.

The analogy between the black hole patch and the Rindler metric, and the Poincaré patch and Minkowski metric was already briefly mentioned earlier, but here the nature of this analogy becomes clearer. More specifically, the analogy between time coordinates is [3]:

$$\begin{aligned} \text{black hole time} &\longleftrightarrow \text{Rindler/Schwarzschild time} \\ \text{Poincaré/global time} &\longleftrightarrow \text{Minkowski time} \end{aligned} \tag{2.187}$$

Firstly, the black hole patch explicitly has a near-horizon Rindler region, as is the case for the Schwarzschild metric. The Unruh effect in the black hole patch can then be related to the Unruh effect in Minkowski space discussed in Sec. (2.4.1), where the black hole patch takes the role of the Rindler metric, and the Poincaré patch (or global patch) takes the role of the Minkowski metric. This is then also related to the Hawking radiation of the Schwarzschild black hole as discussed in Sec. (2.4.1.3), using the same dictionary.

2.4.2.2 Energy fluxes

In order to calculate the bulk energy density of the Unruh heat bath, we need to calculate stress tensor components, as discussed in [24]. More specifically, the stress tensor components representing outgoing and ingoing energy densities are:

$$T_{uu} = \partial_u \phi \partial_u \phi, \qquad T_{vv} = \partial_v \phi \partial_v \phi. \tag{2.188}$$

This operator still requires regularization and renormalization. To this end, we define the renormalized stress tensor by subtracting its expectation value in the vacuum $|0\rangle_u$ associated to the u coordinates (this is a point-splitting regularization):

$$\begin{aligned} :T_{uu}(u_2): &\equiv \partial_u \phi \partial_u \phi - \langle 0 | \partial_u \phi \partial_u \phi | 0 \rangle_u \\ &= \lim_{u_1 \to u_2} \left(\partial_u \phi(u_1) \partial_u \phi(u_2) + \frac{1}{4\pi} \frac{1}{(u_1 - u_2)^2} \right), \end{aligned} \tag{2.189}$$

which is defined and measured by a u-observer with a measuring device calibrated to their vacuum [26]. With respect to the Poincaré vacuum, the CFT expectation value of the renormalized stress tensor then becomes[18]

$$\langle 0| : T_{uu}(u) : |0\rangle_F = -\frac{1}{4\pi} \lim_{u_1 \to u_2} \left(\frac{F'(u_1)F'(u_2)}{(F(u_1) - F(u_2))^2} - \frac{1}{(u_1 - u_2)^2} \right), \tag{2.190}$$

with c the matter central charge[19], and analogously for T_{vv}. These quantities are the energy density of the Unruh heat bath in the Poincaré vacuum, i.e. the energy measured by a u-observer in this vacuum. Switching to the thermal reparameterization $F(y) = \tanh \frac{\pi}{\beta} f(y)$, these expressions can be series expanded as

$$\langle 0| : T_{uu}(u) : |0\rangle_F = -\frac{c}{24\pi} \left\{ \tanh \frac{\pi}{\beta} f(u), u \right\}, \tag{2.191}$$

in terms of the Schwarzian derivative.

On the gravitational saddle, $f(y) = y$, we have $\left\{ \tanh \frac{\pi}{\beta} f(u), u \right\} = -\frac{2\pi^2}{\beta^2}$, such that the Unruh heat bath becomes

$$\langle 0| : T_{uu}(u) : |0\rangle_F = \langle 0| : T_{vv} : |0\rangle_F = c\frac{\pi}{12} T_H^2, \tag{2.192}$$

with T_H the Hawking temperature of the black hole. The total energy density is then

$$E_{\text{bath}}(u, v) = \langle 0| : T_{uu}(u) : |0\rangle_F + \langle 0| : T_{vv}(v) : |0\rangle_F = c\frac{\pi}{6} T_H^2 \tag{2.193}$$

For the full quantum-gravity result, we insert Eq. (2.191) into the Schwarzian path integral and find[20]:

$$\langle : T_{uu} : \rangle_\beta = \langle : T_{vv} : \rangle_\beta = c\frac{\pi}{12} T_H^2 + c\frac{T_H}{16\pi C}, \tag{2.194}$$

where we have left the CFT bra-kets implicit. The quantum effects are entirely contained in the final term, and indeed in the semi-classical limit $C \to \infty$ we get the semi-classical result Eq. (2.192). The total energy density of the Unruh heat bath is then given by

$$E_{\text{bath}}(u, v) = \langle : T_{uu}(u) : \rangle_\beta + \langle T_{vv}(v) : \rangle_\beta = c\frac{\pi}{6} T_H^2 + c\frac{T_H}{8\pi C} \tag{2.195}$$

[18] For a derivation of this result, see Eq. (2.199) with $x^\pm(y^\pm) = F(y^\pm)$.

[19] i.e. the (eigenvalue of the) casimir of the CFT; the operator which commutes with all other symmetry operators.

[20] This path integral has the Lagrangian density as an operator insertion. The trick to solving such a path integral is to take the derivative of the partition function with respect to the prefactor of the action, in this case C. This trick is also used in Chapter 4, where it is explicitly worked out.

In other words, the quantum gravity corrections make for a higher energy density of the Unruh heat bath.

2.4.2.3 Planckian black-body spectrum

The goal is now to obtain an expression for the occupation number of the Unruh modes in function of their frequency/energy. This is in essence a spectral decomposition of the Unruh fluxes [3]. In other words, we want an expression for the occupation number of the positive frequency modes in the observer's reference frame, with respect to the Poincaré vacuum: $\langle 0|N_\omega|0\rangle_P$. Starting with unspecified coordinate frames, the derivation follows [11]. We consider again a massless two-dimensional CFT scalar field ϕ. As before we have the general solution of left and right moving modes which depend only on one of two lightcone coordinates: $\phi(U,V) = \phi(U) + \phi(V)$. Recall the CFT two-point correlation function discussed in Sec. (2.3.4). Since correlators are defined as the vacuum expectation value of field operators, we now have to specify with respect to which vacuum we define a two-point function. Here we write the fields in terms of the general lightcone coordinates $x^+ = u = t + z$ and $x^- = v = t - z$: $\phi(x^\pm)$, and define the two-point function with respect to the vacuum $|0\rangle_x$ of these coordinates:

$$\langle 0|\phi(x_1^\pm)\phi(x_2^\pm)|0\rangle_x = -\frac{1}{4\pi}\ln|x_1^\pm - x_2^\pm|. \tag{2.196}$$

The starting point for the derivation is then the two-point function of the derivatives $\partial_{x_i^\pm}\phi(x_i^\pm) \equiv \partial_\pm\phi(x_i^\pm)$, which can be readily obtained by taking the $\partial_{x_1^\pm}\partial_{x_2^\pm}$ derivative of Eq. (2.196):

$$\langle 0|\partial_\pm\phi(x_1^\pm)\partial_\pm\phi(x_2^\pm)|0\rangle_x = -\frac{1}{4\pi}\frac{1}{(x_1^\pm - x_2^\pm)^2}. \tag{2.197}$$

We now introduce the new lightcone coordinates $y^\pm$, related to the $x^\pm$ coordinates by the conformal transformation $x^\pm(y^\pm)$. A d-dimensional CFT two-point function of (quasi-)primary fields $\phi_{1,2}$ with weights $\Delta_{1,2}$ transforms under a conformal transformation $x \to x'$ as [14]:

$$\langle\phi_1(x_1)\phi_2(x_2)\rangle = \left(\frac{\partial x'}{\partial x}\Big|_{x=x_1}\right)^{\Delta_1/d}\left(\frac{\partial x'}{\partial x}\Big|_{x=x_2}\right)^{\Delta_2/d}\langle\phi_1(x_1')\phi_2(x_2')\rangle\,, \tag{2.198}$$

with the notation $x_i' = x'(x_i)$. For the current case, $d = 1$ (the left- and right-movers individually are one-dimensional) and $\Delta = 1$ (for a massless scalar field), such that Eq. (2.197) transforms under $x^\pm \to y^\pm$ as

$$\langle 0|\partial_\pm\phi(y_1^\pm)\partial_\pm\phi(y_2^\pm)|0\rangle_x = -\frac{1}{4\pi}\left.\frac{dx^\pm}{dy^\pm}\right|_{y_1^\pm}\left.\frac{dx^\pm}{dy^\pm}\right|_{y_2^\pm}\frac{1}{(x^\pm(y_1^\pm) - x^\pm(y_2^\pm))^2}. \tag{2.199}$$

The renormalized version of the quantity in these correlators is given by:

$$: \partial_{\pm}\phi(x_1^{\pm})\partial_{\pm}\phi(x_2^{\pm}) := \partial_{\pm}\phi(x_1^{\pm})\partial_{\pm}\phi(x_2^{\pm}) + \frac{1}{4\pi}\frac{1}{(x_1^{\pm}-x_2^{\pm})^2}, \tag{2.200}$$

which is related to Eq. (2.189) through

$$: T_{\pm\pm}(x^{\pm}) := \lim_{x_1^{\pm}\to x_2^{\pm}} : \partial_{\pm}\phi(x_1^{\pm})\partial_{\pm}\phi(x_2^{\pm}) : . \tag{2.201}$$

Eq. (2.200) transforms to the $y^{\pm}$ coordinates according to

$$: \partial_{\pm}\phi(y^{\pm})\partial_{\pm}\phi(y'^{\pm}) := \left.\frac{dx^{\pm}}{dy^{\pm}}\right|_{y_1^{\pm}} \left.\frac{dx^{\pm}}{dy^{\pm}}\right|_{y_2^{\pm}} \partial_{\pm}\phi(x_1^{\pm})\partial_{\pm}\phi(x_2^{\pm}) + \frac{1}{4\pi}\frac{1}{(y_1^{\pm}-y_2^{\pm})^2}. \tag{2.202}$$

It is from the two-point function $\langle 0| : \partial_{\pm}\phi(y^{\pm})\partial_{\pm}\phi(y'^{\pm}) : |0\rangle_x$ that we can calculate the vacuum expectation value of the number operator. To see this, we write it out explicitly in terms of creation and annihilation operators. For brevity we consider only the right-mover sector y^-, but note that the derivation works irrespective of the choice $y^{\pm}$. Using the plane wave modes $u_{y,\omega} = \frac{1}{\sqrt{4\pi\omega}}e^{-i\omega y^{\pm}}$, i.e. the modes which have a positive frequency with respect to the y frame, and looking at Eq. (2.144) we get

$$\begin{aligned}\langle 0| : \partial_-\phi(y_1^-)\partial_-\phi(y_2^-) : |0\rangle_x = \sum_{ij}\Big[&\langle 0|b_j^\dagger b_i|0\rangle_x \left(\partial_{y_1^-}u_{y,i}\partial_{y_2^-}u^*_{y,j} + \partial_{y_1^-}u^*_{y,j}\partial_{y_2^-}u_{y,i}\right) \\ &+ \left(\langle 0|b_j b_i|0\rangle_x\, \partial_{y_1^-}u_{y,j}\partial_{y_2^-}u_{y,i} + \text{c.c.}\right)\Big].\end{aligned} \tag{2.203}$$

The next step is then to perform the Fourier transformation

$$\int_{-\infty}^{+\infty} dy_1^- \int_{-\infty}^{+\infty} dy_2^- u_\omega(y_1^-)u^*_{\omega'}(y_2^-)\,\langle 0| : \partial_-\phi(y_1^-)\partial_-\phi(y_2^-) : |0\rangle_x\,, \tag{2.204}$$

which can be written in terms of the number operator by using the Klein-Gordon inner product relations for modes:

$$(u_i, u_j) = \delta_{ij}, \qquad (u_i^*, u_j^*) = -\delta_{ij}, \qquad (u_i, u_j^*) = 0. \tag{2.205}$$

The result is

$$\int_{-\infty}^{+\infty} dy_1^- \int_{-\infty}^{+\infty} dy_2^- u_\omega(y_1^-)u^*_{\omega'}(y_2^-)\,\langle 0| : \partial_-\phi(y_1^-)\partial_-\phi(y_2^-) : |0\rangle_x = \frac{1}{4}\,\langle 0|b_\omega^\dagger b_{\omega'}|0\rangle_x\,. \tag{2.206}$$

For $\omega = \omega'$, this is immediately the number operator, such that

$$\langle 0|N_\omega|0\rangle_x = 4\int_{-\infty}^{+\infty} dy_1^- \int_{-\infty}^{+\infty} dy_2^- u_\omega(y_1^-)u^*_{\omega'}(y_2^-)\,\langle 0| : \partial_-\phi(y_1^-)\partial_-\phi(y_2^-) : |0\rangle_x\,. \tag{2.207}$$

Using then Equations (2.202), (2.199) and (2.197), it follows that

$$\begin{aligned}\langle 0| : \partial_- \phi(y_1^-)\partial_- \phi(y_2^-) : |0\rangle_x &= \langle 0|\partial_- \phi(y_1^-)\partial_- \phi(y_2^-)|0\rangle_x + \frac{1}{4\pi}\frac{1}{(y_1^- - y_2^-)^2} \\ &= \langle 0|\partial_- \phi(y_1^-)\partial_- \phi(y_2^-)|0\rangle_x - \langle 0|\partial_- \phi(y_1^-)\partial_- \phi(y_2^-)|0\rangle_y\end{aligned} \tag{2.208}$$

such that

$$\begin{aligned}\langle 0|N_\omega|0\rangle_x = -\frac{1}{\pi}\int_{-\infty}^{+\infty} dy_1^- \int_{-\infty}^{+\infty} dy_2^- u_\omega(y_1^-)u^*_{\omega'}(y_2^-) \\ \times \left[\left.\frac{dx^-}{dy^-}\right|_{y_1^-}\left.\frac{dx^-}{dy^-}\right|_{y_2^-}\frac{1}{(x^-(y_1^-) - x^-(y_2^-))^2} - \frac{1}{(y_1^- - y_2^-)^2}\right].\end{aligned} \tag{2.209}$$

This result has a nice physical interpretation, looking at Eq. (2.208). The production of quanta in the $|0\rangle_x$ vacuum, measured by the observer with local frame y, is related to the deviation of the correlator $\langle 0|\partial_\pm \phi(y_1^\pm)\partial_\pm \phi(y_2^\pm)|0\rangle_x$ from the corresponding value in the $|0\rangle_y$ vacuum [11].

To relate this result to our setup in JT gravity, let $x^\pm$ be the Poincaré lightcone coordinates (U, V) and $y^\pm$ the lightcone coordinates (u, v) of the observer. Recall that the bulk geometry is defined according to the reparameterization field F with $(U = F(u), V = F(v))$, which is then immediately the transformation $x^\pm(y^\pm)$ in Eq. (2.209). Using then the thermal reparameterization $F(y) = \tanh\frac{\pi}{\beta}f(y)$, the Poincaré vacuum expectation value of the occupation number $N_\omega[f] \equiv \langle 0|N_\omega|0\rangle_F$ of the modes $u_\omega(y)$ which have a positive frequency with respect to the observer's local frame y becomes [24]:

$$N_\omega[f] = -\frac{1}{\pi}\int dy_1 \int dy_2 u_\omega(y_1)u^*_\omega(y_2)\left[\frac{f'(y_1)f'(y_2)}{\frac{\beta^2}{\pi^2}\sinh^2\frac{\pi}{\beta}(f(y_1) - f(y_2))} - \left(\frac{1}{y_1 - y_2}\right)^2\right]. \tag{2.210}$$

Where we recognise the first term in the brackets as the Schwarzian bilocal of weight $\Delta = 1$ (recall that this is the case for massless fields). The second term regularises the expression such that the result is finite at $y_1 \to y_2$. The modes are again given by the plane waves

$$u_\omega(y) = \frac{1}{\sqrt{4\pi\omega}}e^{-i\omega y}. \tag{2.211}$$

Let us first discuss the semi-classical result, i.e. the gravitational saddle $f(y) = y$ where the observer's local frame is the black hole patch, following [24]. The occupation number becomes

$$N_\omega[f(y) = y] = \frac{-1}{4\pi^2\omega} \int dy_1 \int dy_2 e^{-i\omega(y_1 - y_2)} \left[\frac{1}{\frac{\beta^2}{\pi^2} \sinh^2 \frac{\pi}{\beta}(y_1 - y_2)} - \left(\frac{1}{y_1 - y_2} \right)^2 \right]. \tag{2.212}$$

We see that the double integral only depends on $y_1 - y_2$. As such, it is constructive to rewrite the integrals in terms of $y_1 + y_2$ and $y_1 - y2 \equiv t$. The former integral factorizes out and results in a divergent prefactor $2\pi\delta(0)$. We get

$$N_\omega[f(y) = y] = -\frac{\delta(0)}{2\pi\omega} \int_{-\infty}^{+\infty} dt e^{-i\omega t} \left[\frac{1}{\frac{\beta^2}{\pi^2} \sinh^2 \frac{\pi}{\beta} t} - \frac{1}{t^2} \right]. \tag{2.213}$$

Both terms have a pole at $t = 0$, so we employ the regularisation $t \to \mp i\epsilon$. For the first term we then use the Fourier transform identity

$$\frac{-1}{2\pi\omega} \int_{-\infty}^{+\infty} dt \frac{1}{\frac{\beta^2}{\pi^2} \sinh^2(\frac{\pi}{\beta}(t \mp i\epsilon))} e^{-i\omega t} = \frac{e^{\mp \frac{\beta}{2}\omega}}{e^{\frac{\beta}{2}\omega} - e^{-\frac{\beta}{2}\omega}}. \tag{2.214}$$

For the second term we get, following from the integral definition of the Heaviside step function,

$$-\frac{1}{2\pi\omega} \int_{-\infty}^{+\infty} dt \frac{1}{(t \mp i\epsilon)^2} e^{-i\omega t} = \mp\Theta(\mp\omega). \tag{2.215}$$

This has a nice physical interpretation. Recall that the second term in Eq. (2.210) originates from the vacuum contribution of the $|0\rangle_y$ vacuum. This is confirmed by the fact that the Heavisides appearing in Eq. (2.215) are the zero temperature ($\beta \to \infty$) limit of Eq. (2.214):

$$\lim_{\beta \to \infty} \frac{e^{\mp \frac{\beta}{2}\omega}}{e^{\frac{\beta}{2}\omega} - e^{-\frac{\beta}{2}\omega}} = \mp\Theta(\mp\omega), \tag{2.216}$$

recall as well that the Poincaré patch is the $\beta \to \infty$ limit of the black hole patch. Putting these together we get

$$\begin{aligned} N_\omega[f(y) = y] &= \frac{e^{\mp \frac{\beta}{2}\omega}}{e^{\frac{\beta}{2}\omega} - e^{-\frac{\beta}{2}\omega}} \pm \Theta(\mp\omega) \\ &= \frac{e^{-\frac{\beta}{2}\omega}}{e^{\frac{\beta}{2}\omega} - e^{-\frac{\beta}{2}\omega}}, \end{aligned} \tag{2.217}$$

where we have omitted the divergent prefactor, and we find that the result is independent of the choice of regularization $t \to \mp i\epsilon$.

In the full quantum gravity picture, however, the situation is different. Much like how quantization introduces order ambiguity when it comes to operators, the quantum

gravity formalism has an order ambiguity when it comes to the regularizations $\mp i\epsilon$, which correspond to the time-ordered ($+i\epsilon$) and anti-time-ordered ($-i\epsilon$) correlators[21]. A priori it isn't clear which ordering to choose, but a posteriori we know that the correct choice is to take the average over time-ordering and anti-time-ordering. The expression to be calculated now involves plugging Eq. (2.210) into the Schwarzian path integral (for this discussion we set $C = 1/2$):

$$\langle N_\omega \rangle_\beta = \int [\mathcal{D}f] N_\omega[f] e^{-I[f]} \tag{2.218}$$

The derivation goes as follows, also following [24]. For certain fields f within the path integral, the expression can in this case be dependent not just on $y_1 - y_2$, but also on either y_i individually. However, since the bilocal operator is invariant under SL(2, $\mathbb{R}$), it commutes with the Hamiltonian of the Schwarzian system [27]

$$[G_\Delta(t_1, t_2), H_{\text{Schw}}] = 0. \tag{2.219}$$

such that the result will again only depend on the time difference $y_1 - y_2$. This can also be seen by looking at Eq. (2.115), which explicitly shows that the correlation function of the bilocal depends only on $\tau_1 - \tau_2$ (this statement also works for Lorentzian times). We again rewrite the integrals in terms of $y_1 \pm y_2$ and the $y_1 + y_2$ integral gives the same divergent prefactor $2\pi\delta(0)$. We get, taking into account the averaging over time orderings[22]:

$$\begin{aligned} N_\omega[f] = -\frac{\delta(0)}{2\pi\omega} \int_{-\infty}^{+\infty} dt e^{-i\omega t} \Bigg[\frac{1}{2} \left(\frac{f'(y_1)f'(y_2)}{\frac{\beta^2}{\pi^2}\sinh^2(\frac{\pi}{\beta}(t+i\epsilon))} + \frac{f'(y_1)f'(y_2)}{\frac{\beta^2}{\pi^2}\sinh^2(\frac{\pi}{\beta}(t-i\epsilon))} \right) \\ - \frac{1}{2} \left(\frac{1}{(t+i\epsilon)^2} + \frac{1}{(t-i\epsilon)^2} \right) \Bigg]. \end{aligned} \tag{2.220}$$

To insert this into the path integral, we get

$$\begin{aligned} \langle N_\omega[f] \rangle = -\frac{\delta(0)}{2\pi\omega} \int_{-\infty}^{+\infty} dt e^{-i\omega t} \\ \times \int [\mathcal{D}f] e^{-S[f]} \Bigg[\frac{1}{2} \left(\frac{f'(y_1)f'(y_2)}{\frac{\beta^2}{\pi^2}\sinh^2(\frac{\pi}{\beta}(t+i\epsilon))} + \frac{f'(y_1)f'(y_2)}{\frac{\beta^2}{\pi^2}\sinh^2(\frac{\pi}{\beta}(t-i\epsilon))} \right) \\ - \frac{1}{2} \left(\frac{1}{(t+i\epsilon)^2} + \frac{1}{(t-i\epsilon)^2} \right) \Bigg] \end{aligned} \tag{2.221}$$

where we have dropped the subscript β in the lhs. The $(t \pm i\epsilon)^-2$ terms can be taken out of the path integral. What remains is then just the partition function, which is

[21] Recall the discussion in Section 2.3.3.1

[22] The notation for this expression is slightly sketchy since the f' fields still depend on the original y_i coordinates, but this issue will resolve itself in the further steps.

cancelled out due to the normalisation. The Fourier transform can then again be evaluated using the definition of the Heaviside function, leading to a term

$$\frac{1}{2}\left(-\Theta(\omega)+\Theta(-\omega)\right). \tag{2.222}$$

For positive frequency modes $\omega > 0$, this becomes $-1/2$. What remains is a path integral over the time-ordered and anti-time-ordered Schwarzian bilocal, which can be evaluated using (the real-time expression of) Eq. (2.115). The time-ordered and anti-time ordered correlators are each others complex conjugate. The exponential factors in Eq. (2.115) become:

$$\begin{aligned} \text{time-ordered:} \quad & e^{-itk_1^2}e^{-(\beta-it)k_2^2} = e^{-it(k_1^2-k_2^2)}e^{-\beta k_2^2} \\ \text{anti-time-ordered:} \quad & e^{itk_1^2}e^{-(\beta+it)k_2^2} = e^{it(k_1^2-k_2^2)}e^{-\beta k_2^2}. \end{aligned} \tag{2.223}$$

Note that the anti-time-ordered expression is the complex conjugate of the time-ordered expression. The occupation number becomes:

$$\begin{aligned} \langle N_\omega[f]\rangle + \frac{1}{2} = \frac{1}{8\pi^3\omega}\frac{1}{Z}\int_{-\infty}^{+\infty} dt e^{-i\omega t}\int d\mu(k_1)d\mu(k_2) \\ \times e^{-\beta k_2^2}\left(e^{-it(k_1^2-k_2^2)}+e^{it(k_1^2-k_2^2)}\right)\Gamma(1\pm ik_1\pm ik_2) \end{aligned} \tag{2.224}$$

where we have again neglected the divergent prefactor and the measure is again given by $d\mu(k) = \sinh(2\pi k)dk^2$.[23] Rewriting this expression as

$$\begin{aligned} \langle N_\omega[f]\rangle + \frac{1}{2} = \frac{1}{8\pi^3\omega}\frac{1}{Z}\int d\mu(k_1)d\mu(k_2)e^{-\beta k_2^2}\Gamma(1\pm ik_1\pm ik_2) \\ \times\int_{-\infty}^{+\infty} dt\left(e^{-it(\omega+k_1^2-k_2^2)}+e^{-it(\omega-k_1^2+k_2^2)}\right), \end{aligned} \tag{2.225}$$

it is clear that the time integrals evaluate to the delta-functions $2\pi\delta(\omega\pm k_1^2\mp k_2^2)$. This has the physical interpretation of energy conservation. Take for instance $\delta(\omega-k_1^2+k_2^2)$: this can be interpreted as a black hole with initial energy k_1^2 (recall that $C=1/2$), which emits a mode with energy ω to end up with a final energy k_2^2. The delta-function enforces $k_1^2=\omega+k_2^2$, which is then simply a bookkeeping result, see Fig. (2.13). We get

$$\begin{aligned} \langle N_\omega[f]\rangle + \frac{1}{2} = \frac{1}{4\pi^2\omega}\frac{1}{Z}\int d\mu(k_1)d\mu(k_2)e^{-\beta k_2^2}\Gamma(1\pm ik_1\pm ik_2) \\ \times\left(\delta(\omega+k_1^2-k_2^2)+\delta(\omega-k_1^2+k_2^2)\right). \end{aligned} \tag{2.226}$$

Using the delta functions, we can eliminate one of the two k-integrals. There is a

[23] Sometimes the convention $d\mu(k) = \sinh(2\pi k)kdk$ is used instead, in which case the prefactor becomes $1/(2\pi^3\omega)$.

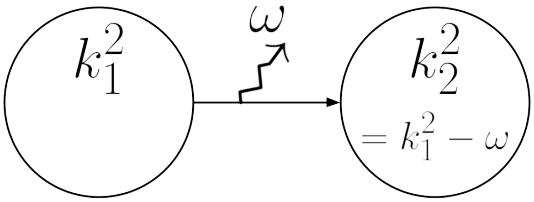

Fig. 2.13: Energy conservation interpretation of $\delta(\omega - k_1^2 + k_2^2)$. A black hole with energy k_1^2 radiates a mode with ω and ends up with energy k_2^2.

subtlety here however, as the two delta's are used to eliminate different k-integrals. We proceed as follows:

$$\delta(\omega + k_1^2 - k_2^2): \quad k_2^2 = \omega + k_1^2$$
$$\Rightarrow \begin{cases} e^{-\beta k_2^2} & \longrightarrow e^{-\beta(\omega + k_1^2)} \\ \Gamma(1 \pm i k_1 \pm i k_2) & \longrightarrow \Gamma\left(1 \pm i k_1 \pm i\sqrt{\omega + k_1^2}\right) \\ \sinh(2\pi k_2) & \longrightarrow \sinh\left(2\pi\sqrt{\omega + k_1^2}\right) \end{cases} \tag{2.227}$$

$$\delta(\omega - k_1^2 + k_2^2): \quad k_1^2 = \omega + k_2^2$$
$$\Rightarrow \begin{cases} \Gamma(1 \pm i k_1 \pm i k_2) & \longrightarrow \Gamma\left(1 \pm i k_2 \pm i\sqrt{\omega + k_2^2}\right) \\ \sinh(2\pi k_1) & \longrightarrow \sinh\left(2\pi\sqrt{\omega + k_2^2}\right). \end{cases} \tag{2.228}$$

Relabeling the remaining k_i to k we get as a final result:

$$\langle N_\omega \rangle_\beta = \frac{1 + e^{-\beta\omega}}{4\pi^2\omega} \frac{1}{Z} \int d\mu(k) \sinh\left(2\pi\sqrt{\omega + k^2}\right) e^{-\beta k^2} \Gamma(1 \pm ik \pm i\sqrt{\omega + k^2}) - \frac{1}{2}. \tag{2.229}$$

This is the full quantum gravity generalization of Eq. (2.217). This integral is solvable numerically, and we can use it to plot the spectral density $\omega N_\omega(\omega)$ (we will also call this the spectrum throughout further discussions). The result, together with the semi-classical result (2.217) are plotted in Fig. (2.14).

One way to verify the result Eq. (2.229) is to compare it to the energy density obtained from the stress tensor components. More specifically, the following equality should hold:

$$\int_0^\infty d\omega\omega \langle N_\omega \rangle = \int_{-\infty}^{+\infty} dy \langle : T_{\pm\pm} : \rangle \tag{2.230}$$

The was verified in detail in [24]. For a brief illustration of this agreement, we know from Eq. (2.195) that the total energy density of the semi-classical heat bath should be lower than that of the exact quantum gravity result. In Fig. (2.14), this would correspond to a lower population of the modes for the semi-classical result, which we do indeed see.

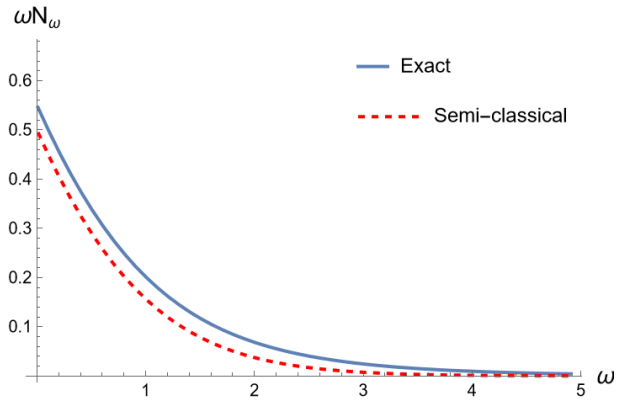

Fig. 2.14: Energy spectral density for the uncharged Unruh effect in JT-gravity with $\beta = 2$. The exact result Eq. (2.229) was calculated numerically. The semi-classical spectrum is given by Eq. (2.217)

This whole setup can be generalized to that of a charged black hole with chemical potential μ emitting charged Unruh radiation with charge Q. This is further explored in Chapter 4.

3 Correlators beyond the black hole horizon

This chapter is the first of two which contains original work, and aims to generalise the setup of bulk correlation functions described in Section 2.3.4 to the case where at least one of the points is located beyond the black hole horizon. Section 3.1 goes over the procedure to define bulk points beyond the horizon and includes first a brief overview of the thermofield double state formalism, but what follows is original work.

3.1 Points beyond the horizon

As discussed before, the radar definition of bulk points using the holographic boundary as an anchor only allows us to define points outside of the black hole, i.e. in the black hole patch. The rest of the spacetime is inaccessible, even though the Poincaré coordinates, and thus the possible values of the field $F(u), F(v)$, reach outside of this area. The setup for defining points beyond the horizon then makes use of the construction of a thermofield double (TFD) state. The idea of introducing a TFD state to define bulk points beyond the black hole patch was already briefly introduced in [2], but not further elaborated on. In essence, we want to use the second boundary of the TFD to anchor points to.

3.1.1 The TFD state

As a brief review of the concept of the thermofield double state, we follow [15]. Consider a quantum field theory with Hamiltonian H and eigenstates $|n\rangle$ with energy E_n. The "trick" of the TFD state is now to double the degrees of freedom, in the sense that we now consider a new QFT consisting of the original QFT and a copy. The two QFT's live in separate spacetimes and a state in the doubled QFT takes the form

$$|m\rangle_1 |n\rangle_2 . \tag{3.1}$$

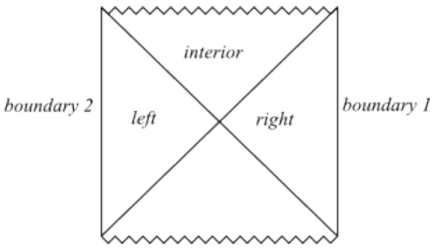

Fig. 3.1: Full, two-sided Penrose diagram for an eternal black hole.

We can now define a specific pure state in the doubled QFT, namely the TFD state:

$$|TFD\rangle = \frac{1}{\sqrt{Z(\beta)}} \sum_n e^{-\beta E_n/2} |n\rangle_1 |n\rangle_2 . \tag{3.2}$$

The density matrix in this state is

$$\rho = |TFD\rangle \langle TFD| , \tag{3.3}$$

such that the reduced density matrix of system 1 becomes

$$\rho_1 = \mathrm{Tr}_2 \, \rho = \sum_n e^{-\beta E_n} |n\rangle_1 \langle n|_1 = e^{-\beta H_1}, \tag{3.4}$$

which is a thermal state. This is the main usefulness of the TFD within quantum field theory: the ability to describe a thermal state of a system as a pure state in the doubled system.

The usefulness for our purposes comes from the analogy between the TFD state formalism and the Penrose diagram for an eternal black hole. Namely, an eternal black hole has a full two-sided Penrose diagram, as can be seen in Fig. (3.1). More specifically for our case, the eternal black hole in AdS has two holographic boundaries, with a copy of the dual CFT on either boundary. The full system is thus dual to the two copies of the CFT, which are in the TFD state.

As an aside, it is worth mentioning that the AdS_2 black holes in JT gravity are not necessarily eternal. In fact, the example in Section 2.2.3.2 explicitly showed the formation of an AdS black hole. While the left and bottom wedge only have physical meaningfulness in the case of an eternal black hole, the construction of the TFD state can still be used as a mathematical framework to define points beyond the horizon in the case of a non-eternal black hole, since this region (i.e. the upper wedge or interior) is always well-defined.

3.1.2 Using the second boundary

Consider an operator $\mathcal{O}(t)$ located on the first holographic boundary. We can access an equivalent operator on the second boundary by performing a sort of Wick rotation. More specifically, we perform the transformation $t \to t \pm i\frac{\beta}{2}$ to access the second boundary[1]. The choice of $+i\frac{\beta}{2}$ or $-i\frac{\beta}{2}$ is not necessarily equivalent, as will become apparent later on. For now we continue with the convention $+i\frac{\beta}{2}$ for convenience of notation. Note that, since Euclidean time is periodic in β, a rotation over $i\beta$ would end up back on the first boundary[2]. Looking at Fig. (3.2), we get for an operator on the second boundary:

$$\widetilde{\mathcal{O}}\left(\widetilde{t}_1\right) = \mathcal{O}\left(t_1 + i\frac{\beta}{2}\right). \tag{3.5}$$

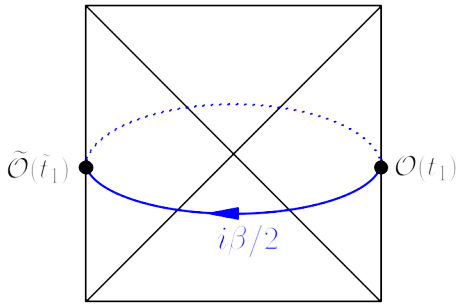

Fig. 3.2: Accessing the second boundary via a wick rotation.

Using this setup, we can now anchor points to the second boundary using a generalisation of the radar definition. More specifically, consider a point $(\widetilde{u}', v')$ located in the interior of the black hole, as can be seen in Fig. (3.3). Before, this point would not be definable using the radar definition introduced in Chapter 2, since the u' coordinate required for the anchoring falls outside of the $t \in]-\infty, +\infty[$ range. We can still shoot out a lightray which reaches this point, providing the v' coordinate in the usual way. However, to get the corresponding u coordinate we now reflect the lightray towards the second boundary instead. For this purpose it is important to make note of the fact that time runs backwards (i.e. from top to bottom in the diagram) in the left wedge. This is generally the case for a two-sided Penrose diagram [15], but in this case it is specifically needed geometrically to be able to interpret the $\widetilde{u}'$ coordinate on the second boundary as indeed being defined by an incoming lightray on the boundary instead of an outgoing one, or in other words as the additive lightcone coordinate $\widetilde{u} = \widetilde{t} + \widetilde{z}$. The new coordinate $\widetilde{u}'$ can now be

[1] The idea stems from a personal communication with Prof. Dr. Thomas G. Mertens, and is also briefly mentioned in [26]

[2] Although this procedure is not necessarily trivial and correlators don't have to be invariant under $t \to t + i\beta$.

related to the coordinate u on the first boundary through the relation $\widetilde{u}' = u' + i\frac{\beta}{2}$. The definition of our point is thus now

$$(\widetilde{u}', v') = (u' + i\frac{\beta}{2}, v'). \tag{3.6}$$

With this lightray definition of points beyond the horizon, we can now construct bulk two-point functions between a point (u, v) on the exterior and a point $(\widetilde{u}', v')$ on the interior of the black hole. We get the relation:

$$\langle G_{bb}(u, v, \tilde{u}', v')\rangle = \left\langle G_{bb}\left(u, v, u' + i\frac{\beta}{2}, v'\right)\right\rangle. \tag{3.7}$$

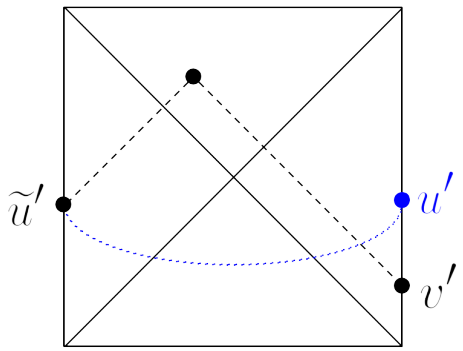

Fig. 3.3: Defining a bulk point $(\widetilde{u}', v')$ beyond the horizon using the second boundary.

3.2 Beyond-horizon correlators

We now move on to the explicit calculation of correlators of the form (3.7).

3.2.1 Semi-classical two-point function

We start with the semi-classical case where the reparameterization is on the gravitational saddle $F(t) = \tanh\frac{\pi}{\beta}t$, i.e. $f(t) = t$. The bulk two-point function is then simply the CFT two-point function, since we don't perform the Schwarzian path integral[3]. In terms of the reparameterization fields this is given by Eq. (2.124):

$$\begin{aligned} G &= \ln\left|\frac{(F(u) - F(u'))(F(v) - F(v'))}{(F(v) - F(u'))(F(u) - F(v'))}\right| \\ &= \ln\left|\frac{(\tanh\frac{\pi}{\beta}f(u) - \tanh\frac{\pi}{\beta}f(u'))(\tanh\frac{\pi}{\beta}f(v) - \tanh\frac{\pi}{\beta}f(v'))}{(\tanh\frac{\pi}{\beta}f(v) - \tanh\frac{\pi}{\beta}f(u'))(\tanh\frac{\pi}{\beta}f(u) - \tanh\frac{\pi}{\beta}f(v'))}\right|, \end{aligned} \tag{3.8}$$

[3]Or rather the path integral is localised on the saddle

where we have omitted the prefactor. Now setting $f(u) = u$ we can write this as:

$$\begin{aligned} G_{f(u)=u} &= \ln \left| \frac{(\tanh \frac{\pi}{\beta} u - \tanh \frac{\pi}{\beta} u')(\tanh \frac{\pi}{\beta} v - \tanh \frac{\pi}{\beta} v')}{(\tanh \frac{\pi}{\beta} v - \tanh \frac{\pi}{\beta} u')(\tanh \frac{\pi}{\beta} u - \tanh \frac{\pi}{\beta} v')} \right| \\ &= \ln \left| \frac{\sinh \frac{\pi}{\beta}(v' - v) \sinh \frac{\pi}{\beta}(u' - u)}{\sinh \frac{\pi}{\beta}(u' - v) \sinh \frac{\pi}{\beta}(v' - u)} \right|. \end{aligned} \tag{3.9}$$

To adapt this result to the case where any one point is beyond the horizon, we simply make the relevant substitutions $t \to \widetilde{t} = t + i\frac{\beta}{2}$.

3.2.1.1 One point beyond the horizon

We first take the case where only one point is beyond the horizon. Let this point be $(\widetilde{u}', v')$ such that we get:

$$\begin{aligned} G_{f(u)=u} &= \ln \left| \frac{\sinh \frac{\pi}{\beta}(v' - v) \sinh \frac{\pi}{\beta}(\widetilde{u}' - u)}{\sinh \frac{\pi}{\beta}(\widetilde{u}' - v) \sinh \frac{\pi}{\beta}(v' - u)} \right| \\ &= \ln \left| \frac{\sinh \frac{\pi}{\beta}(v' - v) \sinh \frac{\pi}{\beta}(u' - u + i\frac{\beta}{2})}{\sinh \frac{\pi}{\beta}(u' - v + i\frac{\beta}{2}) \sinh \frac{\pi}{\beta}(v' - u)} \right|. \end{aligned} \tag{3.10}$$

Using $\sinh(x + iy) = \sinh x \cos y + i \cosh x \sin y$ we get

$$\begin{aligned} G_{f(u)=u} &= \ln \left| \frac{\sinh \frac{\pi}{\beta}(v' - v) \left[\sinh \frac{\pi}{\beta}(u' - u) \cos \frac{\pi}{2} + i \cosh \frac{\pi}{\beta}(u' - u) \sin \frac{\pi}{2} \right]}{\left[\sinh \frac{\pi}{\beta}(u' - v) \cos \frac{\pi}{2} + i \cosh \frac{\pi}{\beta}(u' - v) \sin \frac{\pi}{2} \right] \sinh \frac{\pi}{\beta}(v' - u)} \right| \\ &= \ln \left| \frac{\sinh \frac{\pi}{\beta}(v' - v) \cosh \frac{\pi}{\beta}(u' - u)}{\cosh \frac{\pi}{\beta}(u' - v) \sinh \frac{\pi}{\beta}(v' - u)} \right| \end{aligned} \tag{3.11}$$

where the imaginary units have nicely canceled out. This result is again Eq. (3.9), but where now the $\sinh$'s which have a u' coordinate in their argument have been swapped out for $\cosh$'s.

We can alternatively define the interior point using the transformation $\widetilde{u}' = u' - i\frac{\beta}{2}$. Using $\sinh(x - iy) = \sinh x \cos y - i \cosh x \sin y$, this leads to the expression

$$\begin{aligned} G_{f(u)=u} &= \ln \left| \frac{\sinh \frac{\pi}{\beta}(v' - v) \left[\sinh \frac{\pi}{\beta}(u' - u) \cos \frac{\pi}{2} - i \cosh \frac{\pi}{\beta}(u' - u) \sin \frac{\pi}{2} \right]}{\left[\sinh \frac{\pi}{\beta}(u' - v) \cos \frac{\pi}{2} - i \cosh \frac{\pi}{\beta}(u' - v) \sin \frac{\pi}{2} \right] \sinh \frac{\pi}{\beta}(v' - u)} \right| \\ &= \ln \left| \frac{\sinh \frac{\pi}{\beta}(v' - v) \cosh \frac{\pi}{\beta}(u' - u)}{\cosh \frac{\pi}{\beta}(u' - v) \sinh \frac{\pi}{\beta}(v' - u)} \right| \end{aligned} \tag{3.12}$$

which is the exact same result as when we used $\widetilde{u}' = u' + i\frac{\beta}{2}$.

3.2.1.2 Both points beyond the horizon

We now put both points inside the black hole. In this case we have $\widetilde{u}' = u' + i\frac{\beta}{2}$ and $\widetilde{u} = u + i\frac{\beta}{2}$. The calculations are analogous:

$$\begin{aligned} G_{f(u)=u} &= \ln \left| \frac{\sinh \frac{\pi}{\beta}(v'-v) \sinh \frac{\pi}{\beta}(u'-u+i\frac{\beta}{2}-i\frac{\beta}{2})}{\sinh \frac{\pi}{\beta}(u'-v+i\frac{\beta}{2}) \sinh \frac{\pi}{\beta}(v'-u-i\frac{\beta}{2})} \right| \\ &= \ln \left| \frac{\sinh \frac{\pi}{\beta}(v'-v) \sinh \frac{\pi}{\beta}(u'-u)}{i \cosh \frac{\pi}{\beta}(u'-v)(-i) \cosh \frac{\pi}{\beta}(v'-u)} \right| \\ &= \ln \left| \frac{\sinh \frac{\pi}{\beta}(v'-v) \sinh \frac{\pi}{\beta}(u'-u)}{\cosh \frac{\pi}{\beta}(u'-v) \cosh \frac{\pi}{\beta}(v'-u)} \right| \end{aligned} \tag{3.13}$$

Again the $\sinh$'s of Eq. (3.9) have been replaced by $\cosh$'s where the adapted coordinates appear, with the exception of the argument where they both appear, since there the contributions cancel. Note that we can again consider other combinations of $\pm i\frac{\beta}{2}$, but here as well the result is independent of these choices. Take for example the case where $\widetilde{u} = u - i\frac{\beta}{2}$. In the numerator we get $\sinh \frac{\pi}{\beta}(u' - u + i\beta)$, which becomes $\sinh(\frac{\pi}{\beta}(u'-u) + i\pi) = -\sinh \frac{\pi}{\beta}(u'-u)$. In de denominator we get $i^2 = -1$, such that the cancellation happens even without having to take the modulus. The other combinations of $\pm i\frac{\beta}{2}$ follow analogous arguments.

3.2.1.3 General result

These result are generalisable to the other cases where e.g. one point is in the left wedge. More specifically, the two-point function 3.9 can be easily modified by replacing the $\sinh$'s by $\cosh$'s where only one of the coordinates in the argument is located on the second boundary, but not both. Since each coordinate appears exactly twice in the expression, imaginary units appear in pairs which are multiplied or divided such that the result is always real, even without having to take the modulus.

Interestingly, the semi-classical result is independent of the choice $u \pm i\frac{\beta}{2}$. We will see later on that this is not the case for quantum gravity corrections, analogous to the inequivalence of time orderings for the exact two-point function where both points are on the exterior of the black hole, as discussed in Section 2.3.3.1. Recall also the similarity with the Unruh occupation number of Section 2.4.2.3, where the semi-classical result is also independent of the time-ordering $\pm i\varepsilon$, but the orderings are inequivalent in the quantum gravity result.

3.2.2 Quantum gravity two-point function

The quantum gravity bulk two-point function is given by Eq. (2.134), repeated here:

$$\begin{aligned}\langle G_{bb}(\tilde{t},z,z')\rangle_\beta = \int_0^\infty dM \sinh\left(2\pi\sqrt{M}\right) e^{-\beta M} \int_0^\infty dE \sinh\left(2\pi\sqrt{E}\right) e^{iT\omega} \\ \times \frac{\sin z\omega}{\omega}\frac{\sin z'\omega}{\omega}\Gamma(1\pm i\sqrt{M}\pm i\sqrt{E}),\end{aligned} \tag{2.134}$$

where $T = t - t'$ and $\omega = E - M$. As in the semi-classical case, we will directly adapt this result by substituting the relevant coordinates by their second boundary counterparts. To this end, we will rewrite this expression explicitly in terms of lightcone coordinates:

$$\begin{cases} z = \frac{1}{2}(u-v) \\ z' = \frac{1}{2}(u'-v') \\ T = \frac{1}{2}(u+v-u'-v'), \end{cases} \tag{3.14}$$

such that

$$\begin{aligned}\langle G_{bb}\rangle_\beta = \int_0^\infty dM \sinh\left(2\pi\sqrt{M}\right) e^{-\beta M} \int_0^\infty dE \sinh\left(2\pi\sqrt{E}\right) \\ \times \exp\left[\frac{i}{2}(u-u'+v-v')\omega\right]\Gamma(1\pm i\sqrt{M}\pm i\sqrt{E}) \\ \times \frac{\sin\frac{1}{2}(u-v)\omega}{\omega}\frac{\sin\frac{1}{2}(u'-v')\omega}{\omega}.\end{aligned} \tag{3.15}$$

3.2.2.1 One point beyond the horizon

Taking the case where one point is beyond the horizon ($u' \to \widetilde{u}' = u' + i\frac{\beta}{2}$) we get

$$\begin{aligned}\langle G_{bb}\rangle_\beta = \int_0^\infty dM \sinh\left(2\pi\sqrt{M}\right) e^{-\beta M} \int_0^\infty dE \sinh\left(2\pi\sqrt{E}\right) \\ \times \exp\left[\frac{i}{2}\left(u-u'+v-v'-i\frac{\beta}{2}\right)\omega\right]\Gamma(1\pm i\sqrt{M}\pm i\sqrt{E}) \\ \times \frac{\sin\frac{1}{2}(u-v)\omega}{\omega}\frac{\sin\frac{1}{2}(u'-v'+i\frac{\beta}{2})\omega}{\omega}\end{aligned} \tag{3.16}$$

It is here that we first notice that this result is not independent of $i\frac{\beta}{2} \to -i\frac{\beta}{2}$. In fact, only one case is well-behaved for large energies, since the other is divergent as $E \to \infty$. More specifically, depending on our choice we get the exponential factors

$$\begin{cases} e^{\frac{-5\beta}{4}M} e^{\frac{\beta}{4}E} & \text{if } \widetilde{u}' = u' + i\frac{\beta}{2} \\ e^{\frac{-3\beta}{4}M} e^{\frac{-\beta}{4}E} & \text{if } \widetilde{u}' = u' - i\frac{\beta}{2} \end{cases} \tag{3.17}$$

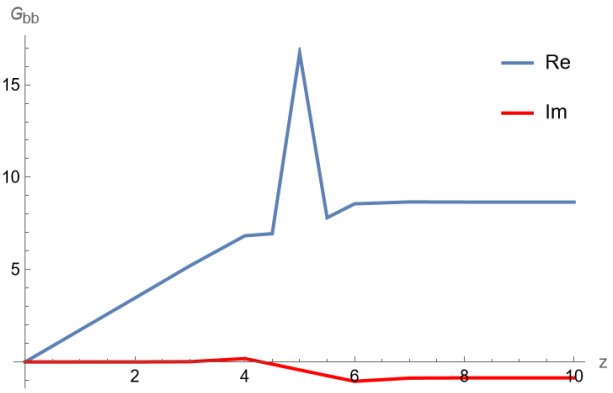

Fig. 3.4: Real and imaginary parts of the (normalised) two-point function where one point $(\widetilde{u}', v')$ is situated on the interior of the black hole in function of z, with $z' = 5$ and $iT = 0.1$.

such that the first case diverges for $E \to \infty$. The correct choice here is thus determined by whichever one ends up with a non-divergent exponential, since a correlation function which is infinite everywhere cannot be meaningfully interpreted. As such from now on we set $\widetilde{u}' = -i\frac{\beta}{2}u'$. Using

$$\begin{aligned}\sin\left(\frac{1}{2}\left(u'-v'-i\frac{\beta}{2}\right)\omega\right) &= \sin\left(\frac{\omega}{2}(u'-v') - i\frac{\omega}{4}\beta\right) \\ &= \sin\omega z' \cosh\frac{\omega\beta}{4} - i\cos\omega z' \sinh\frac{\omega\beta}{4}\end{aligned} \tag{3.18}$$

we get

$$\langle G_{bb}\rangle_\beta = \int_0^\infty d\mu(M) e^{\frac{-3\beta}{4}M} \int_0^\infty d\mu(E) e^{iT\omega} e^{\frac{-\beta}{4}E} \frac{\sin z\omega}{\omega} \frac{\chi^*(z')}{\omega} \Gamma(1 \pm i\sqrt{M} \pm i\sqrt{E}) \tag{3.19}$$

where

$$\chi(z') = \sin\omega z' \cosh\frac{\omega\beta}{4} + i\cos\omega z' \sinh\frac{\omega\beta}{4} \tag{3.20}$$

and $d\mu(M) = \sinh\left(2\pi\sqrt{M}\right) dM$. We can plot this result for a Euclidean time. The result can be seen in Fig. (3.4) and has some similarities with the case where both points are outside of the black hole, see Fig. (2.12). We see a general upwards trend as z increases, with a peak where $z = z'$.

With the coordinate $\widetilde{u}'$ in Eq. (3.18) having been split into its u' part and the contribution from $-i\frac{\beta}{2}$, we would like to have a way of interpreting why there is a peak at $z = z'$. In other words, what is special about the locus $\widetilde{u}' = u' - i\frac{\beta}{2} = z + t' - i\frac{\beta}{2}$. This interpretation is not straightforward however, as will now be illustrated. While the coordinates (u', v') seem like they define a new point (u', v') anchored to the first boundary, the interpretation of these coordinates as lightcone coordinates does not always make sense. Let us call this point (u', v') the "image point" of $(\widetilde{u}', v')$, such

that the peak occurs where the image point has the same z-coordinate as the exterior point. However, because of the geometrical construction of the anchoring, it is possible for the interior point to be located such that $u' < v'$, which is contradictory if we want to interpret $u' = t' + z'$ and $v' = t' - z'$ as lightcone coordinates of the image point, since $z' \geq 0$. As it turns out, the points which have such "anomalous" image points are those which are situated on the right half of the TFD state, i.e. to the right of the vertical center line where the left and right wedge meet. This can be seen in Fig. (3.5).

As an additional check, Fig. (3.6) investigates how an image point moves in relation to the interior point when the interior point is moved parallel to the z-axis, i.e. along a constant time slice. Taking first the case of the non-anomalous blue point, we see that if the interior point moves to the left, so does its image point. For the anomalous red point, the inverse is true: as the interior point moves left, its image point moves right. This, together with $u' < v'$, seems to suggest that when it comes to interpreting the anomalous image points, there is some inversion of the meaning of the z coordinate, $z' \to -z'$. Regardless, the specific way to interpret why there is a peak at $z' = z$ is, as of yet, unclear.

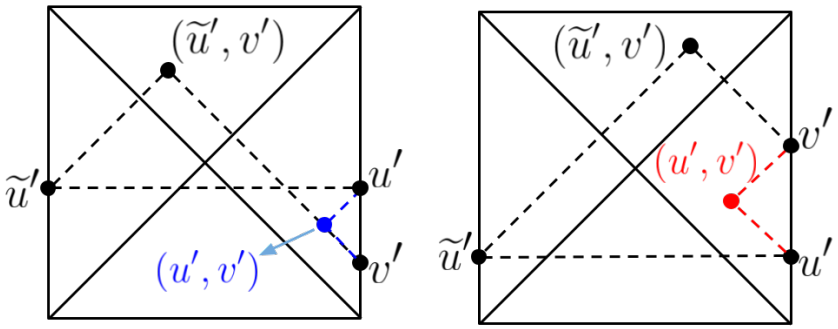

Fig. 3.5: Construction of image points (u', v') from points on the interior of the black hole. Left: interior point has an image point with a valid lightcone coordinate interpretation. Right: interior point has an anomalous image point where $u' < v'$.

It is also worth noting that the correlator has a finite imaginary part. This is not necessarily a problem, as the exact quantum gravity two-point function Eq. (2.115) also has non-trivial imaginary behaviour, as was discussed in Section 2.3.3.1. We can see in Fig. (3.4) that the absolute value of the imaginary part grows in the vicinity of the peak, after which is stays roughly constant.

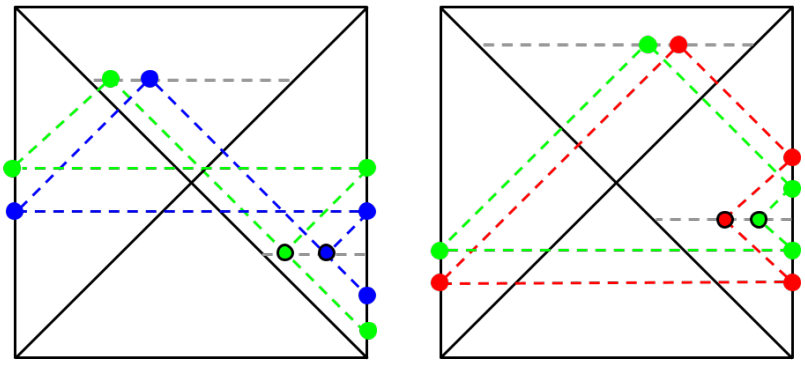

Fig. 3.6: Movement of interior points and their image point along a constant time slice. Image points have a black border. Left: non-anomalous point. If the interior point (blue) moves left (green), its image point also moves left. Right: anomalous point. If the interior point (red) moves left (green), its image point moves right.

3.2.2.2 Both points beyond the horizon

Just as in the semi-classical case we can also look at the case where both points are on the interior of the black hole. We have $\tilde{u} = u \pm i\frac{\beta}{2}$ and $\tilde{u}' = u' \pm i\frac{\beta}{2}$, such that we have four different possible combinations to consider:

$$\begin{aligned} &\text{Case A:} \quad \tilde{u} = u + i\frac{\beta}{2}, \quad \tilde{u}' = u' + i\frac{\beta}{2}, \qquad \text{Case B:} \quad \tilde{u} = u - i\frac{\beta}{2}, \quad \tilde{u}' = u' + i\frac{\beta}{2} \\ &\text{Case C:} \quad \tilde{u} = u + i\frac{\beta}{2}, \quad \tilde{u}' = u' - i\frac{\beta}{2}, \qquad \text{Case D:} \quad \tilde{u} = u - i\frac{\beta}{2}, \quad \tilde{u}' = u' - i\frac{\beta}{2} \end{aligned} \tag{3.21}$$

Case B leads to a divergent exponential in the E-integral, $e^{E\beta/2}$, and is thus discarded. Case A and Case D have no more damping factor for the E-integral, e^0, and are thus also divergent and discarded. For Case C we get:

$$\langle G_{bb} \rangle = \int d\mu(M) e^{-\frac{\beta}{2}M} \int d\mu(E) e^{iT\omega} e^{-\frac{\beta}{2}E} \frac{\chi(z)}{\omega} \frac{\chi^*(z')}{\omega} \Gamma(1 \pm i\sqrt{M} \pm i\sqrt{E}), \tag{3.22}$$

where again $\chi(z)$ is given by Eq. (3.20). This results is variations of Eq. (3.19), with an extra χ function and slightly varying exponential damping factors.

3.3 Points in other wedges

As a final exercise we can calculate the exact two-point function where one point is in another wedge. Recall that this only makes physical sense in the case of an eternal AdS black hole. We will label the wedges as seen in Fig. (3.7), highlighting again the fact that time runs backwards in the left wedge.

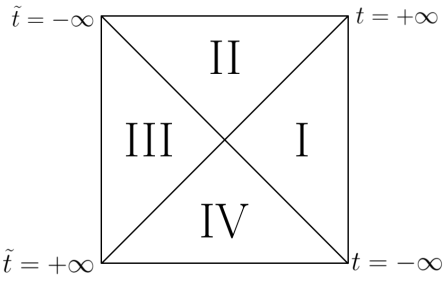

Fig. 3.7: Labeling of the wedges of the TFD state/ Penrose diagram of an eternal AdS black hole.

3.3.1 Wegde IV

A point $(u', \widetilde{v}')$ in wedge IV can be anchored to the second boundary using an outgoing lightray, defining the $\widetilde{v}'$ coordinate, and to the first boundary using the incoming lightray on the boundary, defining the u' coordinate. Substituting this into the exact two-point function we find that $\widetilde{v}' = v' + i\frac{\beta}{2}$ results in a divergent exponential $e^{E\beta/4}$, such that we take the case $\widetilde{v}' = v' - i\frac{\beta}{2}$. Analogous to the previous calculations we get:

$$\langle G_{bb} \rangle = \int d\mu(M) e^{-\frac{3\beta}{4}M} \int d\mu(E) e^{iT\omega} e^{-\frac{\beta}{4}E} \frac{\sin \omega z}{\omega} \frac{\chi(z')}{\omega} \Gamma(1 \pm i\sqrt{M} \pm i\sqrt{E}), \quad (3.23)$$

which is the same result as when the point is in wedge II (3.19), but with $\chi^*(z') \to \chi(z')$. This result is thus also visible in Fig. (3.4), with the sign of the imaginary part flipped.

3.3.2 Wegde III

A point $(\widetilde{u}', \widetilde{v}')$ in wedge III is completely anchored to the second boundary. Again we can consider the four combinations of $\widetilde{u}' = u' \pm i\frac{\beta}{2}$ and $\widetilde{v}' = v' \pm i\frac{\beta}{2}$. Only the case $\widetilde{u}' = u' - i\frac{\beta}{2}$ and $\widetilde{v}' = v' - i\frac{\beta}{2}$ has non-divergent behaviour. The imaginary contributions in the sin's cancel each other out, such that the result becomes

$$\langle G_{bb} \rangle = \int d\mu(M) e^{-\frac{\beta}{2}M} \int d\mu(E) e^{iT\omega} e^{-\frac{\beta}{2}E} \frac{\sin \omega z}{\omega} \frac{\sin \omega z'}{\omega} \Gamma(1 \pm i\sqrt{M} \pm i\sqrt{E}). \quad (3.24)$$

4 The Charged Unruh heat bath in JT gravity

This chapter covers original research. Section 4.1 is a mini-review combining some concepts in the existing literature which are needed as context for the eventual calculations. Section 4.2 starts with the known semi-classical result, followed by an in-between result where only the path integral of the gauge sector is calculated and the gravitational part is left on the saddle. Finally, everything that follows are new calculations which treat both sectors in a full quantum gravity framework. These calculations in essence attempt to generalise the results discussed in Section 2.4.2.3 for a charged black hole with chemical potential μ emitting radiation with a charge Q.

4.1 Charged setup

4.1.1 Number operator

As an introduction, let us consider a massless complex scalar field ϕ in the bulk, following [24]. The matter action is then given by

$$S = \int d^x \sqrt{-g} g^{\mu\nu} \partial_\mu \phi \partial_\nu \overline{\phi}. \tag{4.1}$$

Let ϕ have charge $+Q$, such that it transforms as $\phi \to e^{iQ\Lambda}\phi$ with the gauge transformation $e^{iQ\Lambda} \in U(1)$. Introducing the chemical potential μ, the grand canonical partition function (μVT ensemble) of the matter sector is

$$Z(\beta, \mu) = \text{Tr}\left[e^{-\beta H} e^{-\mu\beta Q}\right]. \tag{4.2}$$

Which can be computed as the vacuum amplitude on the thermal manifold, i.e. in Euclidean time, where the fields exhibit twisted periodicity boundary conditions: $\phi(\tau + \beta) = e^{-Q\mu\beta}\phi$. We can untwist them by redefining the fields as $\partial_\tau \phi = e^{-Q\mu\tau}\partial_\tau \phi$, which leaves the action invariant. Similarly, in lightcone coordinates (u, v), we can redefine the field as $\partial_u \phi = e^{iQ\mu u}\partial_u \phi$ and analogously for v. With these

field redefinitions, the two-point function of the field derivatives with respect to the Poincaré vacuum now becomes

$$\langle 0|\partial_u\phi\partial_u\bar{\phi}|0\rangle_F = -\frac{1}{4\pi}\frac{f'(u_1)f'(u_2)}{\frac{\beta^2}{\pi^2}\sinh^2\frac{\pi}{\beta}(f(u_1)-f(u_2))}e^{iQ\mu(f(u_1)-f(u_2))}. \tag{4.3}$$

Semi-classically, where the bulk frame is fixed to be the black hole frame $f(y) = y$, this becomes

$$\langle 0|\partial_u\phi\partial_u\bar{\phi}|0\rangle_F = -\frac{1}{4\pi}\frac{1}{\frac{\beta^2}{\pi^2}\sinh^2\frac{\pi}{\beta}(u_1-u_2)}e^{iQ\mu(u_1-u_2)}. \tag{4.4}$$

Note that semi-classically, the $U(1)$ frame $\Lambda = 0$ has been chosen, where Λ is the gauge parameter of the background gauge field: $A_\mu \to A_\mu + \partial_\mu\Lambda$. The $U(1)$ part is in this case a free boson system.

We now want an expression in the charged setup for the Poincaré vacuum expectation value of the occupation number of the modes $u_\omega(y)$ which have a positive frequency in the observer's frame $y = u, v$. Using Eq. (2.207), (2.208) and (4.3) we find

$$\begin{aligned} N_{\omega,Q}[f] = -\frac{1}{\pi}\int dy_1 \int dy_2 u_\omega(y_1)u^*_\omega(y_2) \\ \times\left[\frac{f'(u_1)f'(u_2)}{\frac{\beta^2}{\pi^2}\sinh^2\frac{\pi}{\beta}(f(u_1)-f(u_2))}e^{iQ\mu(f(y_1)-f(y_2))} - \frac{1}{y_{12}^2}\right]. \end{aligned} \tag{4.5}$$

This result, however, still needs to be coupled to the background gauge field A_μ. As it stands, the bulk fields are not yet observable since they carry charge and must thus couple to the $U(1)$ field. To do this, we introduce the gauge-covariant derivatives

$$D_\mu = \partial_\mu - iQA_\mu, \tag{4.6}$$

such that the action becomes

$$S = \int d^x\sqrt{-g}g^{\mu\nu}D_\mu\phi\overline{D_\nu\phi}. \tag{4.7}$$

The gauge theory is in fact a background field B and F model (BF-model)[1]. From the dynamics of this particular system it follows that $F = 0$ which means the gauge field is pure gauge: $A_\mu = \partial_\mu\Lambda$ [8]. The boundary dual of the model is then a free boson $\Lambda(t)$ which is coupled to the gravitational degree of freedom f by the chemical potential μ [24]. An observable can then be obtained by extracting the gauge-part of an covariant operator and fixing the gauge. For example, we can take the $U(1)$ gauge-covariant derivative to be

$$D_u\phi \to e^{iQ\Lambda(u)}\partial_u\phi. \tag{4.8}$$

[1]This is elaborated on in Sec. (4.1.2)

Taking again into account the field redefinition $\partial_u \phi \to e^{iQ\mu u}\partial_u \phi$, we can construct the gauge-coupled, and thus observable, two-point function:

$$\langle 0|D_u\phi\overline{D_u\phi}|0\rangle_F = -\frac{1}{4\pi}\frac{f'(u_1)f'(u_2)}{\frac{\beta^2}{\pi^2}\sinh^2\frac{\pi}{\beta}(f(u_1)-f(u_2))}e^{iQ\mu(f(u_1)-f(u_2))}e^{iQ(\Lambda(y_1)-\Lambda(y_2))}. \tag{4.9}$$

This in turn allows us to construct the observable occupation number in the Poincaré vacuum:

$$N_{\omega,Q}[f,\Lambda] = -\frac{1}{\pi}\int dy_1 \int dy_2 u_\omega(y_1)u^*_\omega(y_2) \times \left[\frac{f'(u_1)f'(u_2)}{\frac{\beta^2}{\pi^2}\sinh^2\frac{\pi}{\beta}(f(u_1)-f(u_2))}e^{iQ\mu(f(y_1)-f(y_2))}e^{iQ(\Lambda(y_1)-\Lambda(y_2))} - \frac{1}{y_{12}^2}\right]. \tag{4.10}$$

Since we will eventually want to insert this into a path integral, the question remains what the appropriate action $S[f,\Lambda]$ is for this theory. More specifically, since the action for $\int[\mathcal{D}f]$ is the Schwarzian action, the question is what form the $U(1)$ sector of the action takes.

4.1.2 Action from the IR SYK model

We can construct the action for the charged setup by relating JT gravity to the Sachdev-Ye-Kitaev (SYK) model, a quantum many-body system with random Gaussian couplings introduced in [28]. This section and the next follow [8, 25]. JT gravity as described in Chapter 2 is already related to the SYK model, since the uncharged black hole system in JT gravity is governed by the Schwarzian action, which is the low-energy regime of the SYK model. As such, it is natural to consider the low-energy regime of the complex (charged) SYK model for the charged setup in JT gravity. In this regime, such systems have an emergent $\mathrm{SL}(2,\mathbb{R}) \times U(1)$ symmetry [25]. This is apparent from the fact that the dynamics are governed by an action consisting of the Euclidean thermal Schwarzian action, i.e. the familiar $\mathrm{SL}(2,\mathbb{R})$ gravitational part, coupled to a $U(1)$ BF model describing the gauge field sector [8], also in Euclidean signature:

$$I[f,\Lambda] = -C\int_0^\beta d\tau \left\{\tan\frac{\pi}{\beta}\tau,\tau\right\} + \frac{K}{2}\int_0^\beta d\tau\left(\Lambda'(\tau) - i\mu f'(\tau)\right)^2. \tag{4.11}$$

Where the coupling of Λ to f through μ is now clearer. In the charged setup of JT gravity, the parameter K now determines the strength of the quantum effects of the gauge sector. Recall that in a Euclidean path integral we have e^{-I}, such that the quantum effects are turned off when $K \to \infty$. The fields Λ in this context parameterizes charge fluctuations and are defined up to a constant $\Lambda \sim \Lambda + (\text{constant})$ [8].

The Λ field thus displays a $U(1)_{\text{global}}$ gauge symmetry, like the F-field has an $\text{SL}(2,\mathbb{R})$ gauge invariance, such that a path integral involving the action (4.11) should thus be over $(\text{Diff}(S^1) \times LU(1))/(\text{SL}(2,\mathbb{R}) \times U(1)_{\text{global}})$ [25], where $LU(1)$ is the loop group in $U(1)$[2].

4.1.3 Decoupling the sectors

In the action (4.11), the $\text{SL}(2,\mathbb{R})$ mode f appears in the $U(1)$ sector. Separating the two sectors would allow us to calculate path integrals as the product of two separate path integrals, one for each of the two sectors. As such, we define the field

$$\sigma(\tau) = \Lambda(\tau) - i\mu f(\tau). \tag{4.12}$$

This field then has a twisted periodicity:

$$\sigma(\beta) = \sigma(0) - i\mu\beta + 2\pi m \tag{4.13}$$

where $m \in \mathbb{Z}$ is the winding. The action for σ is thus a completely free scalar with a twisted boundary condition along the thermal circle $e^{i\sigma} \to e^{i\sigma}e^{\mu\beta}$ [25]:

$$I[\sigma] = \frac{K}{2}\int_0^\beta d\tau(\sigma'(\tau))^2 \tag{4.14}$$

A Wick rotation gives the real-time expression $\sigma(t) = \Lambda(t) + \mu f(t)$. Recall that in the semi classical regime we have $\Lambda = 0$ and $f(y) = y$, such that $\sigma'(t) = \mu$.

Since the $\text{SL}(2,\mathbb{R})$ and $U(1)$ sectors are now completely decoupled, the total partition function can be written as

$$\begin{aligned} Z &= \int [\mathcal{D}f][\mathcal{D}\sigma]e^{-I[f,\sigma]} \\ &= \int [\mathcal{D}f]e^{-I[f]}\int [\mathcal{D}\sigma]e^{-I[\sigma]} \\ &\equiv Z_{\text{SL}(2,\mathbb{R})}Z_{U(1)}. \end{aligned} \tag{4.15}$$

$Z_{\text{SL}(2,\mathbb{R})}$ is the familiar Schwarzian partition function, which is given by Eq. (2.99). The $Z_{U(1)}$ partition function can be calculated exactly as well. The derivation follows [25]. The first step is to calculate the partition function for a fixed winding m, and

[2] i.e. the group of maps from S^1 to $U(1)$

since the theory is free the total partition function is then just a sum over m (recall also the twisted periodicity of σ):

$$\begin{aligned} Z_{U(1)} &= \int [\mathcal{D}\sigma] e^{-\frac{K}{2}\int_0^\beta d\tau (\sigma')^2} \\ &= \sqrt{\frac{2\pi K}{\beta}} e^{\frac{K\mu^2\beta}{2}} \sum_m e^{-\frac{2\pi^2 K}{\beta} m^2} e^{-i\frac{2\pi^2 K}{\beta}\frac{\mu\beta}{\pi} m} \\ &= \theta^3\left(i\frac{\beta}{2\pi K}, i\frac{\mu\beta}{2\pi}\right), \end{aligned} \tag{4.16}$$

where θ_3 is the Jacobi theta function, defined by $\theta_3(z,\tau) = \sum_n q^{n^2}\eta^n$ with $q = e^{\pi i \tau}$ and $\eta = e^{2\pi i z}$, such that

$$Z_{U(1)} = \sum_n e^{-\beta\left(\frac{n^2}{2K} - \mu n\right)}. \tag{4.17}$$

Here n can be interpreted as the electric charge, such that this partition function exhibits charge quantization. In 1+1d, the electric field sourced by a particle with charge Q is constant and the energy of the field is given by $\frac{Q^2}{2K}$ [22]. As such, this expression has the interpretation of the trace over the $U(1)$ Hilbert space, with Hamiltonian $\frac{n^2}{2K}$: $Z_{U(1)} = \mathrm{Tr}_{U(1)} e^{-\beta(H-\mu n)}$. We can let the size of $U(1)$ go to infinity. In this case the $m \neq 0$ winding contributions become suppressed. This is not particularly useful for the SYK model, but for our current setup in JT gravity we proceed as such. As a result the charge becomes continuous:

$$Z_{U(1)\to\mathbb{R}} = \int dq e^{-\beta\left(\frac{q^2}{2K} - \mu q\right)}, \tag{4.18}$$

which is simply a Gaussian integral

$$Z_{U(1)\to\mathbb{R}} = \sqrt{\frac{2\pi K}{\beta}} e^{\frac{K\mu^2\beta}{2}}. \tag{4.19}$$

The total partition function is then

$$Z = \left(\frac{2\pi C}{\beta}\right)^{3/2} e^{\frac{2\pi^2 C}{\beta}} \sqrt{\frac{2\pi K}{\beta}} e^{\frac{K\mu^2\beta}{2}} \tag{4.20}$$

Similarly, we can also decouple the two-point function (4.9):

$$\begin{aligned}\langle 0|D_u\phi\overline{D_u\phi}|0\rangle_F &= -\frac{1}{4\pi}\frac{f'(u_1)f'(u_2)}{\frac{\beta^2}{\pi^2}\sinh^2\frac{\pi}{\beta}(f(u_1)-f(u_2))}e^{iQ\mu(f(u_1)-f(u_2))}e^{iQ(\Lambda(y_1)-\Lambda(y_2))}\\ &= -\frac{1}{4\pi}\frac{f'(u_1)f'(u_2)}{\frac{\beta^2}{\pi^2}\sinh^2\frac{\pi}{\beta}(f(u_1)-f(u_2))}e^{Q\mu(f(\tau_1)-f(\tau_2)}e^{iQ(\Lambda(\tau_1)-\Lambda(\tau_2))}\\ &= -\frac{1}{4\pi}\frac{f'(u_1)f'(u_2)}{\frac{\beta^2}{\pi^2}\sinh^2\frac{\pi}{\beta}(f(u_1)-f(u_2))}e^{iQ(\sigma_1-\sigma_2)}\end{aligned} \tag{4.21}$$

where on the second line a Wick rotation $f \to -if$ was used. Note that the Schwarzian bilocal is was left in real-time, while the $U(1)$ part is expressed in Euclidean time. This isn't a problem due to the decoupling of the sectors, which means the two parts will be inserted into separate path integrals. The occupation number in terms of the field σ then becomes:

$$\begin{aligned}N_{\omega,Q}[f,\sigma] = -\frac{1}{\pi}\int dy_1 \int dy_2 u_\omega(y_1)u^*_\omega(y_2)\\ \times\left[\frac{f'(u_1)f'(u_2)}{\frac{\beta^2}{\pi^2}\sinh^2\frac{\pi}{\beta}(f(u_1)-f(u_2))}e^{iQ(\sigma_1-\sigma_2)}-\frac{1}{y_{12}^2}\right].\end{aligned} \tag{4.22}$$

The end goal is now to insert this as an operator into the full path integral

$$\langle N_{\omega,Q}\rangle = \int [\mathcal{D}f][\mathcal{D}\sigma]N_{\omega,Q}[f,\sigma]e^{-I[f,\sigma]}, \tag{4.23}$$

and obtain the spectrum analogous to Fig. (2.14).

4.1.3.1 Energy fluxes

Let us first again discuss the normal ordered components of the stress tensor to obtain an expression for the total energy density of the Unruh heat bath, analogous to Section 2.4.2.2. For this we follow [8]. The stress tensor components are now found by replacing the partial derivatives with gauge-covariant derivatives and taking into account the complex conjugate term:

$$T_{uu} = D_u\phi\overline{D_u\phi} + \overline{D_u\phi}D_u\phi, \quad T_{vv} = D_v\phi\overline{D_v\phi} + \overline{D_v\phi}D_v\phi. \tag{4.24}$$

Again using point-splitting regularisation, the normal ordered components become:

$$\begin{aligned}:T_{uu}(u_2): &= \lim_{u_1\to u_2}\left[D_u\phi(u_1)\,\overline{D_u\phi(u_2)} + \frac{1}{4\pi}\frac{1}{(u_1-u_2)^2} + (c.c.)\right]\\ :T_{vv}(v_2): &= \lim_{v_1\to v_2}\left[D_v\phi(v_1)\,\overline{D_v\phi(v_2)} + \frac{1}{4\pi}\frac{1}{(v_1-v_2)^2} + (c.c.)\right].\end{aligned} \tag{4.25}$$

When taking the CFT expectation value with respect to the Poincaré vacuum, we can expand the two-point functions (4.21) as

$$\langle 0|D_u\phi\overline{D_u\phi}0|\rangle_F = \frac{1}{u_{12}^2} + \frac{iQ\sigma'(u_2)}{u_{12}} + \frac{1}{6}\{F,u_2\} + \frac{1}{2}Q\left(-Q\sigma'(u_2)^2 + i\sigma''(u_2)\right) + \dots \tag{4.26}$$

such that

$$\langle : T_{uu}(u) : \rangle_F = -\frac{1}{12\pi}\{F,u\} + \frac{1}{4\pi}Q^2(\sigma'(u))^2 \tag{4.27}$$

where the first term is recognised as the uncharged term Eq. (2.191) with $c = 2$.

4.2 Planckian black-body spectrum

Using again the plane wave modes $u_\omega(y) = \frac{1}{\sqrt{4\pi\omega}}e^{-i\omega y}$, which have a positive frequency with respect to the y-observer's time coordinate, the full expression for the exact occupation number evaluated in the Poincaré vacuum is:

$$\begin{aligned}\langle N_{\omega,Q}\rangle = -\frac{1}{4\pi^2\omega}\int[\mathcal{D}f][\mathcal{D}\sigma]\int_{-\infty}^{\infty}dy_1\int_{-\infty}^{\infty}dy_2 e^{-i\omega(y_1-y_2)} \\ \times\left[\frac{f'(y_1)f'(y_2)}{\frac{\beta^2}{\pi^2}\sinh^2\frac{\pi}{\beta}(f(y_1)-f(y_2))}e^{iQ(\sigma_1-\sigma_2)} - \frac{1}{y_{12}^2}\right]e^{-I[f,\sigma]}.\end{aligned} \tag{4.28}$$

4.2.1 Semi-classical result

Before tackling the full quantum gravity calculation (4.23), we first consider the semi-classical regime. Recall that the semi-classical regime of saddle is given by $f(t) = t$ and $\sigma'(t) = \mu$, such that the integral (4.28) can be calculated [8]:

$$N_{\omega,Q,\text{cl.}} = \frac{\omega - Q\mu}{\omega}\frac{e^{-\frac{\beta}{2}(\omega-Q\mu)}}{e^{\frac{\beta}{2}(\omega-Q\mu)} - e^{-\frac{\beta}{2}(\omega-Q\mu)}} \tag{4.29}$$

This energy spectrum ωN_ω represents that of a charged black hole with chemical potential μ emitting Unruh radiation with charge Q. The chemical potential of a black hole is related to its charge and can thus, roughly speaking, be read as a sort of Coulomb potential. As such, we can nicely interpret the fact that from Eq. (4.29) it follows that particles with charge $Q > 0$ are preferably emitted by a black hole with chemical potential $\mu > 0$ as can be seen in Fig. (4.1). Note also that this expression is just Eq. (2.217) with an energy shift $\omega \to \omega - Q\mu$ and an additional prefactor $(\omega - Q\mu)/\omega$. The prefactor is necessary to ensure the occupation stays positive, since for $\omega < Q\mu$ the denominator becomes negative.

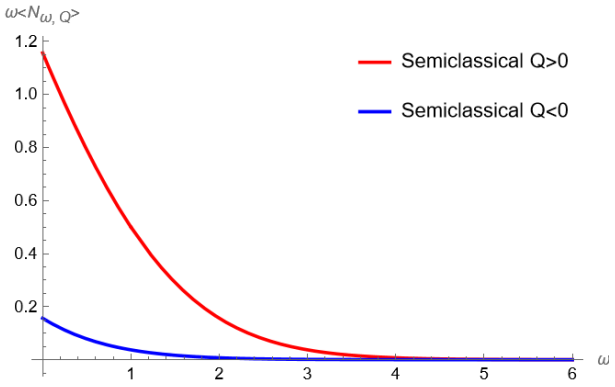

Fig. 4.1: Semi-classical spectrum of the charged Unruh modes for $\mu > 0$.

For the semi-classical case, starting from Eq. (4.27) the energy density becomes:

$$E_{\text{bath}}(u,v) = \langle : T_{uu}(u) : \rangle + \langle : T_{uu}(u) : \rangle = \frac{\pi}{3} T_H^2 + \frac{Q^2\mu^2}{2\pi}. \tag{4.30}$$

This is thus the energy density of the Unruh heat bath of a semi-classical 2d charged black hole with chemical potential μ and Hawking temperature $T_H = \beta^{-1}$.

This spectrum exhibits interesting behaviour in the zero-temperature or extremal black hole limit. Taking explicitly the limit we find:

$$\lim_{\beta\to\infty} N_{\omega,Q,\text{cl.}} = \frac{Q\mu - \omega}{\omega}\Theta(Q\mu - \omega) \tag{4.31}$$

such that only modes with an energy $\omega < Q\mu$ are occupied [8]. These modes which have a non-zero occupation at zero temperature are called superradiant modes. The existence of superradiant modes is entirely due to effects of the electric field. Intuitively, superradiant modes can be understood in a framework similar to the naive interpretation of Hawking radiation, where a particle-antiparticle pair is separated due to the black hole horizon. In the case of the superradiant modes, it is the electric field of the black hole (related to μ), which separates the particle-antiparticle pair of opposite charges, thus allowing radiation at $T = 0$.

4.2.2 Quantum gravity calculation

4.2.2.1 Quantum effects of the gauge sector

Following [8, 22], we now take the zero-temperature result Eq. (4.31) and add only quantum effects of the gauge sector. In other words, the gravitational part stays

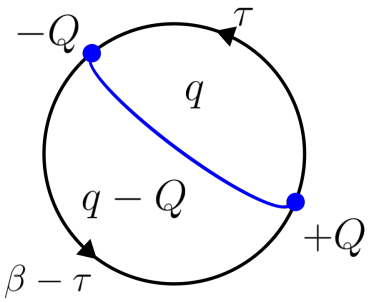

Fig. 4.2: Diagrammatic representation of Eq. (4.35). The charges of the two sectors are written in the bulk.

on the saddle $f(y) = y$ but the path integral over σ is evaluated. The occupation number in this regime becomes:

$$N_{\omega,Q}^{\beta\to\infty}[\sigma] = -\frac{1}{4\pi^2\omega}\int dy_1 \int dy_2 e^{-i\omega(y_1-y_2)}\left[\frac{1}{y_{12}^2}e^{iQ(\sigma(y_1)-\sigma(y_2))} - \frac{1}{y_{12}^2}\right]. \tag{4.32}$$

To include quantum effects of the gauge sector we calculate the path integral

$$\langle N_{\omega,Q}^{\beta\to\infty}\rangle = \frac{1}{Z_{U(1)}}\int [\mathcal{D}\sigma] N_{\omega,Q}^{\beta\to\infty}[\sigma] e^{-\frac{K}{2}\int d\tau(\sigma'(\tau))^2}. \tag{4.33}$$

As with the partition function, we will take $U(1) \to \mathbb{R}$ and thus a continuous charge. The path integral is gaussian, even with the operator insertion $e^{iQ(\sigma_1-\sigma_2)}$: it can be brought to the form

$$\int [\mathcal{D}\sigma] \exp\left(-\int d\tau \int d\tau' \sigma(\tau) A(\tau,\tau')\sigma(\tau') + \int b(\tau)\sigma(\tau)d\tau\right), \tag{4.34}$$

and evaluates to an integral over intermediate charges [8, 22, 23]:

$$\int dq e^{\frac{-q^2}{2K}\tau} e^{\frac{-(q-Q)^2}{2K}(\beta-\tau)} e^{\mu\beta(Q-q)}, \tag{4.35}$$

where the μ originates from the twisted periodicity of σ. This expression has an interpretation in terms of evolution operators along the thermal circle similar to that of Eq. (2.115). Recall that $q^2/2K$ is the energy of the electrical field sourced by a particle with charge q. As such, the first exponential $e^{-\frac{q^2}{2K}\tau}$ represents the time evolution along a Euclidean time period τ of a state with charge q and thus an electric field energy $q^2/2K$. The second exponential $e^{-\frac{(q-Q)^2}{2K}(\beta-\tau)}$ is then the time evolution along the remainder of the thermal circle but with an energy $(q-Q)^2/2K$. This can be interpreted with a charge insertion and extraction $\pm Q$ on two points of the thermal circle, as seen in Fig. (4.2).

Performing then the Fourier transform and using again Eq. (2.215), we get [8, 22]

$$\langle N_{\omega,Q}^{\beta\to\infty}\rangle = \frac{Q\mu - (\omega - \frac{Q^2}{2K})}{\omega}\Theta\left(Q\mu - (\omega - \frac{Q^2}{2K})\right), \tag{4.36}$$

which is exactly Eq. (4.31) but with an energy shift $\omega \to \omega - \frac{Q^2}{2K}$. This can be interpreted as follows. When a quantum is emitted, the total energy consists of the kinetic and rest energy of the particle plus the energy of the electric field it sources. The shift in Eq. (4.36) is then caused by subtracting this self-energy, leaving only the kinematic energy of the particle itself.

4.2.2.2 Full quantum gravity calculation

What follows are the original calculations and interpretations. Using the same arguments as in the uncharged case, the result again depends only on the time difference $t = y_1 - y_2$ and we can rewrite the integrals as dt and $d(y_1+y_2)$. The second integral again factorizes out and gives the divergent prefactor $2\pi\delta(0)$. Also analogous to the uncharged situation, Eq. (4.28) should be adapted to take the average of the time-ordered ($\mathcal{T}$) and anti-time-ordered ($\mathcal{A}$) contributions. The operator insertion in the anti-time-ordered contribution is in fact the complex conjugate of the operator in the time-ordered contribution (cf. Eq. (2.223)). In the path integral here, this flips the sign of the charge in the $U(1)$ sector, essentially causing a simultaneous replacement by particles ($+Q$) with anti-particles ($-Q$). This can be seen from the fact that, when writing the time-ordered and anti-time-ordered two-point functions, the Wightman two-point function is given by the average of $\mathcal{T}\phi^\dagger\phi$ and $\mathcal{A}\phi\phi^\dagger$, where one notices the simultaneous replacement by particle with anti-particle, as one swaps $\mathcal{T}$ with $\mathcal{A}$ [22].

We get

$$\begin{aligned}\langle N_{\omega,Q}\rangle = \frac{1}{2\pi\omega}\int[\mathcal{D}f][\mathcal{D}\sigma]\int dt e^{-i\omega t}e^{-I[f,\sigma]} \\ \times\Bigg[\frac{1}{2}\Bigg(\frac{f'(y_1)f'(y_2)}{\frac{\beta^2}{\pi^2}\sinh^2\frac{\pi}{\beta}(f(y_1)-f(y_2)+i\varepsilon)}e^{iQ\sigma_{12}} \\ +\frac{f'(y_1)f'(y_2)}{\frac{\beta^2}{\pi^2}\sinh^2\frac{\pi}{\beta}(f(y_1)-f(y_2)-i\varepsilon)}e^{-iQ\sigma_{12}}\Bigg) \\ -\frac{1}{2}\left(\frac{1}{(t+i\varepsilon)^2}+\frac{1}{(t-i\varepsilon)^2}\right)\Bigg],\end{aligned} \tag{4.37}$$

where we have omitted the divergent prefactor. For the total occupation number, we need to not only average over the time orderings but also explicitly sum over all particle-antiparticle contributions. As it stands, the current expression consists of

only a time-ordered particle ($+i\varepsilon$ and $+Q$) and an anti-time-ordered antiparticle ($-i\varepsilon$ and $-Q$) contribution. Taking the other two cases into account leads to the following terms:

$$\begin{aligned}
&\frac{1}{2}\Bigg[\frac{f_1' f_2'}{\frac{\beta^2}{\pi^2}\sinh^2\frac{\pi}{\beta}(f_1-f_2+i\varepsilon)}e^{+iQ\sigma_{12}}-\frac{1}{(t+i\varepsilon)^2}\\
&\quad+\frac{f_1' f_2'}{\frac{\beta^2}{\pi^2}\sinh^2\frac{\pi}{\beta}(f_1-f_2+i\varepsilon)}e^{-iQ\sigma_{12}}-\frac{1}{(t+i\varepsilon)^2}\\
&\quad+\frac{f_1' f_2'}{\frac{\beta^2}{\pi^2}\sinh^2\frac{\pi}{\beta}(f_1-f_2-i\varepsilon)}e^{+iQ\sigma_{12}}-\frac{1}{(t-i\varepsilon)^2}\\
&\quad+\frac{f_1' f_2'}{\frac{\beta^2}{\pi^2}\sinh^2\frac{\pi}{\beta}(f_1-f_2-i\varepsilon)}e^{-iQ\sigma_{12}}-\frac{1}{(t-i\varepsilon)^2}\Bigg]\\
&\equiv\frac{1}{2}\left[(\mathcal{T},p)+(\mathcal{T},a)+(\mathcal{A},p)+(\mathcal{A},a)-2\left(\frac{1}{(t+i\varepsilon)^2}+\frac{1}{(t-i\varepsilon)^2}\right)\right]
\end{aligned}\tag{4.38}$$

where $f_i \equiv f(y_i)$ and $\sigma_{12}=\sigma_1-\sigma_2$ and e.g. $(\mathcal{T},p)$ means the time-ordered particle operator contribution. The calculation of the final terms, i.e. the $(t\pm i\varepsilon)^{-2}$ terms, is completely analogous to the uncharged case but with a prefactor of two. Using again Eq. (2.215), this gives an overall term -1 on the right hand side.

Continuing to the operator insertions, we start with the $(\mathcal{T},p)$ contribution. From now, we set $C=1/2$ and $K=2$. This term is then, thanks to the decoupling of the sectors:

$$\frac{1}{4\pi\omega}\int dt e^{-i\omega t}\int[\mathcal{D}f]\frac{f'(y_1)f'(y_2)}{\frac{\beta^2}{\pi^2}\sinh^2\frac{\pi}{\beta}(f(y_1)-f(y_2)+i\varepsilon)}e^{-I[f]}\int[\mathcal{D}\sigma]e^{iQ\sigma_{12}}e^{-I[\sigma]}\tag{4.39}$$

As before, the $\mathrm{SL}(2,\mathbb{R})$ path integral is the two point function Eq. (2.115):

$$\int[\mathcal{D}f]\ldots=\frac{1}{2\pi^2 Z_{SL(2,\mathbb{R})}}\int d\mu(k_1)d\mu(k_2)e^{-it(k_1^2-k_2^2)}e^{-\beta k_2^2}\Gamma(1\pm ik_1\pm ik_2)\tag{4.40}$$

The $U(1)$ part again evaluates to (4.35), with the appropriate normalisation:

$$\int[\mathcal{D}\sigma]\cdots=\frac{1}{Z_{U(1)}}\int dq e^{\frac{-q^2}{4}\tau}e^{\frac{-(q-Q)^2}{4}(\beta-\tau)}e^{\mu\beta(Q-q)}.\tag{4.41}$$

Such that the full expression for the $(\mathcal{T}, p)$ part becomes, with $Z = Z_{\mathrm{SL}(2,\mathbb{R})} Z_{U(1)}$:

$$\begin{aligned}\frac{1}{8\pi^3\omega}\frac{1}{Z}\int d\mu(k_1)d\mu(k_2)e^{-\beta k_2^2}\Gamma(1\pm ik_1\pm ik_2)\\ \times\int dq e^{\mu\beta(Q-q)}e^{-\frac{(q-Q)^2}{4}\beta}\\ \times\int dt e^{-i\omega t}e^{-it(k_1^2-k_2^2)}e^{-\frac{q^2}{4}it}e^{\frac{(q-Q)^2}{4}it}.\end{aligned} \tag{4.42}$$

The time integral evaluates to a delta function:

$$\begin{aligned}\int dt\ldots &= 2\pi\delta\left(\omega+k_1^2-k_2^2+\frac{q^2}{4}-\frac{(q-Q)^2}{4}\right)\\ &= 2\pi\delta\left(\omega+k_1^2-k_2^2+\frac{1}{4}Q(2q-Q)\right)\\ &\equiv 2\pi\delta(\mathcal{T},p),\end{aligned} \tag{4.43}$$

such that we get

$$\begin{aligned}\frac{1}{4\pi^2\omega}\frac{1}{Z}\int d\mu(k_1)d\mu(k_2)e^{-\beta k_2^2}\Gamma(1\pm ik_1\pm ik_2)\\ \times\int dq e^{\mu\beta(Q-q)}e^{-\frac{(q-Q)^2}{4}\beta}\delta(\mathcal{T},p).\end{aligned} \tag{4.44}$$

We will see that, after the dust has settled, the remaining k-integrals are the same for the four terms, but the q-integral differs for each of them.

For the $(\mathcal{A}, p)$ term, the $\mathrm{SL}(2,\mathbb{R})$ part now gives:

$$\int[\mathcal{D}f]\cdots = \frac{1}{2\pi^2 Z_{SL(2,\mathbb{R})}}\int d\mu(k_1)d\mu(k_2)e^{it(k_1^2-k_2^2)}e^{-\beta k_2^2}\Gamma(1\pm ik_1\pm ik_2), \tag{4.45}$$

which is the complex conjugate of Eq. (4.40). The $U(1)$ part now gives:

$$\int[\mathcal{D}\sigma]\cdots = \frac{1}{Z_{U(1)}}\int dq e^{\frac{-q^2}{4}\tau}e^{\frac{-(q+Q)^2}{4}(\beta-\tau)}e^{-\mu\beta(Q+q)} \tag{4.46}$$

which is Eq. (4.41) with $Q\to -Q$.

The time integral now evaluates to the delta function

$$\begin{aligned}\int dt\ldots &= 2\pi\delta\left(\omega-k_1^2+k_2^2-\frac{1}{4}Q(2q+Q)\right)\\ &\equiv 2\pi\delta(\mathcal{A},p).\end{aligned} \tag{4.47}$$

In total we get:

$$\frac{1}{4\pi^2\omega}\frac{1}{Z}\int d\mu(k_1)d\mu(k_2)e^{-\beta k_2^2}\Gamma(1\pm ik_1\pm ik_2) \\ \times\int dq e^{-\mu\beta(Q+q)}e^{-\frac{(q+Q)^2}{4}\beta}\delta(\mathcal{A},p), \tag{4.48}$$

where indeed the only differences lie in the q-integral.

The $(\mathcal{T},a)$ and $(\mathcal{A},a)$ terms consist of different combinations of (4.40) and (4.45), and (4.41) and (4.46). We get:

$$\delta(\mathcal{T},a)=\delta\left(\omega+k_1^2-k_2^2-\frac{1}{4}Q(2q+Q)\right) \tag{4.49}$$

with

$$e^{-\mu\beta(Q+q)}e^{-\frac{(q+Q)^2}{4}\beta}, \tag{4.50}$$

and

$$\delta(\mathcal{A},a)=\delta\left(\omega-k_1^2+k_2^2+\frac{1}{4}Q(2q-Q)\right) \tag{4.51}$$

with

$$e^{\mu\beta(Q-q)}e^{-\frac{(q-Q)^2}{4}\beta}. \tag{4.52}$$

Combining the four different delta functions we get the full expression:

$$\begin{aligned}1+\langle N_{\omega,Q}\rangle &= \frac{1}{4\pi^2\omega}\frac{1}{Z}\int dq\int d\mu(k_1)d\mu(k_2)e^{-\beta k_2^2}\Gamma(1\pm ik_1\pm ik_2) \\ &\quad\times\Big[\delta(\mathcal{T},p)e^{\mu\beta(Q-q)}e^{-\frac{(q-Q)^2}{4}\beta}+\delta(\mathcal{A},p)e^{-\mu\beta(Q+q)}e^{-\frac{(q+Q)^2}{4}\beta} \\ &\qquad+\delta(\mathcal{T},a)e^{-\mu\beta(Q+q)}e^{-\frac{(q+Q)^2}{4}\beta}+\delta(\mathcal{A},a)e^{\mu\beta(Q-q)}e^{-\frac{(q-Q)^2}{4}\beta}\Big] \\ &= \frac{1}{4\pi^2\omega}\frac{1}{Z}\int dq\int d\mu(k_1)d\mu(k_2)e^{-\beta k_2^2}\Gamma(1\pm ik_1\pm ik_2) \\ &\qquad\Big(e^{\mu\beta(Q-q)}e^{-\frac{(q-Q)^2}{4}\beta}[\delta(\mathcal{T},p)+\delta(\mathcal{A},a)] \\ &\qquad+e^{-\mu\beta(Q+q)}e^{-\frac{(q+Q)^2}{4}\beta}[\delta(\mathcal{A},p)+\delta(\mathcal{T},a)]\Big)\end{aligned} \tag{4.53}$$

The first part has a sum of the delta functions $\delta(\omega\pm k_1^2\mp k_2^2+\frac{1}{4}Q(2q-Q))$. Using these delta functions it is possible to eliminate one of the k_i integrals, similar to

the procedure of the uncharged case. Each delta function is used on a different k-integral:

$$\delta(\omega + k_1^2 - k_2^2 + \frac{1}{4}Q(2q-Q)): \quad k_2^2 = \omega + k_1^2 + \frac{1}{4}Q(2q-Q)$$
$$\Rightarrow \begin{cases} e^{-\beta k_2^2} & \longrightarrow e^{-\beta(\omega + k^2 + \frac{1}{4}Q(2q-Q))} \\ \Gamma(1 \pm ik_1 \pm ik_2) & \longrightarrow \Gamma\left(1 \pm ik \pm i\sqrt{\omega + k^2 + \frac{1}{4}Q(2q-Q)}\right) \\ \sinh(2\pi k_2) & \longrightarrow \sinh\left(2\pi\sqrt{\omega + k^2 + \frac{1}{4}Q(2q-Q)}\right) \end{cases} \tag{4.54}$$

and

$$\delta(\omega - k_1^2 + k_2^2 + \frac{1}{4}Q(2q-Q)): \quad k_1^2 = \omega + k_2^2 + \frac{1}{4}Q(2q-Q)$$
$$\Rightarrow \begin{cases} e^{-\beta k_2^2} & \to e^{-\beta k^2} \\ \Gamma(1 \pm ik_1 \pm ik_2) & \to \Gamma\left(1 \pm ik \pm i\sqrt{\omega + k^2 + \frac{1}{4}Q(2q-Q)}\right) \\ \sinh(2\pi k_1) & \to \sinh\left(2\pi\sqrt{\omega + k^2 + \frac{1}{4}Q(2q-Q)}\right). \end{cases} \tag{4.55}$$

Such that the total k-integral becomes:

$$\left[e^{-\beta(\omega + \frac{1}{4}Q(2q-Q))} + 1\right] \int d\mu(k) e^{-\beta k^2} \Gamma\left(1 \pm ik \pm i\sqrt{\omega + k^2 + \frac{1}{4}Q(2q-Q)}\right) \times \sinh\left(2\pi\sqrt{\omega + k^2 + \frac{1}{4}Q(2q-Q)}\right). \tag{4.56}$$

However, there is an additional subtlety when performing the integral over this delta function. Since $k_2^2 > 0$, the delta function can only differ from zero when

$$\omega + k^2 + \frac{1}{4}Q(2q-Q) > 0. \tag{4.57}$$

Since the q-integral goes from $-\infty$ to $+\infty$, this is not guaranteed over the entire domain. As such, we should adjust the bounds of the q-integral to only include the part of the domain where Eq. (4.57) holds true. If we don't, the terms under the square roots in the $\sinh$'s in Equations (4.55) and (4.56) can become negative, leading to an overall imaginary expression, which of course cannot be physically interpreted as an occupation number. The condition for q to ensure the reality of the result becomes:

$$q > -\frac{2}{Q}(\omega + k^2) + \frac{Q}{2} \equiv -\tilde{q}. \tag{4.58}$$

Plugging these results into Eq. (4.53), we get for the first term:

$$\begin{aligned}\frac{1}{4\pi^2\omega}\frac{1}{Z}\int_{-\widetilde{q}}^{+\infty} dq e^{\mu\beta(Q-q)} e^{-\frac{(q-Q)^2}{4}\beta}\left(e^{-\beta(\omega+\frac{1}{4}Q(2q-Q))}+1\right)\\ \times\int d\mu(k) e^{-\beta k^2}\Gamma\left(1\pm ik\pm i\sqrt{\omega+k^2+\frac{1}{4}Q(2q-Q)}\right)\\ \times\sinh\left(2\pi\sqrt{\omega+k^2+\frac{1}{4}Q(2q-Q)}\right)\end{aligned} \tag{4.59}$$

The second term has the delta functions $\delta(\omega \pm k_1^2 \mp k_2^2 - \frac{1}{4}Q(2q+Q))$, so the end result is the same as the first term with $Q \to -Q$. The condition for q is now

$$q < \frac{2}{Q}(\omega + k^2) - \frac{Q}{2} \equiv \widetilde{q}, \tag{4.60}$$

such that for the second term we get

$$\begin{aligned}\frac{1}{4\pi^2\omega}\frac{1}{Z}\int_{-\infty}^{\widetilde{q}} dq e^{-\mu\beta(Q+q)} e^{-\frac{(q+Q)^2}{4}\beta}\left(e^{-\beta(\omega-\frac{1}{4}Q(2q+Q))}+1\right)\\ \times\int d\mu(k) e^{-\beta k^2}\Gamma\left(1\pm ik\pm i\sqrt{\omega+k^2-\frac{1}{4}Q(2q+Q)}\right)\\ \times\sinh\left(2\pi\sqrt{\omega+k^2-\frac{1}{4}Q(2q+Q)}\right).\end{aligned} \tag{4.61}$$

Combining these two results, we get the full expression for the occupation of the charged Unruh modes in the Poincaré vacuum:

$$\begin{aligned}1+\langle N_{\omega,Q}\rangle = \frac{1}{4\pi^2\omega}\frac{1}{Z}\int_0^{+\infty} d\mu(k) e^{-\beta k^2}\\ \times\left[\int_{-\widetilde{q}}^{+\infty} dq e^{-\beta(q\mu+\frac{1}{4}(q^2+Q^2))}\xi_{q,k}(Q) + \int_{-\infty}^{\widetilde{q}} dq e^{-\beta(q\mu+\frac{1}{4}(q^2+Q^2))}\xi_{q,k}(-Q)\right]\end{aligned} \tag{4.62}$$

with

$$\begin{aligned}\xi_{q,k}(Q) =& e^{\beta(\mu+\frac{q}{2})Q}\left(e^{-\beta(\omega+\frac{1}{4}Q(2q-Q))}+1\right)\sinh\left(2\pi\sqrt{\omega+k^2+\frac{1}{4}Q(2q-Q)}\right)\\ &\times\Gamma\left(1\pm ik\pm i\sqrt{\omega+k^2+\frac{1}{4}Q(2q-Q)}\right).\end{aligned} \tag{4.63}$$

Note that, since all combinations of time ordering and particle-antiparticle contributions have been considered, this expression is symmetric under $Q \to -Q$.

4.2.2.3 Plotting the spectrum

We can now attempt to plot $\omega \langle N_{\omega,Q} \rangle$ and compare the result to the semi-classical result Eq. (4.29), as the charged analogue to Fig. (2.14). The result can be seen in Fig. (4.3). The most important point of note for this result is that the spectrum does not approach zero as $\omega \to \infty$. The reason why this is problematic can be viewed in two intuitive ways. Firstly, modes which have an infinite energy should not have any occupation. Secondly, the total energy of the heat bath, $\int d\omega\omega \langle N_{\omega,Q} \rangle$, is infinite if $N_{\omega,Q}$ does not approach zero. Both of these considerations seem to suggest that the result is not physical.

However, it is worth noting that the spectrum does not approach a random value as $\omega \to \infty$, instead it asymptotes to $Q^2/2K$, i.e. exactly the energy of the electric field sourced by a particle with charge Q. This was found to occur regardless of the value of μ, β, C, Q and K. This constant energy shift seems similar to the one in Eq. (4.36). In fact, looking at the expression for $\omega \langle N_{\omega,Q} \rangle$:

$$\begin{aligned}\omega \langle N_{\omega,Q} \rangle = &\frac{1}{4\pi^2}\frac{1}{Z}\int_0^{+\infty} d\mu(k) e^{-\beta k^2} \\ &\times \left[\int_{-\widetilde{q}}^{+\infty} dq e^{-\beta(q\mu+\frac{1}{4}(q^2+Q^2))}\xi_{q,k}(Q) + \int_{-\infty}^{\widetilde{q}} dq e^{-\beta(q\mu+\frac{1}{4}(q^2+Q^2))}\xi_{q,k}(-Q)\right] \\ &- \omega,\end{aligned} \tag{4.64}$$

if we interpret the ω in the last term as having been shifted already as $\omega = \omega - Q^2/2K$, then this would explain an overall addition of $+Q^2/2K$ to the spectrum. We can attempt to counteract this shift by shifting again $\omega \to \omega + Q^2/2K$, which would eliminate the extra term. However, doing so for all ω's appearing in the expression does not seem to fix this issue, see Fig. (4.4). This additional energy shift is thus not employed in further results.

Regardless, as an ad hoc explanation it could be argued that the expression Eq. (4.64) is somehow accidentally measuring the energy of the electric field, on top of the energy due to the occupation of the modes themselves. The reason for this is unclear, but it could nonetheless be interesting to continue on and look at the results with this energy shift corrected for. As such, all the following results have a manual correction of $-Q^2/2K$.

4.2.2.4 Behaviour of the spectrum

As before, we can verify whether the numerical results behave as expected by comparing the results with the total energy density of the Unruh heat bath as

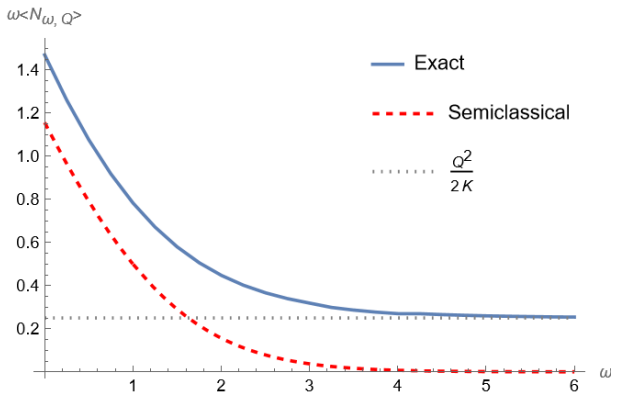

Fig. 4.3: Spectrum of the charged Unruh modes for $\beta = 2$, $\mu = 1$, $Q = 1$, $C = 1/2$ and $K = 2$.

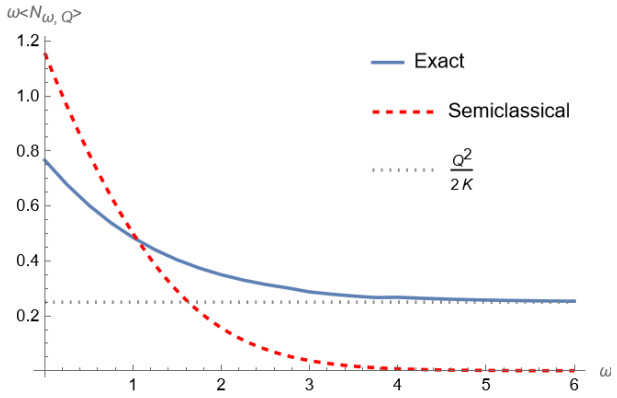

Fig. 4.4: spectrum of the charged Unruh modes with the shift $\omega \to \omega + \frac{Q^2}{2K}$ in an attempt to fix the asymptotic behaviour. $\beta = 2$, $\mu = 1$, $Q = 1$, $C = 1/2$ and $K = 2$.

calculated from the normal ordered components of the energy-stress tensor. For the exact result, we need to insert Eq. (4.27) into the full path integral[3]. We get:

$$\begin{aligned}\langle : T_{uu}(u) : \rangle &= \frac{1}{Z}\int [\mathcal{D}f][\mathcal{D}\sigma]\left(-\frac{1}{12\pi}\{F,u\} + \frac{Q^2}{4\pi}\dot{\sigma}^2(u)\right)e^{-I[f,\sigma]} \\ &= \frac{1}{Z_{\mathrm{SL}(2,\mathbb{R})}}\int [\mathcal{D}f]\frac{-1}{12\pi}\{F,u\}\,e^{-I[f]} + \frac{1}{Z_{U(1)}}\int [\mathcal{D}\sigma]\frac{Q^2}{4\pi}\dot{\sigma}^2(u)e^{-I[f,\sigma]}\end{aligned} \tag{4.65}$$

where in each term the remaining path integral over the other sector is cancelled out by the normalisation. The $\mathrm{SL}(2,\mathbb{R})$ term is known from the uncharged case and is given by Eq. (2.194). The $U(1)$ part involves a path integral where the operator insertion is exactly the Lagrangian density. As such, we can calculate it using the

[3] More specifically we take the expectation value of (4.27), since we normalise with the partition function.

known expression for the partition function Eq. (4.19). We start from the derivative of the partition function with respect to K, written in Lorentzian signature:

$$\begin{aligned}
\frac{\partial Z_{U(1)}}{\partial K} = \frac{\partial}{\partial K}\left(\sqrt{\frac{2\pi K}{\beta}}e^{\frac{K\mu^2\beta}{2}}\right) &= \frac{\partial}{\partial K}\left(\int [\mathcal{D}\sigma]e^{iS[\sigma]}\right) \\
\Leftrightarrow \frac{1}{2K}\sqrt{\frac{2\pi K}{\beta}}e^{\frac{K\mu^2\beta}{2}}\left(K\mu^2\beta+1\right) &= \frac{\partial}{\partial K}\int [\mathcal{D}\sigma]e^{\frac{iK}{2}\int_0^{-i\beta}dt\dot{\sigma}^2(t)} \\
&= \frac{i}{2}\int_0^{-i\beta}dt\int [\mathcal{D}\sigma]\dot{\sigma}^2(t)e^{iS[\sigma]} \\
&= \frac{\beta}{2}\int [\mathcal{D}\sigma]\dot{\sigma}^2(u)e^{iS[\sigma]}
\end{aligned} \tag{4.66}$$

where in the last line we used the fact that there is no preferential location on the thermal circle, so the integral over t simply evaluates to $-i\beta$. Including the normalisation we now directly get the expectation value of the $\dot{\sigma}^2$ operator:

$$\begin{aligned}
\langle\dot{\sigma}^2(u)\rangle &= \frac{1}{\sqrt{\frac{2\pi K}{\beta}}e^{\frac{K\mu^2\beta}{2}}}\left(\frac{1}{\beta K}\sqrt{\frac{2\pi K}{\beta}}e^{\frac{K\mu^2\beta}{2}}\left(K\mu^2\beta+1\right)\right) \\
&= \frac{1}{\beta K}\left(1+K\mu^2\beta\right)
\end{aligned} \tag{4.67}$$

The expectation value of the stress tensor component thus becomes

$$\langle :T_{uu}(u): \rangle = \langle :T_{vv}(v): \rangle = \frac{\pi}{6}T_H^2 + \frac{T_H}{8\pi C} + \frac{Q^2\mu^2}{4\pi} + \frac{Q^2}{4\pi\beta K}. \tag{4.68}$$

The final term is due to the quantum effects of the gauge sector and indeed for $K \to \infty$ this term disappears. Since this term is positive, we expect the exact quantum gravity result to have a higher occupation than the semi-classical case Eq. (4.30) (repeated here for convenience):

$$E_{\text{bath}}(u,v) = \langle :T_{uu}(u): \rangle + \langle :T_{uu}(u): \rangle = \frac{\pi}{3}T_H^2 + \frac{Q^2\mu^2}{2\pi}. \tag{4.30}$$

Firstly, we can look at the effect of differing the charge Q for a fixed chemical potential μ. The results can be seen in Fig. (4.5). Note that for $Q \lesssim 0.6$ the numerical accuracy of the results tend to break down, producing clearly nonsensical plots, and as such no lower values are discussed here. We can see that as Q increases, the spectrum eventually has a lower occupation than the semi-classical case, which is in disagreement with Eq. (4.68). This because the quantum gravity contribution is purely positive with respect to the semi-classical case, such that, due to

$$\int d\omega\omega \langle N_{\omega,Q}\rangle = \int dy \langle :T_{\pm\pm}: \rangle, \tag{4.69}$$

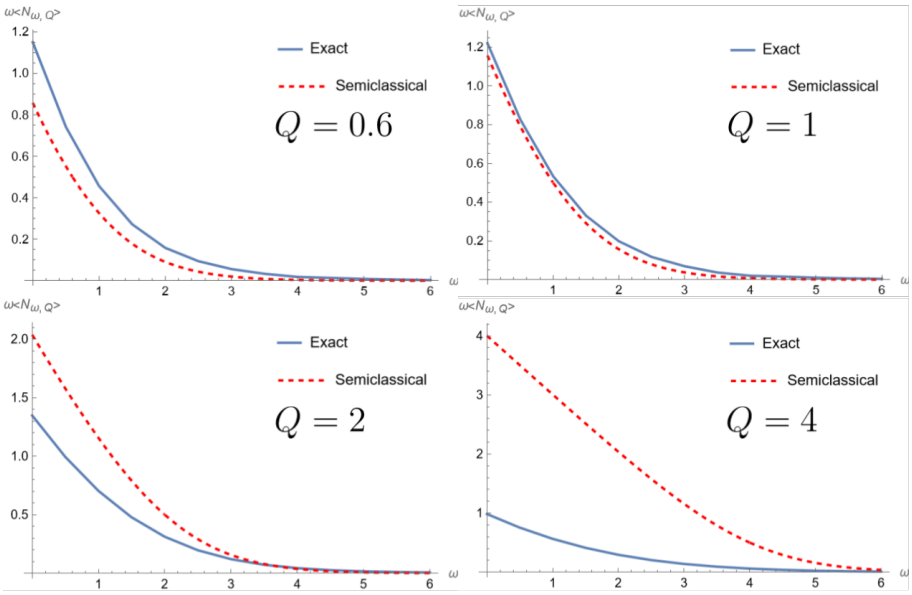

Fig. 4.5: Comparison of the corrected exact and semi-classical charged Unruh spectrum for different values of the charge Q. $\beta = 2$, $\mu = 1$, $K = 2$ and $C = 1/2$.

the area under the exact curve should always be bigger than the area under the semi-classical curve. Since the exact curve falls completely under the semi-classical one, this is impossible. Regardless of the comparison with the semi-classical case, looking at Eq. (4.68), the area under the exact curve should increase for increasing Q. To verify this, $\int d\omega\omega \langle N_{\omega,Q}\rangle$ was calculated numerically for different values of Q, the results for which can be seen in Fig. (4.6). We see that initially, the area increases as is expected. However, eventually this behaviour flips and disagrees with Eq. (4.68). It is unclear whether this behaviour is due to the actual nature of the expression, or if it is due to numerical inaccuracy for higher values of Q, similar to how the numerical results break down for small Q. However, since the behaviour is quite gradual and the curve does not display the same erratic behaviour as associated with the breakdown for small Q, this seems unlikely. Both the comparison problem and the area-under-curve problem could be alleviated if the charge contribution to the energy density had relative minus sign instead, but as it stands the validity of the result (4.62) is further called into question.

We can repeat this process for a varying chemical potential μ and a fixed charge Q, the results of which can be seen in Fig. (4.7). Here we can instantly see that the area under the curve, and thus the occupation, increases for increasing μ.[4] This is in line with what we expect from Eq. (4.68). However, we see that for increasing μ the exact curve eventually falls under the semi-classical result, which should not be possible looking at Eq. (4.68). In fact, varying μ should affect the exact result in the same way as the semi-classical one, since the μ contribution is identical in both. Because of this, we do expect the difference between the exact and semi-classical

[4]This was also verified by numerical integration.

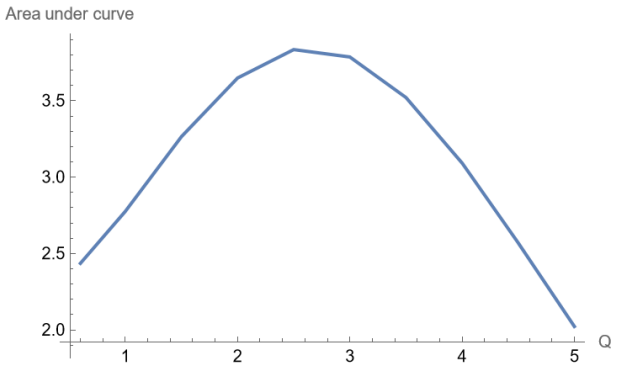

Fig. 4.6: Area under the corrected $\omega \langle \omega N_{\omega,Q} \rangle$ curve for different values of the charge Q. $\beta = 2$, $\mu = 1$, $K = 2$ and $C = 1/2$.

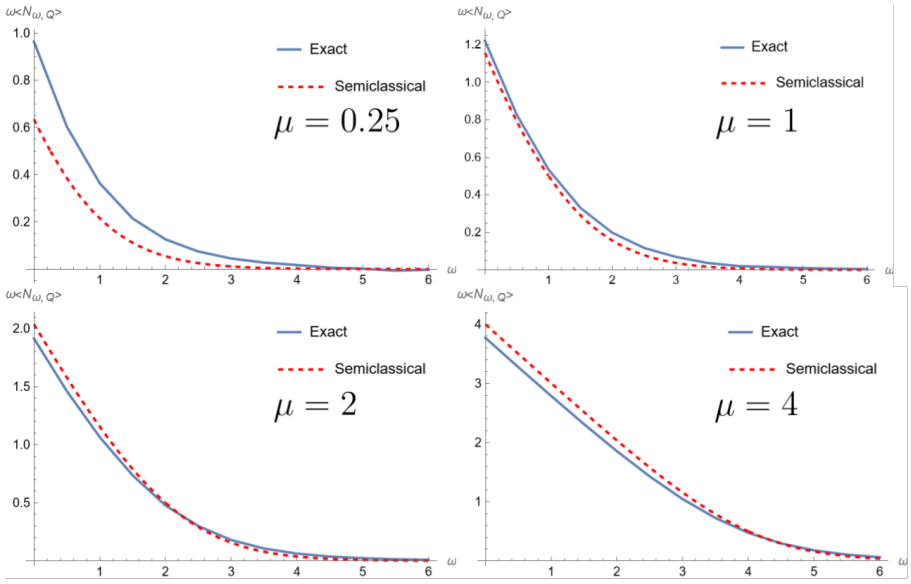

Fig. 4.7: Comparison of the corrected exact and semi-classical charged Unruh spectrum for different values of the chemical potential μ. $\beta = 2$, $Q = 1$, $K = 2$ and $C = 1/2$.

curve to be smaller for large μ, since the quantum corrections are then smaller in relation to the total energy density. This behaviour can slightly be recognised in the figures, but not with enough certainty to say that it is completely in line with expectations, especially considering the aforementioned issue of the area under the curve. However, since the we expect the curves to be closer together for large μ, and the exact curve is only slightly below the semi-classical one, this effect might be due to numerical inaccuracy. To determine whether this is the case, further numerical analysis would be required.

Finally we can also look at the $\beta \to \infty$ limit to investigate the existence of superradiant modes. The result for $\beta = 50$ can be seen in Fig. (4.8). Care needs to be taken not to increase β too much, as this also leads to a decrease in numerical accuracy. We do see the expected behaviour in Fig. (4.8), as only modes which have an energy $\omega < Q$ seem to have a non-zero occupation. The main difference for the exact result

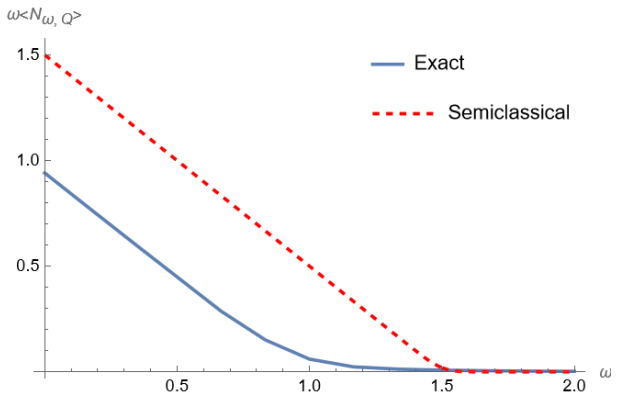

Fig. 4.8: Comparison of the corrected exact and semi-classical charged Unruh spectrum for $\beta = 50$, $Q = 1.5$, $K = 2$ and $C = 1/2$.

is that the superradiant part of the semi-classical spectrum is completely linear, while this is not the case for the exact result. In this regime as well, the area under the curve of the exact result is contradictorily smaller than that of the semi-classical curve.

4.2.2.5 Final remarks

Zero charge limit

In the case $Q \to 0$, Eq. (4.62) should coincide with the known expression for the uncharged Unruh occupation, Eq (2.229):

$$\langle N_\omega \rangle = \frac{1+e^{-\beta\omega}}{4\pi^2\omega} \frac{1}{Z_{\mathrm{SL}(2,\mathbb{R})}} \int d\mu(k) \sinh\left(2\pi\sqrt{\omega+k^2}\right) e^{-\beta k^2} \Gamma(1 \pm ik \pm i\sqrt{\omega+k^2}) - \frac{1}{2}. \tag{2.229}$$

The ξ function becomes in this regime:

$$\xi(k,q,0) = \left(e^{-\beta\omega}+1\right) \Gamma\left(1 \pm ik \pm i\sqrt{\omega+k^2}\right) \sinh\left(2\pi\sqrt{\omega+k^2}\right) \equiv \xi(k). \tag{4.70}$$

The bounds of the integrals become

$$\lim_{Q\to 0} \widetilde{q} = \lim_{Q\to 0} \left(\frac{2}{Q}(\omega+k^2) - \frac{Q}{2}\right) = +\infty \tag{4.71}$$

Such that

$$\langle N_{\omega,Q=0} \rangle = \frac{1}{4\pi^2\omega} \frac{1}{Z} \int d\mu(k) e^{-\beta k^2} \int_{-\infty}^{+\infty} dq e^{-\left(\frac{q^2}{4}+q\mu\right)\beta} 2\xi(k) - 1 \tag{4.72}$$

where the remaining q integral gets exactly canceled by the $U(1)$ partition function Eq. (4.19), since Gaussian integrals are independent of the sign of the linear term in the exponential. We get

$$\langle N_{\omega,0}\rangle = \frac{1+e^{-\beta\omega}}{4\pi^2\omega}\frac{1}{Z_{\mathrm{SL}(2,\mathbb{R})}}\int d\mu(k)\sinh\left(2\pi\sqrt{\omega+k^2}\right)e^{-\beta k^2}\Gamma\left(1\pm ik\pm i\sqrt{\omega+k^2}\right)-1 \tag{4.73}$$

which is exactly twice Eq. (2.229). This is perhaps not surprising, as the uncharged case has no addition of particle-antiparticle contributions. In fact, redoing the derivation of Section 4.2.2.2 but averaging over the particle-antiparticle contributions instead, we retrieve exactly the uncharged result in the $Q \to 0$ limit. However, averaging over the contributions of particles and antiparticles is less apparent as a valid approach, taking into account the interpretation of the result as an occupation number.

Semi-classical and zero-temperature limit

If the result Eq. (4.62) is valid, it should reduce to Eq. (4.29) in the semi-classical, i.e. $C \to \infty$ and $K \to \infty$ limit. Additionally, it should equal Eq. (4.36) in the appropriate $\beta \to \infty$ and $C \to \infty$ limit. However, there is a subtlety to these limits, as carelessly taking for example the zero-temperature limit without also adjusting C would not lead to the required behaviour. In any case, taking the correct combination of limits would be a good additional check of the validity of Eq. (4.62), or any other possible results for the occupation number of the charged modes.

5 Conclusion and outlook

5.1 Correlators beyond the horizon

In order to define points beyond the AdS_2 black hole horizon, one can employ a technique where the point is anchored to the second boundary of a TFD state. This interior point then has coordinates $(\widetilde{u}', v')$, where $\widetilde{u}'$ is located on the second boundary and related to a coordinate on the first boundary by a kind of Wick rotation $\widetilde{u}' = u' \pm i\frac{\beta}{2}$. It was found that the choice of $\pm i\frac{\beta}{2}$ is equivalent in the semi-classical treatment, i.e. quantum matter on classical gravity, but inequivalent in the full quantum gravitational treatment. This is in analogy to e.g. the boundary two-point function, where the time orderings of the operators, defined by the choice $\pm i\varepsilon$, is also equivalent only in the semi-classical regime.

The exact quantum gravity bulk two-point function where the point $(\widetilde{u}', v')$ is located on the interior of the black hole was found by directly substituting these coordinate transformations into the known result, and can be written as:

$$\langle G_{bb} \rangle_\beta = \int_0^\infty d\mu(M) e^{\frac{-3\beta}{4}M} \int_0^\infty d\mu(E) e^{iT\omega} e^{\frac{-\beta}{4}E} \frac{\sin z\omega}{\omega} \frac{\chi^*(z')}{\omega} \Gamma(1 \pm i\sqrt{M} \pm i\sqrt{E}) \tag{5.1}$$

where

$$\chi(z') = \sin \omega z' \cosh \frac{\omega\beta}{4} + i \cos \omega z' \sinh \frac{\omega\beta}{4}, \tag{5.2}$$

$T = t - t'$ and $\omega = E - M$. When plotted numerically for a fixed time difference (see Fig. (3.4)), this result has some similarities to the case where both points are on the exterior of the black hole, most notably a peak where $z = z'$. However, the interpretation of this behaviour is less straightforward. The projected $u' = \widetilde{u}' + i\frac{\beta}{2}$ coordinate on the first boundary can have a contradictory definition as a valid lightcone coordinate, namely when $u' < v'$, such that the physical meaning of z' is not always clear. As such, a comprehensible interpretation of the result Eq. (5.1) is as of yet lacking. Intuitively, one would perhaps not expect the correlation function across a black hole horizon to have a peak anywhere, as there is no clear spatial relationship between the two points.

In the case of the eternal AdS_2 black hole, the other wedges of the TFD state or two-sided Penrose diagram are also meaningful. As such, we can extend the above treatment for points belonging to those wedges. The results are slight variations of Eq. (5.1) with different exponential damping factors and either $\chi^*(z') \to \chi(z')$ or $\to \sin \omega z'$.

5.1.1 Outlook

The interpretation of Eq. (5.1) is still very much an open problem. Further analytical analysis of this result could provide some further insight. One possible avenue in this regard is a pure state decomposition, similar to the discussion in Section 2.3.4.1. This could then further be analysed in the near-horizon regime, since the horizon is the least understood area of the black hole. Concretely, taking the near-horizon limit corresponds to taking the limits $u \to \infty$ and $\widetilde{u} \to \infty$. Another interesting limit to take would be the semi-classical limit $C \to \infty$, in order to then compare the result with the semi-classical approximation as a way of verifying its validity.

Another possibility is a more thorough numerical analysis of the result, more specifically a more sophisticated version of the plot in Fig. (3.4), as well as plots of the other results could be insightful. Since the integral is quite numerically intensive to compute, more intricate numerical methods could prove useful in this regard. Furthermore, it would be interesting to see a clear interpretation of why there is a peak in the correlator at the locus $z' = z$. To this end, the geometrical meaning of the coordinates could further be refined. Perhaps some interpretation of, or insight into the significance of, the imaginary part of the correlator could also prove useful.

5.2 Charged Unruh heat bath

The occupation of charged Unruh radiation with charge Q emitted by a charged black hole with chemical potential μ was computed within the JT gravity framework. The occupation number, with respect to the Poincaré vacuum, of the charged modes which have a positive frequency with respect to the observer's local frame was found to be:

$$1 + \langle N_{\omega,Q} \rangle = \frac{1}{4\pi^2\omega}\frac{1}{Z}\int_0^{+\infty} dk^2 \sinh(2\pi k) e^{-\beta k^2} \times \left[\int_{-\widetilde{q}}^{+\infty} dq e^{-\beta(q\mu + \frac{1}{4}(q^2+Q^2))}\xi_{q,k}(Q) + \int_{-\infty}^{\widetilde{q}} dq e^{-\beta(q\mu+\frac{1}{4}(q^2+Q^2))}\xi_{q,k}(-Q)\right] \tag{5.3}$$

with

$$\begin{aligned}\xi_{q,k}(Q) =& e^{\beta(\mu+\frac{q}{2})Q}\left(e^{-\beta(\omega+\frac{1}{4}Q(2q-Q))}+1\right)\sinh\left(2\pi\sqrt{\omega+k^2+\frac{1}{4}Q(2q-Q)}\right)\\ &\times\Gamma\left(1\pm ik\pm i\sqrt{\omega+k^2+\frac{1}{4}Q(2q-Q)}\right),\end{aligned} \tag{5.4}$$

and

$$\widetilde{q}=\frac{2}{Q}(\omega+k^2)-\frac{Q}{2}. \tag{5.5}$$

The resulting spectral density $\omega\langle N_{\omega,Q}\rangle$ was plotted in Figures (4.3 - 4.8). This result was found to have multiple problems.

Firstly, the spectrum does not approach zero as $\omega\to\infty$, which would mean that the total energy of the heat bath is infinite. There is a caveat, as the spectrum does not approach a random value but rather $Q^2/2K$, which is exactly the energy of the electric field sourced by a particle with charge Q. Attempts were made to correct for this energy surplus by shifting ω in a somewhat natural way, but no progress was made. In terms of interpretation, it could be argued that the expression Eq. (5.3) accidentally measures the energy of the electric field on top of the energy of the occupation of the modes themselves, but the reason why this would be the case is unclear. Nonetheless moving further, the energy surplus was manually subtracted from the spectrum.

Secondly, the total energy $\int d\omega\omega\langle N_{\omega,Q}\rangle$, i.e. the area under the curve of the spectrum, was found not to agree with the expectation. More specifically, since it is related to the normalised stress tensor components through

$$\int d\omega\omega\langle N_{\omega,Q}\rangle=\int dy\langle:T_{\pm\pm}:\rangle, \tag{5.6}$$

we can compare both the spectrum and the normalised stress tensor components to their semi-classical counterparts and see if the behaviour matches. To this end, the exact quantum gravity normalised stress tensor components for the charged JT setup were calculated and were found to be

$$\langle:T_{uu}(u):\rangle=\langle:T_{vv}(v):\rangle=\frac{\pi}{6}T_H^2+\frac{T_H}{8\pi C}+\frac{Q^2\mu^2}{4\pi}+\frac{Q^2}{4\pi\beta K}, \tag{5.7}$$

where the semi-classical result consists only of the first and third term, i.e. the quantum effects of respectively the $\mathrm{SL}(2,\mathbb{R})$ and $U(1)$ gauge sector are contained entirely within the second and fourth term. A first conclusion we can take from this is that the area under the curve of the exact spectrum should always be bigger than that of the semi-classical curve, since the quantum contributions are both positive. This was not found to be the case for the spectrum of Eq. (5.3), where the exact

curve can even fall completely under the semi-classical curve for some combinations of the parameters.

Furthermore, the behaviour for varying Q or μ does not match the expectations when looking at Eq. (5.7). For example, looking at Eq. (5.7) one would expect the area under the curve to continually increase as Q increases. Instead, it was found that the energy increases until $Q \approx 2.5$, after which it decreases. This could be the result of a loss of numerical accuracy for higher values of Q, but this is as of yet unconfirmed. Looking at the behaviour for varying μ, it was found that the area under the curve increases for increasing μ, which is in line with Eq. (5.7). However, as μ increases, the exact curve again eventually falls completely under the semi-classical curve, which should not be possible. Aside from this, since μ only appears in a term which shared by both regimes, we expect the difference between the semi-classical curve and the exact curve to become smaller as μ increases, since the quantum corrections become smaller in comparison. This does appear to happen in the obtained results, but whether the numerical relationship is exactly as expected was not verified. Regardless, the area under the exact curve should never become smaller than that of the semi-classical curve. As a final note, a lot of this behaviour could be better explained if the sign of the last two terms of Eq. (5.7) were flipped, but this result seems less likely to be erroneous than Eq. (5.3) itself.

The zero temperature limit $\beta \to \infty$ was also investigated, as the charged spectrum should exhibit the existence of superradiant modes. This was found to be the case, with the spectrum of the superradiant modes forming a concave decreasing curve. This in contrast with the semi-classical case, where the superradiant modes have a linear spectrum. The $Q = 0$ limit was also investigated, as this should reduce to the known result for the uncharged occupation number. This was verified, up to a prefactor of 2, which originates from the summing over particle-antiparticle contributions which is absent in the uncharged case.

5.2.1 Outlook

When it comes to verifying the result Eq. (5.3), a lot of the evidence seems to suggest that the result is, at least partially, wrong. There are however some additional checks which can be performed in order to get more closure. Firstly is taking the different combinations of limits of the parameters K, C and β. $K \to \infty$ corresponds with turning off quantum effects of the gauge sector, $C \to \infty$ turns off quantum effects of the gravitational sector and $\beta \to \infty$ sets the temperature to zero. Taking then appropriate combinations of these limits should reduce Eq. (5.3) to Eq. (4.29) or Eq. (4.36).

Another possibility to further explore these results is to perform a more accurate numerical analysis. More specifically, the behaviour for increasing Q should be repeated with higher accuracy to test whether the erroneous behaviour is surely due to the result, and not due to numerical accuracy. Additionally, the behaviour for increasing μ can also be further explored. Since the curve for larger values of μ is only slightly below the semi-classical case, this could feasibly be due to numerical inaccuracy as well, especially since one expects the difference between the two curves to become smaller for large μ. A more sophisticated numerical analysis could shed some light on this issue.

Finally there is still the issue of the interpretation of the energy surplus $Q^2/2K$. As it stands, the current explanation, where the result somehow measures the energy of the electric field on top of that of the modes, is ad hoc at best. For this explanation to be satisfactory, it should be more clear where in the derivation this effect comes into play.

Bibliography

[1] Ahmed Almheiri and Joseph Polchinski. *Models of AdS_2 Backreaction and Holography*. 2015. arXiv: 1402.6334 [hep-th] (cit. on p. 16).

[2] Andreas Blommaert, Thomas G. Mertens, and Henri Verschelde. „Clocks and rods in Jackiw-Teitelboim quantum gravity“. In: *Journal of High Energy Physics* 2019.9 (Sept. 2019) (cit. on pp. 3, 17, 25, 26, 29, 30, 34, 37, 38, 59).

[3] Andreas Blommaert, Thomas G. Mertens, and Henri Verschelde. „Unruh detectors and quantum chaos in JT gravity“. In: *Journal of High Energy Physics* 2021.3 (Mar. 2021) (cit. on pp. 47, 48, 50).

[4] Adam R. Brown, Hrant Gharibyan, Alexandre Streicher, et al. „Falling toward charged black holes“. In: *Physical Review D* 98.12 (Dec. 2018) (cit. on p. 11).

[5] John L. Cardy. *Conformal Invariance and Statistical Mechanics*. Santa Barbara, CA, June 1988 (cit. on p. 34).

[6] Sean M. Carroll. *Spacetime and Geometry: An Introduction to General Relativity*. Cambridge University Press, 2019 (cit. on pp. 4, 13).

[7] Bo-Hung Chen and Dah-Wei Chiou. „Response of the Unruh-DeWitt detector in a gravitational wave background“. In: *Physical Review D* 105.2 (Jan. 2022) (cit. on p. 47).

[8] Julian De Vuyst and Thomas G. Mertens. „Operational islands and black hole dissipation in JT gravity“. In: *Journal of High Energy Physics* 2023.1 (Jan. 2023) (cit. on pp. 22, 72, 73, 76–80).

[9] Bryce S. DeWitt. „QUANTUM GRAVITY: THE NEW SYNTHESIS“. In: *General Relativity: An Einstein Centenary Survey*. 1980, pp. 680–745 (cit. on p. 47).

[10] Julius Engelsöy, Thomas G. Mertens, and Herman Verlinde. „An investigation of AdS2 backreaction and holography“. In: *Journal of High Energy Physics* 2016.7 (July 2016) (cit. on pp. 18, 19).

[11] A. Fabbri, J. Navarro-Salas, and G. J. Olmo. „Particles and energy fluxes from a conformal field theory perspective“. In: *Physical Review D* 70.6 (Sept. 2004) (cit. on pp. 50, 52).

[12] Eduardo Fradkin. *Quantum field theory*. en. Princeton, NJ: Princeton University Press, Mar. 2021 (cit. on pp. 34, 35).

[13] Ping Gao, Daniel L. Jafferis, and David K. Kolchmeyer. „An effective matrix model for dynamical end of the world branes in Jackiw-Teitelboim gravity“. In: *Journal of High Energy Physics* 2022.1 (Jan. 2022) (cit. on p. 16).

[14]Paul Ginsparg. *Applied Conformal Field Theory*. 1988. arXiv: hep-th/9108028 [hep-th] (cit. on p. 50).

[15]Thomas Hartman. *Lectures on Quantum Gravity and Black Holes*. 2015 (cit. on pp. 11, 12, 28, 43, 44, 59, 61).

[16]Michal P. Heller. *Quantum black holes and holography - lecture notes*. 2024 (cit. on p. 5).

[17]Roman Jackiw. „Lower dimensional gravity". In: *Nuclear Physics B* 252 (1985), pp. 343–356 (cit. on p. 1).

[18]Satyanad Kichenassamy. *Fuchsian Reduction: Applications to Geometry, Cosmology, and Mathematical Physics*. Birkhäuser Boston, 2007 (cit. on p. 8).

[19]Hagen Kleinert. *Path Integrals in Quantum Mechanics, Statistics, Polymer Physics, and Financial Markets*. WORLD SCIENTIFIC, May 2009 (cit. on p. 29).

[20]Ho Tat Lam, Thomas G. Mertens, Gustavo J. Turiaci, and Herman Verlinde. „Shockwave S-matrix from Schwarzian quantum mechanics". In: *Journal of High Energy Physics* 2018.11 (Nov. 2018) (cit. on p. 32).

[21]Juan Maldacena, Douglas Stanford, and Zhenbin Yang. *Conformal symmetry and its breaking in two dimensional Nearly Anti-de-Sitter space*. 2016. arXiv: 1606 . 01857 [hep-th] (cit. on p. 23).

[22]Thomas Mertens. *Jackiw-Teitelboim trans-Planckian Unruh heat baths, unpublished notes*. 2023 (cit. on pp. 75, 78–80).

[23]Thomas G. Mertens. „The Schwarzian theory — origins". In: *Journal of High Energy Physics* 2018.5 (May 2018) (cit. on p. 79).

[24]Thomas G. Mertens. „Towards black hole evaporation in Jackiw-Teitelboim gravity". In: *Journal of High Energy Physics* 2019.7 (July 2019) (cit. on pp. 3, 32, 45, 48, 52–54, 56, 71, 72).

[25]Thomas G. Mertens and Gustavo J. Turiaci. „Defects in Jackiw-Teitelboim quantum gravity". In: *Journal of High Energy Physics* 2019.8 (Aug. 2019) (cit. on pp. 73, 74).

[26]Thomas G. Mertens and Gustavo J. Turiaci. „Solvable models of quantum black holes: a review on Jackiw–Teitelboim gravity". In: *Living Reviews in Relativity* 26.1 (July 2023) (cit. on pp. 3, 4, 6–8, 10, 16–18, 20–25, 27–33, 46, 49, 61).

[27]Thomas G. Mertens, Gustavo J. Turiaci, and Herman L. Verlinde. „Solving the Schwarzian via the conformal bootstrap". In: *Journal of High Energy Physics* 2017.8 (Aug. 2017) (cit. on pp. 32, 54).

[28]Subir Sachdev and Jinwu Ye. „Gapless spin-fluid ground state in a random quantum Heisenberg magnet". In: *Physical Review Letters* 70.21 (May 1993), 3339–3342 (cit. on p. 73).

[29]Matthew D. Schwartz. *Statistical mechanics Lecture Notes*. Cambridge, MA, 2021 (cit. on p. 38).

[30]Marcus Spradlin and Andrew Strominger. „Vacuum states for AdS2 black holes". In: *Journal of High Energy Physics* 1999.11 (Nov. 1999), 021–021 (cit. on pp. 3, 9, 12, 45, 46).

[31]Douglas Stanford and Edward Witten. „Fermionic localization of the schwarzian theory". In: *Journal of High Energy Physics* 2017.10 (Oct. 2017) (cit. on p. 28).

[32]Thomas Strobl. *Gravity in Two Spacetime Dimensions*. 2000. arXiv: hep-th/0011240 [hep-th] (cit. on p. 4).

[33]Robert H Swendsen. *An introduction to statistical mechanics and thermodynamics*. Oxford Graduate Texts. London, England: Oxford University Press, Mar. 2012 (cit. on p. 38).

[34]W. G. Unruh. „Notes on black-hole evaporation“. In: *Phys. Rev. D* 14 (4 1976), pp. 870–892 (cit. on pp. 3, 47).

[35]Henri Verschelde. „Kwantum zwarte gaten en holografie“. Lecture Notes. 2022 (cit. on pp. 6, 39, 43).

Colophon

This thesis was typeset with LaTeX 2$_\varepsilon$. It uses the *Clean Thesis* style developed by Ricardo Langner. The design of the *Clean Thesis* style is inspired by user guide documents from Apple Inc.

Download the *Clean Thesis* style at `http://cleanthesis.der-ric.de/`.